UNIVERSITY OF KWAZULU-NATAL
INYUVESI YAKWAZULU-NATALI

WASH R&D CENTRE

Water Sanitation & Hygiene Research & Development Centre

DEVELOPMENT AND TESTING OF A FAECAL SLUDGE GREENHOUSE SOLAR DRYER

by

Pareshin Naidoo

212523981

In fulfilment of MScEng | Chemical Engineering,

College of Agriculture, Engineering and Science, UKZN

Supervisor:	Dr Santiago Septien
Co-supervisor:	Prof Craig McGregor
Submitted:	13-07-2023

As the candidate's Supervisors, we agree/do not agree to the submission of this thesis.

Signed:

Supervisor

……

Co-Supervisor

……

Form EX1-5

COLLEGE OF AGRICULTURE, ENGINEERING AND SCIENCE

DECLARATION 1 – PLAGIARISM

I, Pareshin Naidoo, declare that

1. The research reported in this thesis, except where otherwise indicated, is my original research.
2. This thesis has not been submitted for any degree or examination at any other university.
3. This thesis does not contain other persons' data, pictures, graphs or other information, unless specifically acknowledged as being sourced from other persons.
4. This thesis does not contain other persons' writing, unless specifically acknowledged as being sourced from other researchers. Where other written sources have been quoted, then:
    a. Their words have been re-written but the general information attributed to them has been referenced
    b. Where their exact words have been used, then their writing has been placed in italics and inside quotation marks, and referenced.
5. This thesis does not contain text, graphics or tables copied and pasted from the Internet, unless specifically acknowledged, and the source being detailed in the thesis and in the References sections.

Signed:

……

Form EX1-6

COLLEGE OF AGRICULTURE, ENGINEERING AND SCIENCE

DECLARATION 2 – PUBLICATIONS

Details of contribution to publications that form part and/or include research presented in this thesis (include publications in preparation, submitted, in press and published and give details of the contributions of each author to the experimental work and writing of each publication)

S.Septien, S. B. M. A. S. J. K. C., 2020. Effect of drying on the physical and chemical properties of faecal sludge for its reuse. *Journal of Environmental Chemical Engineering*, 8(1).

Dr. Santiago Septien Stringel, M. T. M. M. A. S. D. F. I., 2019. *Drying of Faecal Sludge using*, Gezina: Water research commission.

Ekechukwu, O. N. B., 1999. *Review of Solar-Energy Drying Systems II: An Overview of Solar Drying Technology. Energy Conversion and Management, 40, pp.615-655*. s.l.:s.n

Signed: 

……

Acknowledgements

There are a few people that participated in the development and testing of a greenhouse solar dryer. It would not have been possible without assistance from these people and organizations. My supervisors played a critical role in the entire development process. Their direction and knowledge guarantee that all of the research and design are precise and effective. The collaboration of friends and colleagues helped greatly in the development of a successful faecal sludge greenhouse solar dryer. Without my family and wife's support, it would not have been possible for me to complete my MSc thesis.

I would like to thank the following people and organizations for their contribution to the development and testing of the greenhouse solar dryer prototype:

1. Water Research Commission (WRC).
2. Technical and administrative staff from the WASH R&D Centre: Poovalingum Govender, Nombuso Mtshali, Kerry-Lee Philp, Luyanda Madlala, Ridwan Kebeje.
3. Colleagues and vacation students: Adheesh Ganapathie, Akhil Ramlucken, Renaldo Soni, Yashlin Pather.
4. Supervisors: Dr Santiago Septien, Prof Craig McGregor.
5. Family and spouse: Managie Naidoo, Prishen Naidoo, Perumal Naidoo, Noval Naidoo.

All of the above-mentioned people and organisations played a crucial role in the completion of the development and testing of the greenhouse solar dryer prototype.

Abstract

Faecal sludge poses a significant global challenge, contributing to pollution and disease transmission if not managed appropriately. Thermal drying presents a viable treatment method, reducing sludge mass and eliminating pathogens. However, the high energy requirements associated with conventionally powered methods of thermal drying raise operating costs, and to address this issue, solar drying was evaluated as an efficient and sustainable alternative for this process. This project aims to develop and test a solar thermal drying system for the treatment of faecal sludge, measure its performance characteristics, and identify areas of improvement and optimization.

This project presents an adaptation of a greenhouse-type solar dryer developed by the WASH R&D Centre at the University of KwaZulu-Natal for the treatment of faecal sludge. Greenhouse solar dryers utilise solar thermal energy and ventilation to dry a product. This dryer consists of seven subsystems: an enclosure, absorber wall, ventilation and circulation system, sludge mixing system, drainage system, drying tray, and testing instrumentation. Polymethyl methacrylate and aluminium were used in the construction of the enclosure, which measures 2 × 1.5 × 2 m (length × width × height). A ventilation and circulation system were installed in the greenhouse to remove moisture from the dryer and to improve moisture evaporation by enhancing external mass transfer at high air velocities. A rake system was designed to mix sludge and promote homogenous drying. The sludge was placed in a suspended grid where it could be dried from the top and bottom. A temperature and humidity control system was developed to record both the humidity and temperature at seven different areas in the dryer. The dryer was tested in Durban during the winter season of 2022 using feedstock consisting of water, wet soil, and synthetic sludge as a proxy of real faecal sludge, at UKZN, Howard College campus on the roof of the Chemical Engineering building.

Temperatures higher than 40 °C were recorded inside the dryer with ambient outside temperatures lower than 30 °C were recorded, leading to relative humidity lower than 40 %. Functionality tests were conducted to ensure the various subsystems were operating correctly, after which, the system was tested with feedstock. During the water tests, 7 small crucibles filled with water were used in the greenhouse dryer to determine how well water evaporated. Adjustments of both the ventilation and circulation fan speeds were made to determine the best airflow rates for the drying of water. Lower fan speeds proved more effective for water evaporation so the lowest fan speed combinations, ventilation speed 1 (V1) and circulation speed 1 (C1) were used in the wet soil tests and synthetic sludge. Tests with soil and sludge were conducted at these speeds. A large reduction of the moisture content of wet soil was observed during a single day from around 70 % moisture content to less than 20 % in the space of 5 hours. Synthetic sludge was made and tested during the winter season. Synthetic sludge has very similar properties and texture to faecal sludge and therefore is an effective feedstock for measuring the dryer's performance.

A 10 kg sample of synthetic sludge was tested in the greenhouse solar dryer between the dates of 05-08-2022 and 08-08-2022. Synthetic sludge with an 80 % moisture content was reduced to 6.5 % over 4 days. Drying times ranged from 5 to 6 hours a day, with an overall drying rate of 0.36 kg/h on average, a specific energy consumption (SEC) of approximately 655 kWh/t and an overall dryer efficiency of 9.6 %. A second test was conducted on the dates of 14-08-2022 and 15-08-2022. Better weather conditions on the second test enabled the dryer to dry 80 % moisture content sludge to 12 % in 2 days. The overall dryer efficiency of approximately 18 % and average SEC of 363 kWh/t were calculated over the two days of testing. The greenhouse solar dryer research and testing indicated that solar thermal dryers can potentially address the drying and disposal of faecal sludge, a matter that is a major problem in developing countries. Further steps to conclude the study include tests with real faecal sludge, improvement and optimization of the system, and the development of a techno-economic analysis.

Table of Contents

Acknowledgements ..... **V**

Abstract ..... **VI**

List of Figures ..... **XI**

List of Tables ..... **XIV**

List of Equations ..... **XVI**

Acronyms & Abbreviations ..... **XVI**

Chapter 1: Introduction **1**
1.1. Aim and Specific Objectives 2
1.2. Scope of Work 3
1.3. Research Questions 3
1.4. Initial Assumptions 3
1.5. Outline 4

Chapter 2: Literature Review **5**
2.1. Faecal Sludge 5
2.1.1. Faecal Sludge Management 6
2.1.2. Faecal Sludge Collection Systems 7
2.1.3. Resource Recovery 7
2.2. Solar Energy 8
2.2.1. Solar Spectrum 9
2.2.2. Solar Irradiance 9
2.2.2.1. Global Horizontal Irradiation (GHI) 10
2.2.2.2. Direct Normal Irradiation (DNI) 11
2.2.2.3. Diffuse Horizontal Irradiation 11
2.2.2.4. Latitude Tilt Irradiation 12
2.2.3. Solar Energy Conversion Routes 12
2.2.3.1. Photovoltaic systems 12
2.2.3.2. Photosynthetic and photoelectrochemical systems 13
2.2.3.3. Solar thermal systems 13
2.3. Thermal Drying 14
2.3.1. Drying Principle 14
2.3.2. Drying Kinetics 15
2.3.3. Psychrometry in Drying 17
2.3.4. Thermal Dryers 17
2.4. Solar Thermal Drying 18
2.4.1. Solar Thermal Dryers 18
2.4.2. Solar Thermal Drying of Waste Sludge 20
2.4.3. Greenhouse Solar Dryers 21
2.5. Summary of Literature 23

Chapter 3: Material & Methods **24**
3.1. Design Ideology 24
3.2. Description of the Greenhouse Solar Dryer 24
3.2.1. Enclosure 27
3.2.2. Absorber Wall 27
3.2.3. Ventilation and Circulation Systems 28
3.2.4. Rake System 29
3.2.5. Instrumentation and Control Systems 30
3.3. Testing of the Prototype 31
3.3.1. Functionality Tests 31
3.3.1.1. Enclosure temperature tests 31
3.3.1.2. Ventilation and circulation tests 32
3.3.1.3. Absorber wall temperature fluctuation tests 33
3.3.1.4. Rake system and testing instrumentation 33
3.3.1.5. Greenhouse dryer integrated functionality tests 33
3.3.2. Feedstock Tests 33
3.3.2.1. Water evaporation tests 33
3.3.2.2. Wet soil tests 34
3.3.2.3. Synthetic sludge tests 36
3.4. Data Treatment and Analysis 37
3.4.1. Output Parameters 37
3.4.2. Performance Parameter Calculations 37
3.4.3. Statistics/Uncertainties 38

Chapter 4: Results & Discussion **40**
4.1. Functionality Tests 40
4.2. Water Test Results 42
4.3. Wet Soil Drying Tests 45
4.3.1. 1.4 kg Wet Soil Drying Test 45
4.3.2. 15 kg Wet Soil Drying Test 47
4.4. Test 3 (Synthetic sludge) 50
4.4.1. Synthetic sludge test 1 50
4.4.2. Synthetic sludge test 2 53
4.4.3. Evaluation of synthetic sludge tests 1 and 2 55

Chapter 5: Conclusion **57**

Chapter 6: Observations & Recommendations **59**

Appendix A: Psychrometric Chart **65**

Appendix B: Support for the Literature Review **66**
B-1. Belt Dryers 67
B-2. Fluidized Bed Dryers 67
B-3. Drum Dryers 68
B-4. Direct-Type Solar Dryers 68
B-5. Passive Direct-Type Solar Dryers 69
B-6. Greenhouse Dryers 69
B-7. Active Direct Solar Dryers 70
B-8. Indirect-Type Solar Dryers 70

B-9. Passive Indirect Solar Dryers 71
B-10. Active Indirect Solar Dryers 71
B-11. Passive Hybrid Solar Dryer 72
B-12. Active Hybrid Solar Dryer 72

Appendix C: Thermal Drying Modelling 73
C-1. The Mathematical Model for Thermal Drying 73

Appendix D: CFD Simulations 74
D-1. Air Flow Direction 74
D-2. Temperature Fluctuations 75

Appendix E: Design Calculations 79
E-1. Design Assumptions 79
E-1.1. Change in Moisture Content 79
E-1.2. Drying time 80
E-1.3. Mass flow rate of air 81
E-1.4. Water Activity vs Moisture Content 81
E-1.5. Rake system calculation 83

Appendix F: Material Specifications of the Greenhouse Dryer 84
F-1. Selection of Material 84
F-1.1. Enclosure 86
F-1.1.1. Polycarbonate (PC) 86
F-1.1.2. Poly(methyl methacrylate) (PMMA) 86
F-1.1.3. Polyethylene Terephthalate Glycol (PETG) 86
F-1.1.4. Polyetherimide (PEI) 86
F-1.2. Absorber Wall 88
F-1.2.1. Metal absorber wall 88
F-1.2.2. Concrete absorber wall 88
F-1.3. Ventilation 89
F-1.3.1. Axial fans 90
F-1.3.2. Fan speed controller 90
F-1.4. Circulation Fans 91
F-1.5. Rake System 91
F-1.5.1. Linear Actuator 91
F-1.5.2. Guide Rail and Carriage 92
F-1.6. Drying Tray 92
F-1.6.1. Perforated Steel wire mesh 92
F-1.6.2. Aluminium angle (76 × 76 × 2 mm) 92
F-1.7. Drainage system 93
F-2. Testing Instrumentation 93
F-2.1. Temperature and Humidity Testing Instrumentation 93
F-2.1.1. Temperature and humidity sensors 93
F-2.1.2. Power module 94
F-2.1.3. Microcontroller 94
F-2.1.4. MicroSD card module 95
F-2.2. Air Flow Meters/Anemometer 95
F-3. Costing 96

Appendix G: Greenhouse Dryer Prototype Testing 97
G-1. Testing Procedure 97
G-1.1. Functionality Testing 97
G-1.2. Tests with Water 97
G-1.3. Tests with Wet Soil 98
G-1.4. Tests with Synthetic Sludge 98
G-1.5. Safe Operating Procedures (SOPs) for Moisture Analyser 99
G-2. Testing Results 99
G-2.1. Water Tests 101
G-2.2. Soil Tests 104
G-2.3. Synthetic Sludge 109

Appendix H: Drawings 114
H-1. Enclosure Frame 114
H-2. Absorber Wall 120
H-3. Rake System 122
H-4. PMMA Acrylic Sheet 131
H-5. Drying Tray 138
H-6. Floor Sheet Metal 141
H-7. Final Assembly 143

List of Figures

Figure 2-1: Treatment routes for human excreta (Abraham, 2016). 5
Figure 2-2: Faecal sludge management chain (Linda Strande, 2014). 6
Figure 2-3: Illustration of a VIP latrine, UDDT and ABR facility (Getahun, 2020). 7
Figure 2-4: Solar spectrum (Amyx, 2019). 9
Figure 2-5: Propagation of radiation on earth (Kevin R. Mallon, 2017). 9
Figure 2-6: GHI map of the Earth for 2019 (Marcel Suri,Tomas Cebecauer, 2023). 10
Figure 2-7: GHI map of South Africa (Jarvis, 2019). 11
Figure 2-8: DNI map of South Africa (Jarvis, 2019). 11
Figure 2-9: Solar Energy conversion routes (Gcep, 2006). 12
Figure 2-10: Residential PV system and utility grid (Smith, 1995). 12
Figure 2-11: Sunlight used to produce hydrogen using a particle and electrode solution. 13
Figure 2-12: Examples of some of the solar thermal technologies. 14
Figure 2-13: Relationship between dry-weight and wet-weight basis (Perry, 2007). 15
Figure 2-14: Classification of the solar thermal dryers (Ekechukwu, 1999). 19
Figure 2-15: Examples of active and passive solar dryer designs (Ekechukwu, 1999). 19
Figure 3-1: Greenhouse Solar Thermal Dryer –front/side of the greenhouse (left) and back/side of the greenhouse (right). 26
Figure 3-2: Enclosure after its construction. 27
Figure 3-3: Absorber wall. 27
Figure 3-4: Fan electrical connections. 28
Figure 3-5: Rake system and drying table. 29
Figure 3-6: Position of the temperature and humidity sensors. 30
Figure 3-7: Electrical control boxes. 30
Figure 3-8: Water test drying setup 34
Figure 3-9: Wet soil test with 15 kg soil at 70 % moisture content. 35
Figure 3-10: Synthetic sludge spread on the drying tray inside the dryer 37
Figure 4-1: Greenhouse temperature for different circulation and ventilation flow rate combinations. 42
Figure 4-2: Greenhouse humidity for different circulation and ventilation flow rate combinations. 43
Figure 4-3: Surface chart of SEC vs the fan speeds for selected data from water tests. 45
Figure 4-4: Surface chart of dryer efficiency vs fan speeds for selected data from water tests. 45
Figure 4-5: Drying curves for 1.4 kg soil tests with and without the rake system. 46
Figure 4-6: Drying curve for 15 kg soil tests with and without rake system operating. 47
Figure 4-7: Drying rate vs time for 15 kg soil tests with and without rake system operating. 48
Figure 4-8: Krischer curve for 15 kg soil tests with and without the rake system in operation. 48

Figure 4-9: Moisture content vs time for Test1 with synthetic sludge drying. 52
Figure 4-10: Drying rate vs moisture content for the 4 days of drying synthetic sludge. 53
Figure 4-11: Drying curve for duplicate drying test. 54

Figure A-1: Psychrometric chart. 65
Figure B-1: Treatment of sewage sludge. 66
Figure B-2: Belt drying system for sludge (Andritz, n.d.). 67
Figure B-3: Fluid bed dryer system for drying sludge. 67
Figure B-4: Drum dryer for drying sludge (Andritz, n.d.). 68
Figure B-5: Example of direct solar drying application. 68
Figure B-6: Composition of a solar cabinet dryer (Ekechukwu, 1999). 69
Figure B-7: Typical example of airflow in a solar dryer (Ekechukwu, 1999). 69
Figure B-8: A forced convection greenhouse dryer and a forced convection transparent roof solar barn (Ekechukwu, 1999). 70
Figure B-9: Working principle of indirect solar dryers (Sharma, 2009) 70
Figure B-10: A distributed-type natural circulation solar maize dryer (Ekechukwu, 1999). 71
Figure B-11: Active Indirect solar dryer (Ekechukwu, 1999). 71
Figure B-12: Working principle of a hybrid solar dryer (Ekechukwu, 1999). 72
Figure B-13: Features of a typical mixed mode active solar dryer (Ekechukwu, 1999). 72
Figure D-1: Velocity air stream within the dryer. 75
Figure D-2: Velocity air stream within the dryer. 75
Figure D-3: Air temperature distribution over table and drying tray (left) and air temperature fluctuations inside the greenhouse enclosure during operation (right). 76
Figure D-4: Temperature of air flowing over faecal sludge. 76
Figure D-5: Airflow pattern result 1. 77
Figure D-6: Airflow pattern result 2. 77
Figure D-7: Airflow pattern result 3. 77
Figure D-8: Airflow pattern result 4. 77
Figure D-9: Airflow pattern result 5. 77
Figure D-10: Airflow pattern result 6. 77
Figure D-11: Airflow pattern result 7. 78
Figure D-12: Airflow pattern result 8. 78
Figure D-13: Air volume rendering result 1. 78
Figure D-14: Air volume rendering result 2. 78
Figure E-1: Moisture content vs water activity. 82
Figure F-1: Transparent properties of various plastics (Ekechukwu, 1999). 84

Figure F-2: UV properties of transparent plastic (Ekechukwu, 1999). 85
Figure F-3: Axial fan. 90
Figure F-4: ebm-papst variable control switch. 90
Figure F-5: Square-mounted circulation fans. 91
Figure F-6: Igus belt-driven linear actuator. 91
Figure F-7: Igus linear guide rail. 92
Figure F-8: DHT- 22 temperature and humidity sensor 93
Figure F-9: WROOM power module. 94
Figure F-10: ESP32 development board. 94
Figure F-11: MicroSD card module. 95
Figure G-1: Thermal imaging taken using a FLIR 1 camera. 100
Figure G-2: Graph of Temperature vs Time. 106
Figure G-3: Graph of Humidity vs Time. 107
Figure G-4: Graph of DR vs MC for 15 kg wet soil dried with the rake system in operation. 108
Figure G-5: Drying rate vs moisture content. 109
Figure G-6: Drying rate vs moisture content. 113

List of Tables

Table 2-1: Drying thermal technologies for sewage sludge application. 18
Table 2-2: Solar thermal drying technologies. 20
Table 2-3: Solar thermal drying technology for sewage sludge. 21
Table 2-4: Solar drying technology for the treatment of sewage sludge. 22
Table 3-1: Greenhouse dryer design specifications. 25
Table 3-2: Ventilation and Circulation flow rates 32
Table 3-3: Water evaporation testing specifications. 34
Table 3-4: Wet soil testing specifications. 35
Table 3-5: Ingredient for 10 kg batch of synthetic sludge. 36
Table 3-6: Synthetic sludge testing specifications. 36
Table 4-1: Testing data recorded during functionality tests 41
Table 4-2: Performance parameters at varying ventilation rates and constant circulation rate (C3) during the water tests 43
Table 4-3: Performance parameters at varied circulation rates and constant ventilation rate (V1) during the water tests 44
Table 4-4: Performance parameters for 1.4 kg wet soil test with and without the rake system in operation. 46
Table 4-5: Performance parameters for 15 kg wet soil test with and without the rake system in operation. 49
Table 4-6: Evolution of synthetic sludge in the 4 days of testing during Test 1. 51
Table 4-7: Performance data for Test 1 with synthetic faecal sludge. 52
Table 4-8: Performance data for Test 2 with synthetic faecal sludge. 54
Table 4-9: Overall performance data for Test 1 and Test 2 with synthetic faecal sludge. 55

Table E-1: Design assumptions 79
Table F-1: UV light categories 87
Table F-2: Properties of metals. 88
Table F-3: Stone to concrete properties. 89
Table F-4: Technical specifications of the axial fan. 90
Table F-5: Technical specifications of the fan potentiometer. 91
Table F-6: Technical specifications of the square-mounted fan. 91
Table F-7: Technical specifications of the linear guide rail. 92
Table F-8: Technical specifications of the temperature and humidity sensor 93
Table F-9: Technical specifications of the power module. 94

Table F-10: Technical specifications of the microcontroller. 94
Table F-11: Material costing. 96
Table G-1: Ventilation and Circulation calibration. 99
Table G-2: Power consumption for the various electrical components. 100
Table G-3: Enclosure dry tests. 100
Table G-4: Water tests circulation speed 3 (28-07-2022). 101
Table G-5: Performance calculations from C3 test data. 101
Table G-6: Circulation speed 10 vs Ventilation performance parameters (02-08-2022). 102
Table G-7: Performance parameters calculated for circulation speed 10. 102
Table G-8: Circulation 6 and no circulation testing data (04-08-2022). 102
Table G-9: Performance Parameters Calculated for No Circulation and Circulation Speed 6. 103
Table G-10: Water Test for Circulation Speed 10 (05-08-2022). 103
Table G-11: Performance parameters for circulation speed 10. 103
Table G-12: Water Test for Circulation Speed 0 (No Circulation) (27-08-2022). 103
Table G-13: Performance parameters for water tests with no circulation. 104
Table G-14: Testing data of 1.4 kg soil dried with the rake system, not in operation. 104
Table G-15: Performance calculations for 1.4 kg soil without the use of the rake system. 105
Table G-16: Overall performance calculations for 1.4 kg soil without the use of the rake system. 105
Table G-17: Testing data of 1.4 kg soil dried with the rake system in operation (11-08-2022). 105
Table G-18: Performance calculations for 1.4 kg soil with the use of the rake system. 105
Table G-19: Testing data for 15 kg sample of soil dried without the use of rake system (12-08-2022). 106
Table G-20: Performance parameters for 15 kg soil tests without the rake system operating. 106
Table G-21: Performance parameters to dry wet soil without the use of the rake system. 107
Table G-22: Testing data for 15 kg of wet soil with the rake system in operation (17-08-2022). 108
Table G-23: Calculated performance data for 15 kg wet soil with the use of the rake system (17-08-2022). 108
Table G-24: Performance data calculated from soil test with the use of rake system (17-08-2022). 109
Table G-25: Day 1 testing data for synthetic sludge (05-09-2022). 110
Table G-26: Performance data for day 1 of testing (05-09-2022). 110
Table G-27: Day 2 testing data for synthetic sludge (06-09-2022). 110
Table G-28: Performance data for day 2 of 15 kg synthetic sludge testing (06-09-2022). 110
Table G-29: Day 3 testing data for synthetic sludge (07-09-2022). 111
Table G-30: Performance calculations for 15 kg synthetic sludge day 3 (07-09-2022). 111
Table G-31: Day 4 (08-09-2022). 111
Table G-32: performance data for day 4 of testing (08-09-2022). 112
Table G-33: Day 1 of duplicate synthetic sludge testing data (14-09-2022). 112

Table G-34: Calculated performance parameters for day 1 of duplicate testing (14-09-2022). 112
Table G-35: Day 2 synthetic sludge duplicate testing data (15-09-2022)..... 113
Table G-36: Calculated performance parameters for day 2 of duplicate testing (15-09-2022). 113

List of Equations

Equation 1: Moisture removal..... 37
Equation 2: Drying rate..... 38
Equation 3: Dryer efficiency..... 38
Equation 4: Specific energy consumption (SEC). 38
Equation 5: Change in moisture content 79
Equation 6: Conserved energy in a system 80
Equation 7: Drying time..... 80
Equation 8: Mass flow balance 81
Equation 9: Mass flow balance 81
Equation 10: Evaporated moisture..... 81
Equation 11: Volumetric flow rate of water 81
Equation 12: Torque equation..... 83

Acronyms & Abbreviations

ABR	Anaerobic Baffled Reactors
CFD	Computational Fluid Dynamics
DHI	Direct Horizontal Irradiation
DNI	Direct Normal Irradiation
EMC	Equilibrium Moisture Content
GHI	Global Horizontal Irradiation
LTI	Latitude Tilt Irradiation
PMMA	Poly(methyl methacrylate)
SEC	Specific Energy Consumption
UDDT	Urine Diversion Dry Toilet
UKZN	University of KwaZulu-Natal
VIP	Ventilated Improved Pit
WRC	Water Research Commission

Chapter 1: Introduction

Many regions around the world have no access to a sewer system, which contributes to a lack of sanitation. Human excreta is the source of faecal and sewage waste. Human excreta includes faeces and urine, as well as any waste that contains such material. In areas without sewer access, faecal sludge is generated by faecal sludge collection systems. Septic tanks, dry toilets, and pit latrines are examples of waste sludge collection systems. Faecal waste is a partially digested or semi-solid by-product of excreta collection, storage, or treatment (Linda Strande, 2014). The treatment of faecal sludge waste in underdeveloped nations has been hampered by a lack of resources and expertise (Koné, 2010).

Faecal sludge that is not managed properly causes public health issues, water pollution, and poor sanitation. This necessitates the development of cost-effective technology to aid in the processing of faecal sludge waste. Faecal waste management programs aiming at resource recovery may result in long-term, dependable, and safe collection and treatment of faecal waste sludge. Use in agriculture as fertilizer or soil conditioner is one of the possible re-use routes for faecal sludge. Onsite sanitation is one of the most practical solutions to the world's 2.4 billion people's lack of sanitation in poor countries.

Since it is difficult and expensive to connect the entire population to a sewage system in developing countries, many areas of the world rely on onsite sanitation. Additionally, onsite sanitation is the most practical solution for providing sanitation to underserved communities. In developed areas and cities, it can also be used to shift the way sewage sanitation is done into one that is more water-sensitive and sustainable, especially in areas where the sewage system needs urgent maintenance, the wastewater treatment facilities aren't working properly, and the water supply is running low. The build-up of faecal waste at the source is one of the major problems with on-site sanitation. Therefore, techniques for its in-situ treatment as well as its collection and transportation to a facility that treats faeces must be developed to dispose of it and eventually recover its resource potential.

The removal of wastewater from faecal sludge is a critical procedure for keeping waste bulk and volume to a minimum (Andritz, n.d.). Drying enables the removal of moisture through evaporation and kills pathogens found in faecal matter. Drying is an important step in the treatment of faecal sludge. Thermal drying can be utilized effectively to produce a dry and pasteurized bio-solid from faecal waste, which can be used as agricultural goods or fuel. Since commercial thermal dryers consume a lot of energy to dry faecal sludge, various energy sources are being studied to find the most efficient way to dry sludge (Ekechukwu, 1999).

Thermal solar technologies are extensively researched to find the best technology capable of effectively drying faecal sludge and producing a biomass or biosolid that can be used as an agricultural product or a fuel. Solar energy is a promising resource that can be used to effectively dry sludge. There are many dryers available today that utilize solar energy effectively to dry fruits, vegetables and even sewage

sludge. Technologies such as greenhouses can be modified to dry faecal sludge. Greenhouses utilize solar thermal energy thereby reducing energy costs incurred from heating a product.

Solar energy has been used in various ways for centuries. The sun radiates heat and light that sustain life on Earth. Plants require sunlight to flourish, while people as well as animals rely on plants for food and oxygen. This clean free energy is abundant in nature and has become a popular energy source in these times due to fossil fuel energy sources being depleted. Solar energy is renewable and if utilized effectively can prove an efficient and unlimited energy source. Solar energy technology has a lengthy history. Between 1860 and 1914, devices were developed to generate steam by harnessing the sun's heat to power irrigation pumps and engines (Smith, 1995). Solar energy can be an efficient resource for thermal drying waste sludge. Greenhouse dryers are capable of capturing the sun’s radiation energy within an enclosure. Greenhouse solar dryers rely on the capture of heat through the greenhouse effect and ventilation for the removal of moisture. Transparent mediums such as glass or clear plastics can be used to isolate the drying product from the outside environment. A transparent material is an effective tool for both holding air in an enclosure and also allowing solar thermal energy to pass into a system to heat the circulating air (Belloulid, et al., 2017). Active direct greenhouse dryers offer various benefits and simplicity as compared to the various other dryer types.

Since very little emphasis (S. Septien, 2019) has been put on faecal sludge solar thermal drying, the focus of the project is to develop solar drying technology that can be put in place to treat faecal sludge in areas with onsite sludge collection systems. The majority of the literature is concerned with the treatment of sewage sludge since very limited technology is available for the treatment of faecal sludge. Nonetheless, faecal sludge and sewage sludge portray similar properties, therefore similar treatment routes and techniques applied to sewage sludge can be used for faecal sludge treatment.

The project at hand will utilize solar energy to dry faecal sludge and create a biosolid. The development of a solar dryer design will effectively help in the treatment of faecal waste in places that require waste treatment. Unsanitary faecal sludge can be successfully dried using a solar dryer to create a dry, pasteurized biosolid. The creation of faecal sludge treatment technology can aid in converting waste streams into material and financial resource streams, encouraging safe reuse techniques.

1.1. Aim and Specific Objectives

The study aims to create and evaluate a cost-effective solar drying method for the wastewater treatment of faecal sludge.

The study's objectives are to investigate various technical methods and solar thermal drying technologies, to construct a feasible or cost-effective design that can be implemented in places that are not connected to a sewage system, to test the functionality and performance of various sub-systems of

the greenhouse dryer and integrated system, to evaluate the use of the prototype for the drying of sludge and its implementation in the field.

1.2. Scope of Work

The methodological approach is to develop a solar thermal greenhouse solar dryer for dealing with faecal sludge waste treatment. A prototype will be developed and stationed on the UKZN, Howard College, Chemical Engineering building roof. The prototype will be made up of different sub-systems. The several subsystems' functionality will be tested both individually and with each one fully incorporated into the dryer. To ascertain the dryer's performance, tests will be done using soil, water, and artificial sludge. After all the tests are concluded performance parameters will be calculated. To assess whether the dryer may be a useful instrument for drying sludge, performance characteristics will be compared to the literature.

There were a few limitations to the testing of the prototype. The limitations include tests being conducted during one season in the year which was the winter season, during the day and not at night, on sunny days and with synthetic sludge and not real faecal sludge. Weather conditions had a major impact on testing as the weather was not consistent on testing days. There are some very windy and cloudy days. The performance parameters calculated are significantly influenced by these weather conditions.

1.3. Research Questions

- What is the maximum temperature the greenhouse dryer can reach?
- What is the lowest humidity the greenhouse dryer can reach?
- Can the dryer lower the sludge's moisture content?
- Does the mixing of sludge improve the drying rate?
- Do ventilation and circulation improve drying conditions and performance parameters?

1.4. Initial Assumptions

- The greenhouse solar dryer prototype will aim to remove as much moisture from inside the dryer to the external environment
- Drying will promote humidity build but this can be alleviated by adjusting the ventilation power and circulation fans in the dryer.
- A black absorber wall will raise air temperatures in the greenhouse dryer and will ensure higher temperatures are reached inside the dryer.

1.5. Outline

The topic and the investigation are introduced. The research and literature discussed in the study are summarised in Chapter 2. The creation of the prototype, its testing, and the handling and analysis of the data are all covered in Chapter 3. Chapter 4 includes the testing results and discussion. Chapter 5 is the conclusion and Chapter 6: lists the observations and recommendations for further development of the prototype.

Chapter 2: Literature Review

Faecal sludge, solar energy, thermal drying, and solar thermal drying methods make up the literature review's four main sections. Faecal sludge is the product to be dried, solar energy will provide radiation and act as a heating element, thermal drying will be the process implemented and by combining solar energy and thermal energy, solar thermal technology can be developed.

2.1. Faecal Sludge

Faecal sludge and sewage sludge come from human excreta (A. Murray Muspratt, 2014) Human excreta refers to faecal and urinary discharges, as well as any waste that contains such material.

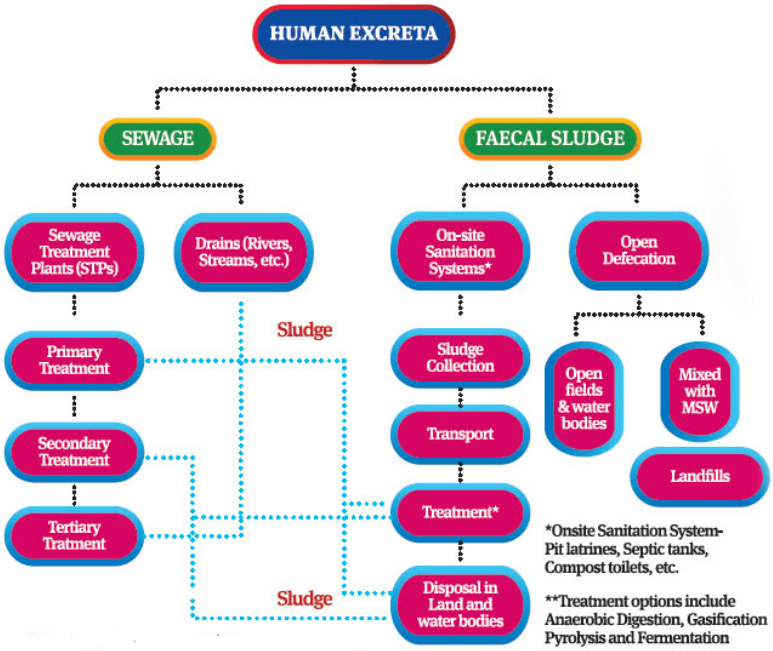

Figure 2-1: Treatment routes for human excreta (Abraham, 2016).

In areas without access to a sewer, onsite sanitation is where faeces are treated. Pit latrines, dry toilets, and septic tanks are examples of onsite sanitation technology. Faecal sludge is a slurry or semi-solid that is produced when excreta and blackwater are collected, stored, or treated (Linda Strande, 2014). Faeces, urine, anal cleansing supplies, and occasionally hazardous waste make up faecal sludge (Niwagaba, 2014).

Faecal sludge produced by an estimated 2.4 billion people causes environmental damage when it is left untreated (Koné, 2010). Faecal sludge and septage are the results of the frequent emptying of the onsite sanitation systems (Brdjanovic, 2015). The high volumes of faecal sludge with pathogens, organic matter and water can lead to offensive odour, disease outbreaks and continuous disposal costs (Mawioo,

2016). Due to this, there is an increasing need for safe faecal sludge emptying, transportation, and disposal (Montangero, 2004).

Public health problems, water pollution and poor sanitation are a result of faecal sludge that is not managed correctly. Plans for managing faecal sludge that is created to recover resources may result in a sustainable, dependable, and secure collection and treatment of faecal sludge. Faecal sludge could be recycled in agriculture as fertilizer, soil conditioner, and biofuel, among other uses. Faecal sludge's ability to be heated is increased when dried. Dried faecal sludge would resemble wood in terms of properties as a biofuel (S.Septien, 2020).

2.1.1. Faecal Sludge Management

Figure 2-2 shows the management sequence for the usage or disposal of faecal sludge. Emptying, collecting, moving, treating, and discarding faecal sludge make up the faecal sludge management component. The inability of households and communities to pay for professional sludge collection and transportation is one of many important variables that has a detrimental impact on the chain of faecal sludge management. There are few treatment facilities for faecal sludge, which creates expensive transport costs for the transportation of sludge in remote areas. The best way to overcome these factors is to effectively apply a sustainable FSM chain that meets every step in the service chain.

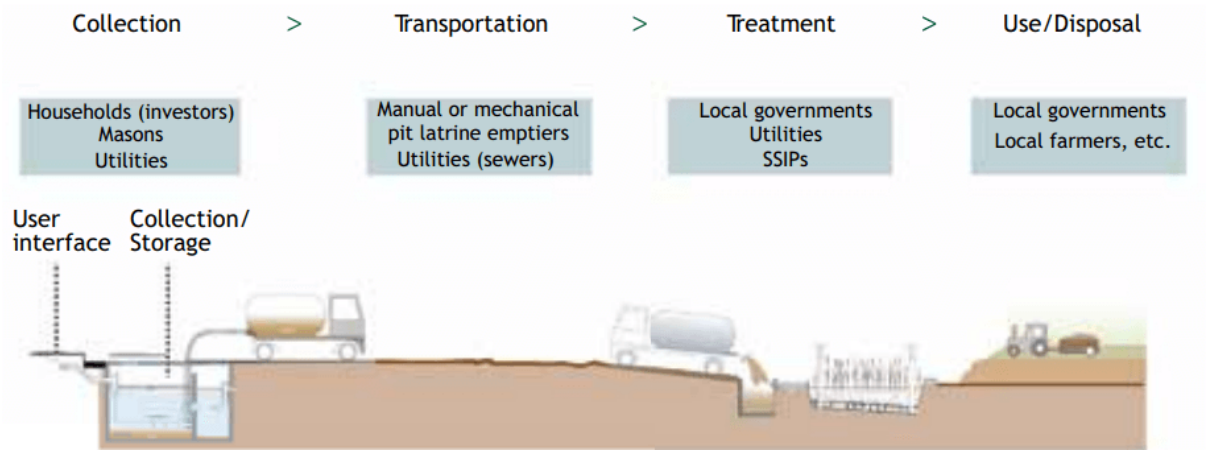

Figure 2-2: Faecal sludge management chain (Linda Strande, 2014).

Onsite treatment incurs expensive transportation costs due to the long distances between collection and treatment points. Determining the end use of the treated faecal sludge will greatly impact the design of the treatment technology. It is therefore conceivable to work backwards to achieve the treatment goals after the end-user has been identified. For example, the design of the treatment of faecal sludge to obtain a commercial fuel, that can be used in industry, will incorporate a different design from that of the treatment of faecal sludge to obtain a biosolid for agricultural purposes.

2.1.2. Faecal Sludge Collection Systems

The eThekwini Municipality (Durban metropolis, South Africa) utilizes ventilated improved pit (VIP) latrines, urine diversion dry toilets (UDDT), sceptic tanks and anaerobic baffled reactors (ABR) facilities to accumulate raw sludge. Figure 2-3 shows a schematic of VIP latrines, UDDT and ABR facilities. VIP latrines are sealed pits with ventilation pipes for the removal of foul odour.

VIP latrines typically contain excreta and urine but can also contain household waste (Getahun, 2020). Limited data found in the literature indicate VIP latrines contain faecal sludge with moisture contents of more than 50 % up to values of 95 % moisture content wet sludge (Phindile Madikizela, 2022). Emptying the pits can be difficult and water is sometimes added to aid in the emptying of VIP latrines, this contributes to the high moisture content of the collected sludge.

Without using water for flushing, the UDDT separates and collects urine and faeces in separate compartments. As a result, the majority of it is made up of excreta, but there is also a significant amount of sand, which is utilized to keep the faeces vault dry. UDDT vaults are generally easier to empty as they are designed with access doors for emptying. Faecal sludge samples collected from UDDT vaults have significantly lower moisture contents as compared to samples collected in VIP latrines. This is due to separate urine collection tanks and the addition of sand to keep the vaults dry. Faecal sludge of around 50 % up to values of 70 % moisture content sludge is present in UDDT vaults (Getahun, 2020).

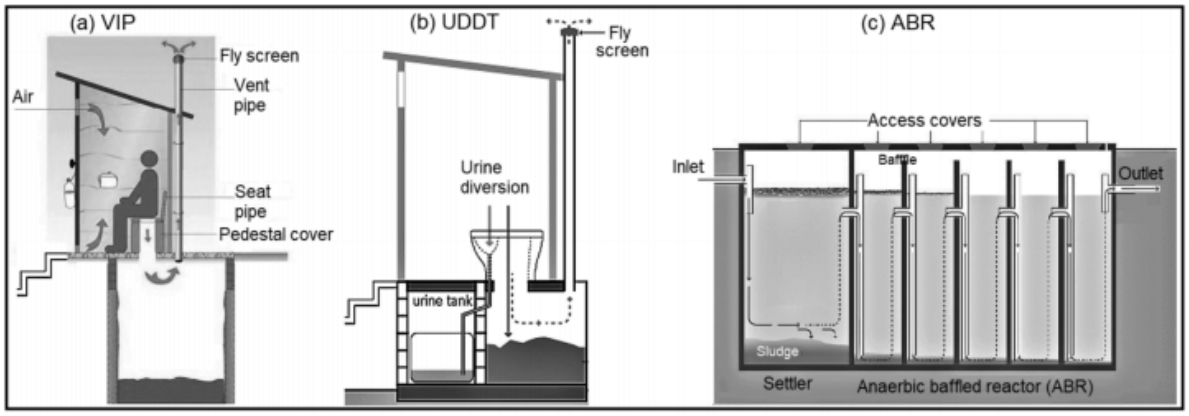

Figure 2-3: Illustration of a VIP latrine, UDDT and ABR facility (Getahun, 2020).

2.1.3. Resource Recovery

Faecal sludge management schemes that are created to recover resources may result in a sustainable, dependable, and secure collection and treatment of faecal sludge. Faecal sludge could be recycled in agriculture as a fertilizer or soil conditioner. High quantities of phosphorus found in dried faecal sludge made it suitable for use as fertilizer in agriculture. Dried faecal sludge's properties as a biofuel could be comparable to those of wood (S.Septien, 2020).

Agriculture may be viewed as the most natural usage of faecal sludge given that 60–70 % of the nutrients from crop fields are considered to be present in human excreta. Excreta utilization in agriculture can reduce the requirement for artificial fertilizers, resulting in the more sustainable production of agricultural fertilisers. Excreta feeds the soil with nutrients, enhances the soil's structure and water-holding ability, gets rid of pests, and neutralizes heavy metals and soil toxins, all of which cannot be done with synthetic fertilizers (Sapienza, 2005).

Similar to how sewage sludge is used in the cement industry, processed faecal sludge can be an efficient biofuel or a by-product of cement (Okuna, 2000). Faecal sludge can even be used in the production of ceramic-type products (M.M. Jordan, 2005). Faecal sludge has been reported to have heating values up to 17 MJ/kg in nations like Ghana and Senegal, which are comparable to the heating values of firewood and sawdust. Industrial fuel is a final application that could enable an economical and environmental solution for expensive and successful faecal sludge management (A. Murray Muspratt, 2014).

There are fewer treatment plants for the treatment of faecal sludge in South Africa. Wastewater treatment plants for the treatment of sewage sludge are more common. Wastewater facility's treatment processes include sludge stabilization, dewatering, incineration and drying of sewage sludge. Municipal sludge treatment facilities utilize a combination of these processes. Faecal sludge and sewage sludge have similar characteristics. Drying technology such as bed dryers, belt dryers and drying beds applied to sewage sludge can be effective in the treatment of faecal sludge. Therefore, if stabilized sewage sludge can be made a viable fuel, then faecal sludge stands to be a very attractive feedstock. Cost-effective methods for drying faecal sludge are required for commercial and large-scale viability.

2.2. Solar Energy

The sun is the nearest star to Earth, and despite being 150 million kilometres away, its gravitational force keeps the Earth in orbit. All life on Earth depends on the sun's radiation of heat and light. Sunlight is essential for plant growth because both animals and people depend on plants for food and oxygen. This clean free energy is abundant in nature and has recently become a popular energy source as fossil fuel energy sources become depleted. Electromagnetic waves carry solar energy to Earth primarily. Large amounts of solar energy are absorbed by Earth, which serves as a solar energy collector. This energy manifests in a variety of ways, including direct sunlight for plants, heated air masses that cause wind, and evaporation of water from oceans that results in rain. The energy that the sun provides to the earth in a single hour is greater than the energy used by the entire world in a single year. Each year, Earth receives roughly ten times more energy from sunlight than it does from fossil fuels like coal, oil, natural gas, and uranium (Robert Foster, 2009).

Solar energy is a renewable resource that, when used wisely, has the potential to be both effective and limitless. Oil, coal, and natural gas have all contributed to the emission of greenhouse gases into the

atmosphere, which has led to global warming. Alternative fuels such as solar energy for the production of electricity and as a heat source are becoming increasingly popular as renewable energy sources. Solar energy has been used in various ways for centuries. Solar energy is renewable and if utilized effectively can prove an efficient and unlimited energy source. Some of the advantages of solar energy are that it is non-polluting, carbon-free and a sustainable energy resource. Solar energy can be converted to provide power and heat through various conversion routes (Caramori, 2016).

2.2.1. Solar Spectrum

The light from the sun comes to Earth with different frequencies. These frequencies make up the solar spectrum. A solar spectrum shows the energy in solar irradiation in the form of electromagnetic waves of a wide spectrum. It progresses from low-energy infrared to visible light, followed by high-energy ultraviolet (UV). Infrared has a larger range of wavelengths on the solar spectrum as compared to visible light and UV light. Infrared wavelength represents around 51 % of the solar spectrum. About 47 % of the solar spectrum is made up of visible light. Around 2 % of the solar spectrum is made up of UV light. Long wavelengths have less energy than shorter wavelengths. The solar spectrum shows the radiation energy over all wavelengths (Amyx, 2019) . The wavelength and intensity of light in a solar spectrum are depicted in Figure 2-4.

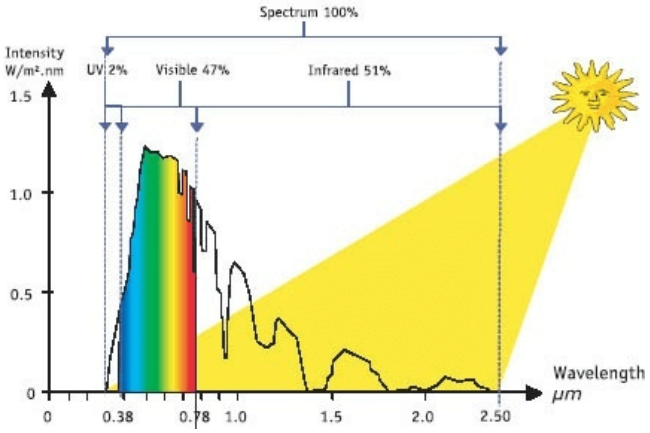

Figure 2-4: Solar spectrum (Amyx, 2019).

2.2.2. Solar Irradiance

The rate at which light strikes a surface is known as solar irradiance, which is used to gauge solar power. Different radiation types are produced as a result of the various pathways through which solar energy travels to Earth. Direct, diffuse, and reflected radiation are the three different forms of radiation. The solar energy that is sent to Earth directly, without any changes or significant interference, is known as direct radiation. On a cloudless day, direct radiation is observed. Diffuse radiation is solar radiation that is scattered and alters direction on its way to the earth's surface. The scattering of sunlight can be caused by cloud cover and moisture in the air. The percentage of solar energy deflected by the earth's surfaces, buildings,

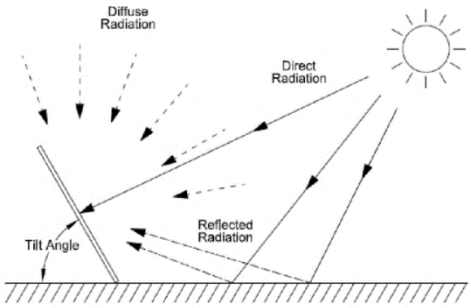

Figure 2-5: Propagation of radiation on earth (Kevin R. Mallon, 2017).

and glossy surfaces is referred to as reflected radiation (Ahmad Siouti, 2019). Figure 2-5 shows how radiation is propagated to Earth.

Irradiance quantifies the amount of radiation energy per square meter of area. There are 4 main parameters of solar irradiance. These parameters include latitude tilt irradiance (LTI), diffuse horizontal irradiance (DHI), direct normal irradiance (DNI), and global horizontal irradiance (GHI).

2.2.2.1. Global Horizontal Irradiation (GHI)

The total radiation emitted from a surface that is parallel to the ground is known as GHI. GHI, which comprises both DNI and DHI, is a crucial factor to consider in solar installations. GHI values are measured using pyranometers. The thermopile pyranometer and the silicon photo-electric pyranometer are the two varieties of pyranometers that are employed (Mohamed Khalifa Boutahir, 2022). The formula for calculating GHI is shown below:

$$GHI\ (Global\ Horizontal) = DNI\ (Direct\ Normal) \times cos(\theta) + DHI\ (Diffuse\ Horizontal)$$

Where:

θ = Angle made between the surface and the sunlight rays

GHI maps illustrate the solar radiation distribution across a region. Figure 2-6 shows an average GHI map of the planet for the year 2019.

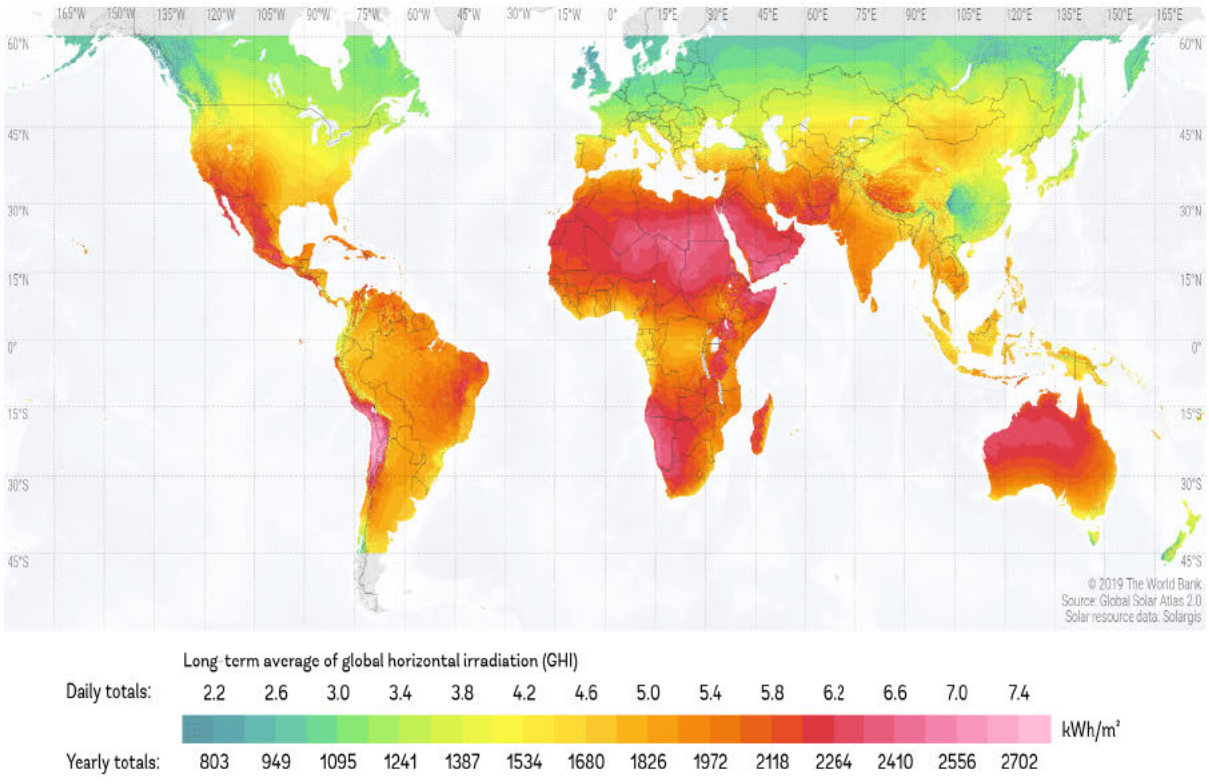

Figure 2-6: GHI map of the Earth for 2019 (Marcel Suri,Tomas Cebecauer, 2023).

The map shows high GHI values in Africa, therefore, indicating the continent has a large potential for utilizing solar technologies. Africa receives more than 2,000 kWh/m² averaged GHI annually (Jarvis, 2019). South Africa also receives an important amount of radiation. The east coastlines exhibit lower GHI values as these areas are more inland towards the northwest. Durban experiences more than 1,000 kWh/m² annually. Figure 2-7 shows an average GHI map of South Africa for the year 2018.

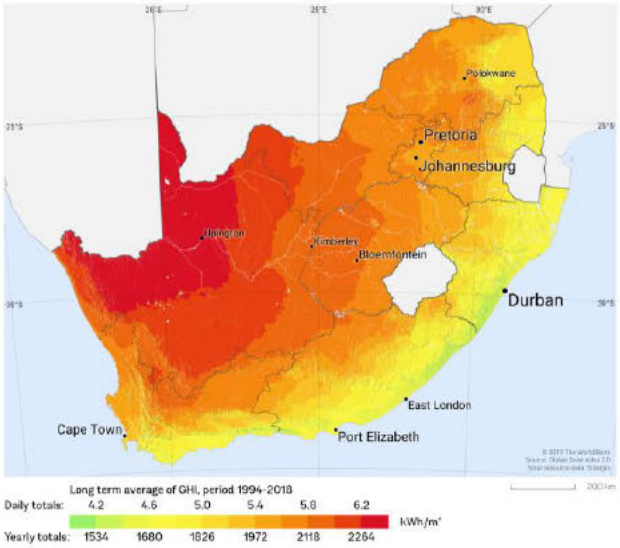

Figure 2-7: GHI map of South Africa (Jarvis, 2019).

2.2.2.2. Direct Normal Irradiation (DNI)

DNI measures the amount of solar radiation that reaches a surface normal to or perpendicular to the sun's rays coming in a straight line from the direction of the sun per unit area of the surface. The most DNI is observed on days with no cloud cover and little additional interference. This form of irradiation can be deflected and concentrated to a precise spot by using mirrored surfaces, glazing and other light-reflecting materials (Mohamed Khalifa Boutahir, 2022).

The formula to calculate DNI is:

$$DNI = \frac{GHI - DHI}{cos(\theta)}$$

Maintaining a surface normal to incoming radiation will maximize the quantity of irradiance it receives each year. DNI plays an essential role in solar concentration installations shows a DNI irradiation map of South Africa. Durban and along the coastline experience DNI values of more than 1,500 kWh/m² annually (Jarvis, 2019). Figure 2-8 shows the DNI map of South Africa between 1994 and 2018.

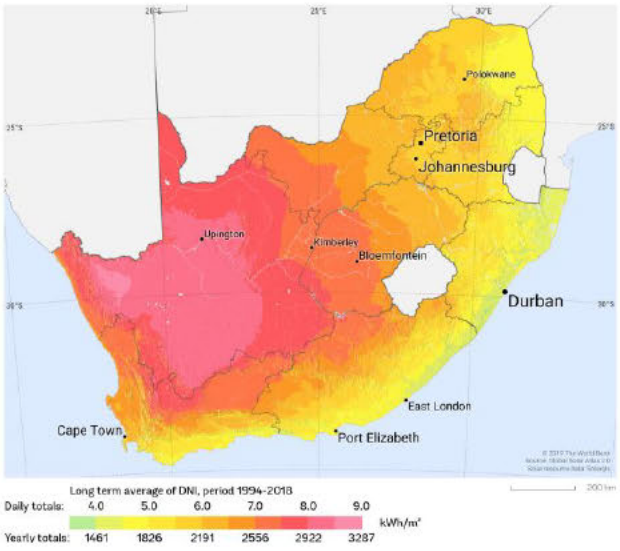

Figure 2-8: DNI map of South Africa (Jarvis, 2019).

2.2.2.3. Diffuse Horizontal Irradiation

The DHI is the irradiance a horizontal surface receives which is scattered or diffused by the atmosphere. The main cause of DHI is due to cloud cover or rain (Mohamed Khalifa Boutahir, 2022).

2.2.2.4. Latitude Tilt Irradiation

LTI denotes the largest quantity of radiation that a surface can absorb at its optimum tilt and position. The LTI angle changes with the earth's latitude (Mohamed Khalifa Boutahir, 2022).

2.2.3. Solar Energy Conversion Routes

Solar energy has been utilized in many ways all over the world showing the different methods of utilizing solar energy (Gcep, 2006). Figure 2-9 shows the reuse routes of solar energy.

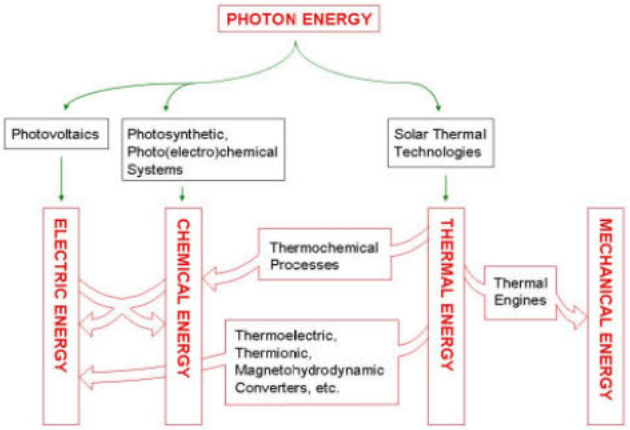

Figure 2-9: Solar Energy conversion routes (Gcep, 2006).

2.2.3.1. Photovoltaic systems

Photovoltaic (PV) systems utilize PV panels that generate electricity from solar energy. When the sun shines on a solar panel, the PV cells on the panel absorb the energy from the sun's beams. This energy produces moving electrical charges in response to an internal electric field within the cell, which produces electricity (Energy Efficiency & Renewable Energy, 2023). A basic residential photovoltaic system can include solar panels, inverters, cables, deep cycle batteries and other electrical and mechanical hardware. PV systems can be used together with the utility grid or can operate independently as an off-grid PV system. Figure 2-10 shows an example of a residential PV system and the utility grid.

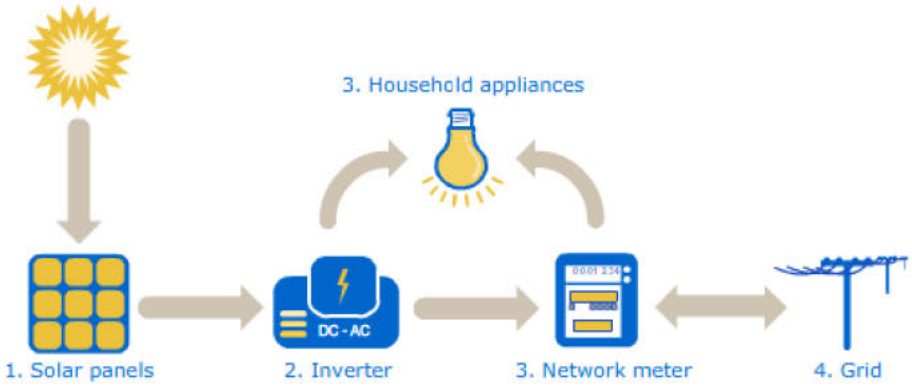

Figure 2-10: Residential PV system and utility grid (Smith, 1995)

2.2.3.2. Photosynthetic and photoelectrochemical systems

Chemistry is used in the design of materials and systems for solar energy conversion into electricity and fuel in photosynthetic and photoelectrochemical systems. Both photosynthetic and photoelectrochemical solar cells have significantly improved hydrogen production. The most well-known wet chemical process for turning solar energy into electrical energy or chemical fuels uses semiconductors or liquid junctions (Caramori, 2016). Figure 2-11 shows a labelled illustration of these systems to produce hydrogen.

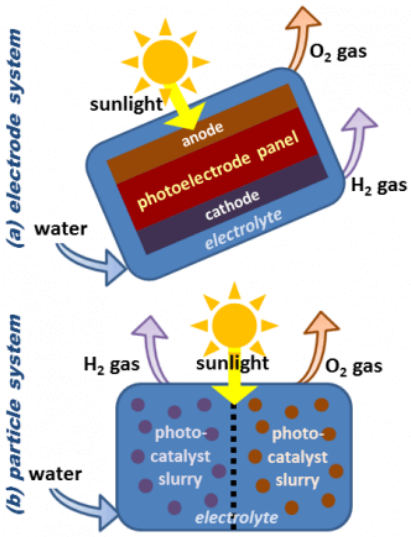

Figure 2-11: Sunlight used to produce hydrogen using a particle and electrode solution.

2.2.3.3. Solar thermal systems

Through solar thermal technologies, solar energy can meet heating needs. For many years, solar thermal technology has been available on the market. Solar thermal technologies such as solar thermal collector systems convert solar radiation into useful heat. Other solar thermal devices include solar geysers, solar dryers, and solar ovens (Bradford F Mills, 2008). Figure 2-12 shows the ethylene propylene diene monomer collector, flat plate collector, evacuated tubes and parabolic through solar thermal technologies used presently. Concentrating solar thermal power systems are also used to produce energy. Sunlight can be reflected onto a receiver by using mirrors and other reflective surfaces. The fluid inside the receiver can heat up to extremely high temperatures, and this thermal energy can drive an engine or spin a turbine to produce electricity (Energy Efficiency & Renewable Energy, 2023).

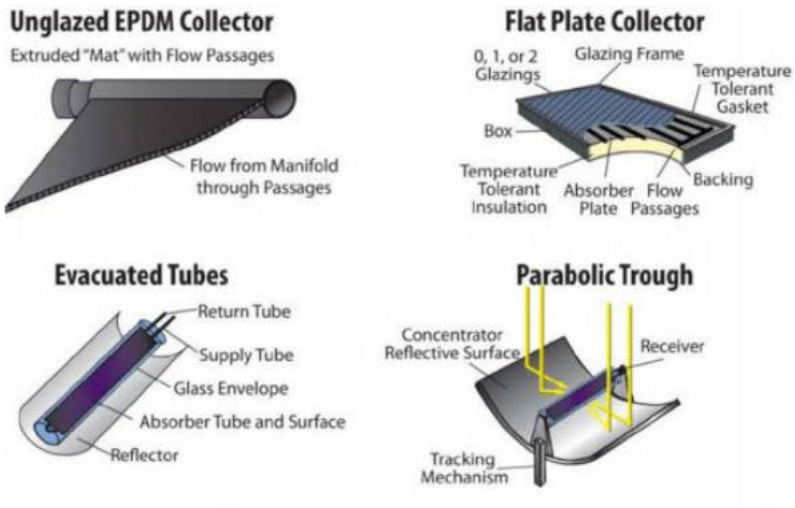

Figure 2-12: Examples of some of the solar thermal technologies.

2.3. Thermal Drying

Biomass and waste are frequently processed into fuels using thermal drying. The bulk reduction and eradication of pathogens from faecal sludge involve several steps, one of which is drying. Their energy characteristics are improved by reducing the moisture content. Thermal drying utilizes heat to dry a product or sample. Faecal waste can be successfully thermally dried to create a dry, pasteurized bio-solid that can be used for biofuel or agricultural products. By removing water, drying concentrates the sludge's energy and raises its calorific value (Samuel Getahun, 2020). There are various drying technologies available commercially today for the drying of sewage sludge. These technologies can be modified to dry faecal sludge.

2.3.1. Drying Principle

One of the oldest, most frequent, and most varied chemical engineering procedures is drying. Using heat, a liquid is evaporated from a solid, semi-solid, or liquid during the drying process. Essential characteristics of the drying process include phase shift and the creation of a solid product (Devahastin, 2013). Faecal sludge holds a lot of water. The air is used to remove the water vapour. A solid may include water in several forms, such as unbound or bonded moisture form, which directly affects the drying process. Drying is caused by the difference in thermodynamic activity between water vapour in the air and moisture in a wet product.

Since the water activities of the moisture in the product being dried and the vapour in the air are identical at thermodynamic equilibrium, further drying of the product is difficult. The moisture content of a solid, when it is in thermal equilibrium with the humidity of the air around the solid is known as equilibrium moisture content (EMC). Evaporation of liquid water into vapour requires a large amount of energy (2,258 kJ/kg at 101.3 kPa). Moisture content can be expressed on both wet (x_w) and dry (x_d) basis. The

weight of moisture per unit of wet material is known as moisture content on a wet basis (Visavale, 2012).

$$x_w = \frac{m_w}{m_w + m_d}$$

Where:

m_w = Mass of moisture in sludge (kg).

m_d = Mass of solids in sludge (kg).

The ratio of water content to the weight of dry material is used to express the moisture content on a dry basis (x_d):

$$x_d = \frac{m_w}{m_d}$$

While agricultural goods are expressed on a wet basis, the most practical way to express moisture for mathematical calculations is on a dry basis (Visavale, 2012). Figure 2-13 shows the relationship between dry and wet basis.

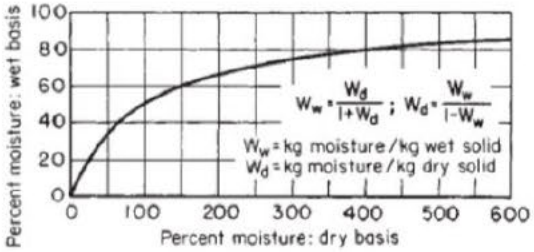

Figure 2-13: Relationship between dry-weight and wet-weight basis (Perry, 2007).

Convection (convective or direct dryers), conduction (contact or indirect dryers), or radiation (solar, infrared, microwave, dielectric) can all be used to generate heat for drying. The drying medium in the vast majority of industrial dryers is hot air or gases from direct combustion. Before being carried away by the carrier gas, the liquid must leave the top surface of the substance. The following mass transfer methods may be used to transport moisture from within a solid (Devahastin, 2013):

- **Liquid diffusion**: Occurs when the wet solid is at a temperature lower than the liquid's boiling point.
- **Vapour diffusion**: Occurs when liquid is vaporized within the material.
- **Hydrostatic pressure differences**: This happens when the rate of internal vaporization is higher than the rate of vapour transport from the solid to the surroundings.
- **Capillary flow**: Capillary suction, which is brought on by a gradient in capillary pressure ranging from large to small capillaries, is responsible for this phenomenon.

2.3.2. Drying Kinetics

The rate of moisture loss as a function of time is known as drying kinetics. An understanding of drying kinetics aids in the selection of appropriate drying methods and process management. When designing

and using technologies, it is crucial to comprehend the impact drying kinetics has on drying. Drying kinetics is studied with the use of drying curves. The drying curve charts the progression of a product's moisture content loss. The constant rate phase, the first falling rate period, and the second falling rate period are the three stages that typically make up a drying curve (Wei Ling, 2022).

When the product reaches wet bulb temperature and the drying rate reaches a specific level, the constant rate stage starts. The hot air evaporates the liquid on the surface of the wet product during the constant rate period, which causes the surface temperature and rate of product evaporation to remain constant. The heat is mostly utilized to evaporate the water on the outer surface of faecal sludge, which often has a body of loose water. Loose or unbound water is usually removed during this stage. Most of the loose water is occasionally already removed during the drying of faecal sludge, hence a constant rate period may not always be observed (Wei Ling, 2022).

The loose water starts to evaporate during the first falling rate period, and water from the sludge body starts to diffuse to the surface (Erbay Z., 2010). The sludge becomes less saturated in a liquid because the rate of evaporation is higher than the rate at which water diffuses to the surface. The surface of the sludge eventually dries out and is no longer wet. Since there isn't much water on the sludge's surface to be evaporated, the temperature of the sludge begins to rise above the wet-bulb temperature. At this point, the available heat is used to partially evaporate the water and heat the sludge. Once this starts to occur drying transitions into the second falling rate period (Wei Ling, 2022).

The temperature inside the drying product declines and approaches the dry-bulb temperature during the second falling rate. The product's surface has dried entirely at this point. At this point, the product has a high temperature and a low moisture content. It is more difficult to transfer heat to products of higher temperatures (Deng W., 2011). With regards to sludge, the further removal of moisture in this stage can result in the sludge structure becoming brittle and cause it to crumble or break down. Once the moisture content of sludge cannot be reduced further it can be assumed the EMC has been reached (Erbay Z., 2010).

The faecal sludge surface experiences mass heat transfers when subjected to convective heat transfer. The moisture in faecal sludge changes phases from liquid to gas when subjected to hot air and radiation. Factors that influence the drying kinetics are as follows:

- **Temperature:** Heat raises the temperature of sludge and causes moisture on sludge surfaces to evaporate (Ali I., 2016). For faecal sludge with the same moisture content, the rising air temperature decreases drying time and increases the drying rate (Bennamoun L., 2014)
- **Relative humidity**: Relative humidity is a measure of how well the air can absorb moisture. The moisture gradient that exists before the air humidity and sludge humidity can reach

equilibrium is one of the driving forces for moisture transport from inside the sludge to the outside air

- **Particle size**: At the same temperature a larger surface or mass of sludge will take longer to dry. Larger surfaces will have a higher resistance to mass heat transfer and therefore lead to longer drying times (Zhao G., 2020)
- **The velocity of air**: Increased air velocity will result in a larger quantity of air coming in contact with the faecal sludge, therefore, increasing the potential of moisture removal by the air. The higher air velocity accelerates the water vapour diffusion rate while maintaining the pressure difference between the air surrounding the sludge surface and the water vapour there (Zheng Q., 2021)

2.3.3. Psychrometry in Drying

Psychrometry is important in the drying process as it refers to the properties of an air-vapour mixture that controls the rate of drying and the thermodynamic equilibrium. As the EMC and drying kinetics depend on the temperature and relative humidity of the air, it is then necessary to know the thermodynamic properties of air. Psychrometric charts are important tools for showing the thermodynamic properties of an air-vapour mixture at constant pressure (Hyndman, 2020). A psychrometric chart can be found in Appendix A. The typical properties of a psychrometric chart are (Hsuan-Yu Chen, 2022):

- **Dry-bulb temperature:** The thermometer's reading of the air's temperature.
- **Wet-bulb temperature:** The temperature of a surface saturated in condensed vapour water in balance with the surrounding air is the wet-bulb temperature.
- **Relative** humidity**:** Ratio between the saturated vapour pressure at the same temperature and the actual vapour pressure. The percentage of relative humidity is used to express it.
- Dew point **temperature:** Water vapour condenses at this temperature.
- Humidity **ratio:** Air moisture content represented as the weight of water vapour per unit weight of dry air on a dry basis.
- **Enthalpy:** Energy content of the air (kJ/kg).

2.3.4. Thermal Dryers

Thermal dryers are commonly used to dry sludge (GROSS, 2007). There are various thermal drying technologies available commercially. There are very few thermal drying technologies applied to faecal sludge. Thermal drying of faecal sludge is effective in reducing or deactivating pathogens and bacteria. The common thermal dryers available today used to dry sewage sludge include drum dryers, belt dryers and bed dryers. These technologies could be potentially used to dry faecal sludge. Table 2-1 lists some

of the thermal drying technology used to dry sludge. More details about these dryers can be found in Appendix B.

Table 2-1: Drying thermal technologies for sewage sludge application.

Thermal drying type	**Dryer type**	**Energy transfer medium**	**Operating Temp.**
Convective Drying *(Roediger, 2011)*	Belt dryers	Air	80–140 °C
	Fluidized Bed dryers	Thermal oil/Steam	50–600 °C
	Drum dryer	Fuel/Natural gas/Air	+400 °C
Conductive Drying *(Dexiao Ma, 2021) (KWS Conveying Solutions, 2023)*	Hot wall sludge dryers	Thermal conductivity/Air	60–180 °C
	Thermal screw conveyor	Thermal conductivity/Air	120–300 °C
Radiation Drying *(Eva Kocbek, 2020)*	Microwave drying	Microwave radiation	+100 °C
Solar thermal Drying *(Alice Sorrenti, 2022)*	Greenhouse dryer	Solar energy/Air	35–60 °C
	Cabinet dryers	Solar energy/Air	35–60 °C
	Bed dryer	Solar energy/Air	±25 °C
	Transparent wall screw conveyor	Solar energy/Air/ Thermal conductivity	35–60 °C

2.4. Solar Thermal Drying

Solar thermal drying uses solar radiation's thermal energy to dry a product. Solar thermal energy can be a useful energy source for drying faecal sludge. Devices known as solar dryers use solar energy to dry materials, commonly used in the food industry. Solar thermal drying is conducted using solar thermal systems that harness solar energy.

2.4.1. Solar Thermal Dryers

There are two types of sun drying systems: passive solar energy drying systems and active solar energy drying systems. These systems are classified according to how solar energy is utilized and their heating modes (Visavale, 2012). There are also direct and indirect dryer types. Figure 2-14 shows the classification of solar thermal dryers.

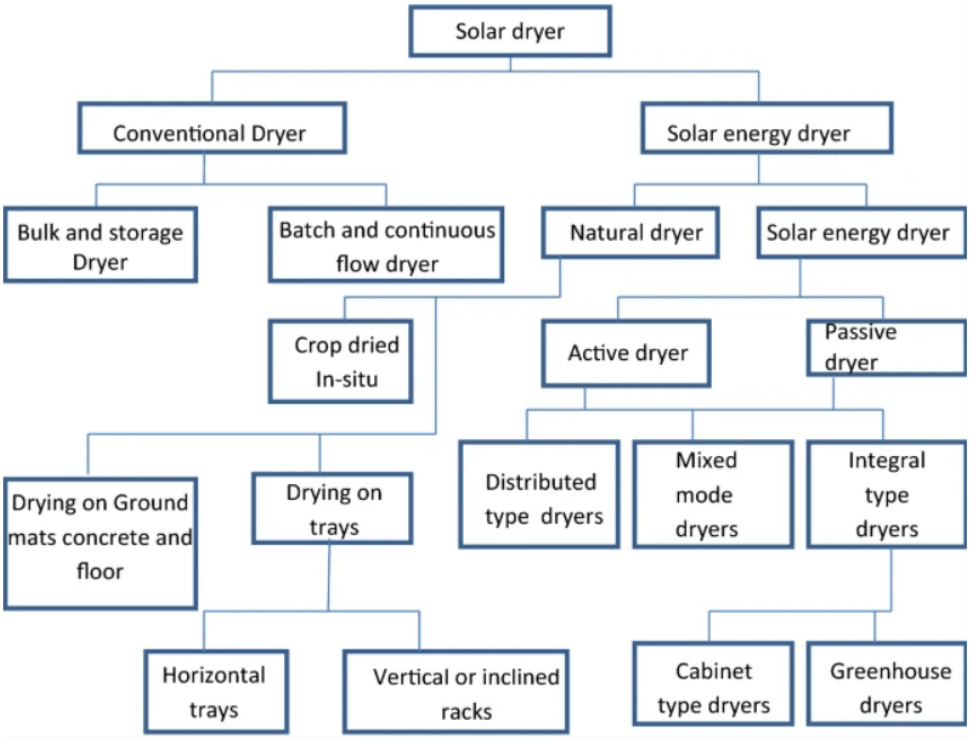

Figure 2-14: Classification of the solar thermal dryers (Ekechukwu, 1999).

The study focuses on both active and passive solar drying devices. Passive solar drying systems utilize airflow by natural convection for drying whereas active systems induce air forcefully into the systems with the use of electric fans. These two systems are subdivided into three categories. These modes are classified as direct, disseminated, or mixed. Direct-type solar dryers allow sunshine to enter the drying chamber directly and dry the goods. Indirect dryers use collectors to absorb or use sunlight to heat air, which is then routed through the drying chamber to dry a product. Mix mode dryers are a combination of direct and indirect dryers. The sub-classes of solar dryer design are shown in Figure 2-15.

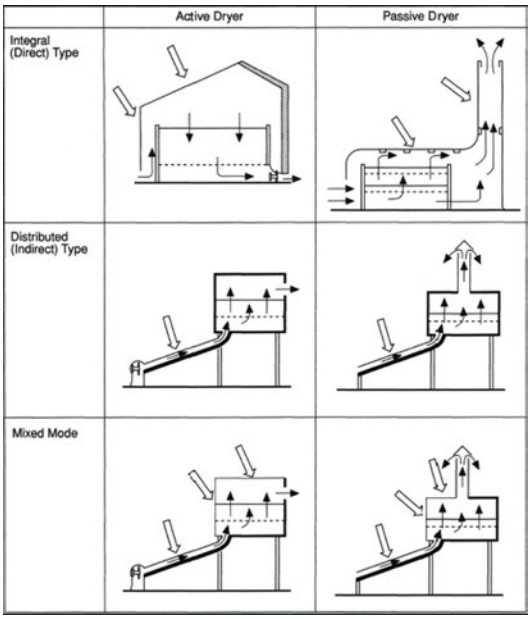

Figure 2-15: Examples of active and passive solar dryer designs (Ekechukwu, 1999).

Table 2-2 shows the types of solar dryer technology that can be used to dry faecal sludge. Further illustrations and information regarding solar thermal dryers are shown in Appendix B.

Table 2-2: Solar thermal drying technologies.

Dryer type	**Description**
Passive direct solar dryer	These solar dryers expose the product, which is mainly crops, to direct sunshine. This enhances the colour ripening desired in fruits, coffee and the development of roasted beans. Passive direct dryers utilize chimneys at the top of the dryers for air to moist air to escape or be expelled from within the dryer (Visavale, 2012).
Active direct solar dryers	The key difference between these and passive direct solar dryers is that the ventilation system is driven by electricity. There are three types of active direct sun dryers: absorption, storage, and greenhouse dryers.
Passive indirect solar dryers	These are indirect sun dryers that use natural air convection to dry. More than one drying attempt can be employed to increase the volume of drying. Trays can be stacked on vertical racks with enough room between them. In general, passive indirect solar dryer designs include an air-heating solar energy collector, insulated ducting, a drying chamber, and a chimney (Visavale, 2012)
Active Indirect solar dryers	These dryers include a collection, drying chamber, ducting, and an air circulation fan. Because of the independent air heating unit, these systems may achieve high temperatures with flow rate control. Certain designs use recirculation of drying air to optimize energy efficiency, ensuring low exhaust temperatures of air (Ekechukwu, 1999).
Hybrid solar dryers	These dryers combine the features of both direct and indirect type solar energy dryers. Here the necessary heat required for the drying process was produced by the combined action of the air heated in the collector and the incident direct solar radiation on the product to be dried (Visavale, 2012).

2.4.2. Solar Thermal Drying of Waste Sludge

Waste sludge treatment systems using solar thermal drying have been developed. There are various types of solar thermal technology available for the treatment of sludge. Large amounts of sludge are generated during the treatment of wastewater, and this sludge needs to be disposed of to protect the environment. In many places around the world, solar drying has been chosen as an alternative to treating sewage sludge for its safe disposal. Open-air drying such as beds was commonly used to dry faecal sludge but closed systems such as cabinet and greenhouse dryers dry sludge faster and are more effective. The use of solar drying to address the treatment of sewage sludge is gaining interest in numerous countries. Greenhouse solar dryers are frequently employed in the sludge treatment process.

The majority of the sewage sludge used for fuel came from activated sludge systems, and it may have undergone several procedures whereby microorganisms decompose waste sludge in the absence of oxygen. In both situations, stabilization takes place, greatly lowering the sludge's calorific value (Tchobanoglous, 2003). Research shows after primary settling the calorific value of sewage sludge will average around 25 MJ/kg of dry solids but this value was halved after anaerobic digestion (Fytili, 2008). Very little technology has been developed and implemented for the drying and treatment of faecal sludge but quite a few solar technologies have been implemented for the drying of sewage sludge. The technology implemented and their performance parameters for the solar thermal drying of sewage sludge are shown in Table 2-3.

Table 2-3: Solar thermal drying technology for sewage sludge.

Dryer type	**Drying rate**	**Specific Energy Consumption**	**Moisture Content reduction**	**Average temperature**	**Effective area**
Modified Solar Greenhouse (Alice Sorrenti, 2022)	0.30	450	±80	±40	0.6200
Solar Absorber Drying Chamber (Ataollah Khanlari, 2020)	0.80	5400	-	40–80	0.0324
Cabinet Dryer (Panli Wang, 2019)	0.21	106.75	±74	±45	0.0320

2.4.3. Greenhouse Solar Dryers

Solar thermal energy is used by greenhouse solar dryers to dry products. Many applications of greenhouse type dryers have been applied to the drying of sewage sludge. Direct greenhouse solar dryers generally utilize transparent walls to allow solar radiation to pass into an enclosure to heat and dry sewage sludge. The dried sludge was put in a thick layer above the ground in the greenhouse and periodically mixed using either mechanical or manual means to homogenize the distribution and avoid crust development (Alice Sorrenti, 2022).

Due to the sludge's absorption of some of the solar energy that enters the greenhouse through its glass walls, heat is produced inside the greenhouse, which causes moisture to evaporate. Be mindful that a very small amount of the radiation was lost due to the clear wall's reflectance, absorption, and sludge reflectance. The greenhouses typically have a ventilation system to remove the evaporated moisture and mixing fans to increase turbulence, which speeds up the mass transfer and increases drying rates.

Circulation fans are also a useful tool in distributing air throughout the dryer. Some of the solar drying technology used in the treatment of sewage sludge is listed in Table 2-4.

Table 2-4: Solar drying technology for the treatment of sewage sludge.

Location	**Drying rate**	**Specific Energy Consumption**	**MC reduction**	**Average temperature**	**Effective area**
Palermo, Italy (Alice Sorrenti, 2022)	0.012–0.3	450	92	40	0.62
Kavala, Greece (V. L. Mathioudakis, 2013)	0.3–0.5	52–83	±80	-	66
Stuttgart, Germany (Bux M., 2002)	0.008–0.28	70–110	90	30	700
Fethiye, Turkey (Mayis Kurt, 2014)	0.007–0.01	-	±85	-	2000
De Mallorca, Spain (I., 2011)	0.2	±60	40–50	-	20000

2.5. Summary of Literature

Faecal sludge was researched extensively to determine its proeprties and charecteristics. Faecal sludge is a hazardous waste product and therefore makes it difficult to handle. Faecal waste is sometimes difficult to obtain from onsite collection facilities. This makes it difficult to apply safe and effective faecal sludge management to dealing with raw sludge. Understanding the drying properties of faecal sludge is important to consider in the design of a dryer to ensure an efficient treatment process can be developed. Thermal drying is one of the best ways to treat and process faecal sludge to yield a cleaner and useable final product. Faecal sludge management schemes incur high transportation costs. A good way of minimizing costs will be to develop drying technology close to sludge collection facilities to lower transportation costs.

Thermal drying was found to be an effective tool utilized in the treatment of sewage sludge. Many different thermal dryers can be used for the treatment of faecal sludge. Given their nature-related similarities, sewage sludge and faecal sludge could be potentially treated using the same technology. Sludge from sewage treatment plants has been dried using thermal dryers, which then yield useful bioproducts. Commercial dryers used for sewage sludge treatment incur high manufacturing and operating costs. Large amounts of power and resources are required to operate these technologies therefore it is important to develop more affordable drying technologies adapted to the treatment of faecal sludge. South Africa receives an abundance of solar thermal energy. Solar energy can be a useful energy source to help aid the drying of faecal sludge because thermal dryers for the treatment of sewage sludge have significant operating expenses and energy demands.

Greenhouse dryers utilize solar energy to dry a product with the aid of solar energy. A greenhouse dryer is an effective tool for utilizing solar energy to dry faecal sludge. The design of a transparent enclosure can assist in allowing certain wavelengths of light from the solar spectrum to pass into the enclosure. A greenhouse solar dryer would be an effective tool to dry faecal sludge. Dryers for greenhouses come in a variety of designs, including active, passive, direct, indirect, and hybrid dryers. An active greenhouse dryer offers better versatility. The development of a faecal sludge greenhouse dryer can help bridge the gap between faecal sludge and sewage sludge treatment technologies. Sewage sludge treatment technologies can be used to treat faecal sludge.

Chapter 3: Material & Methods

The materials and methods focus on the process and activities that are undertaken to develop and test the greenhouse dryer. Descriptions and design specifications of the greenhouse solar dryer and the various sub-systems are discussed. Feedstock and the testing procedures are discussed and explained in the materials and methods.

3.1. Design Ideology

The design aims to develop a greenhouse dryer to maximise exposure to sunlight and hot air over faecal sludge and remove as much moisture from the faecal sludge and the drying chamber to effectively dry faecal waste. Transparent walls will allow light to pass into the enclosure and shield faecal sludge from the outside environment. The air entering and already inside the dryer will be heated with the help of an absorber wall. The greenhouse dryer combines various sub-systems to improve the drying process in different ways. The dryer was separated into three different sections. These 3 sections are the collector, top and lower drying chamber. Due to the simplicity of construction and the transparency of the walls, which will allow sunlight to enter the dryer, the dryer's effectiveness is not greatly impacted by the dryer's shape.

Dry air will enter the collector where it is preheated and thereafter moves into the top and bottom drying chambers. Air will flow over the drying table and faecal sludge in the top chamber and under the faecal sludge product through the drying tray on the lower chamber side. Moist air will be expelled from the drying chambers. The drying chambers should be positioned in the most effective position ensuring maximum exposure to sunlight. The collector side will receive minimum sunlight but the absorber wall will be heated from the drying chamber side increasing the temperature of the absorber wall surface on the collector side.

3.2. Description of the Greenhouse Solar Dryer

A greenhouse solar dryer has been developed to dry faecal sludge in this project. The chemical engineering building roof at Howard College, University of KwaZulu-Natal (Durban, South Africa), where the solar dryer was located (coordinates 29.8671° South and 30.9831° East). The dryer includes an enclosure, ventilation system, circulation fans, a sludge hanging bed (drying tray), a rake system, an absorber wall, and temperature and humidity sensors. The dryer was made up of 3 main sections, these sections are the collector, top drying chamber and lower drying chamber. Air enters through the back face of the dryer and passes over the absorber wall and into the top and lower drying chamber through the holes on the bottom of the absorber wall. A drying table separates the top and lower drying chambers.

The drying tray was situated on the top drying chamber which was exposed to sunlight. The absorber wall was heated from the drying chamber side of the dryer.

The enclosure was developed to house the drying product and allow sunlight to pass into the dryer to aid the drying process. Ventilation and circulation fans were installed to bring ambient air into the dryer, distribute air throughout the dryer and remove moisture from within the dryer. An absorber wall was implanted to raise the air temperature entering the dryer collector and the drying chamber. A rake system was implemented to mix the sludge. These subsystems are described in detail in section 3.2. The temperature and humidity control system recorded temperature and humidity at different points in the dryer and measured ambient temperature and humidity outside near the inlet of the dryer. The greenhouse solar dryer specifications are listed in

Table 3-1. Drawings of the various structural components needed are shown in Appendix H.

Table 3-1: Greenhouse dryer design specifications.

Component	**Specification**	**Explanation**
Enclosure	Transparent dryer walls and roof.	PMMA plastic allows sunlight to pass into the dryer.
	Metal frame.	Ensure transparent walls are mechanically stable.
	Ensure materials are corrosion-resistant.	Due to moisture material must be corrosion-resistant.
	Materials to have excellent UV stability.	To prevent the decomposition of transparent material due to daily radiation exposure.
	Dimensions are to be limited to $2 \times 2 \times 2$ m.	To allow enough space to enter the dryer for cleaning and allow a considerably high volume of FS to be dried.
Absorber wall	High thermal conductivity.	To allow fast and homogenous heating of the material.
	Black or dark surface (matt paint).	To increase solar radiation absorbance
	Ports for air to flow through.	To allow air to pass from the collector into the drying chamber.
Rake system	Automatic timed operation.	To allow regular operation
	Linear actuator equipped with a motor.	To move linearly the rake system across faecal sludge.
	Blades rotating.	To homogenise the sludge during drying and avoid crust formation.
Drying tray	Finely perforated steel mesh support.	To allow sludge to be dried from the bottom through the holes in the mesh.
	Corrosion-resistant material.	To avoid corrosion of the material exposed to wet surfaces of faecal sludge over long periods.

Component	**Specification**	**Explanation**
Ventilation system	Fans are positioned on the front and rear of the dryer.	To allow dry air to enter and expel moist air on the rear side of the dryer.
	Adjustable fan speed	To change the ventilation rate
	Ventilation capacity to dry sludge at 80% moisture content.	To install a ventilation system with a minimum volume flowrate capacity of 1,714 $m^3/h/kg$ of air (as calculated in Appendix E).
Circulation fans	Fans are positioned inside the sides of the dryer above the drying tray.	To increase the air velocity at the surface of the sludge bed (increasing the mass transfer coefficient).
	Adjustable fan speeds	To change the air circulation rate
Instrumentation	Temperature and humidity sensors were positioned in the dryer and connected to the temperature control system.	To determine temperature and humidity at determined points in the dryer.
	Data was stored on a microSD card and transferred to a computer.	To store and record data.

A *CMP3* flat class C pyranometer was used to determine solar irradiance. The pyranometer was connected to a separate control unit in a plastic box. The control unit was made up of an Arduino board, date and time sensor, microSD adapter and dc power supply. The control unit reads and stores the date, time and irradiance. Figure 3-1 shows the completed prototype.

Figure 3-1: Greenhouse Solar Thermal Dryer –front/side of the greenhouse (left) and back/side of the greenhouse (right).

3.2.1. Enclosure

Two rectangular bases were constructed by welding 1.5 × 2 m lengths of aluminium angle. Four vertical braces were developed to connect the top and bottom bases at each corner. The aluminium angle was TIG welded using tungsten welding rods. Thereafter the weld was ground to form a smooth finish. The vertical braces and base frame together with PMMA were assembled using M12 × 20 self-tapping galvanized set screws. A door was developed using an aluminium frame, PMMA sheet and hinges. The door allows easy access to the inside of the enclosure. The door frame was constructed using 25 mm square tubing. The PMMA door was fastened onto the frame using M12 self-tapping screws. The frame was important to reinforce PMMA as the plastic was very flexible. Hinges were fastened onto the door and enclosure frame. A lock was installed to pull the door tight against the aluminium angle. Figure 3-2 shows the enclosure after its construction and before placing the other parts.

Figure 3-2: Enclosure after its construction.

3.2.2. Absorber Wall

Aluminium sheet metal 3 mm thick was used as an absorber wall inside the greenhouse. The sheet was painted black to retain heat within the dryer. 10 mm holes were drilled on the bottom of the absorber wall to allow airflow into the dryer to pass into the drying chamber where faecal sludge was to be dried. 25 × 10 mm holes were drilled from the bottom of the absorber wall to a height of 600 mm. The absorber wall was mounted nearest to the back of the dryer using self-tapping set screws. Dry air will flow over the absorber wall, which will thereby heat the air stream through convection. Air was then forced through the 10 mm holes into the drying chamber. The thermal conductivity of aluminium is shown in Appendix F in comparison to other materials. Figure 3-3 shows the black absorber wall developed.

Figure 3-3: Absorber wall.

3.2.3. Ventilation and Circulation Systems

For 10 kg sludge at 80 % moisture content a flow rate of approximately 1,714 m³/h was calculated as shown in calculations in Appendix F. Four RS PRO AC 220V axial fans with an effective diameter of 204 mm and a flow rate of 1,002.4 m³/h were used within the greenhouse dryer: two fans were mounted near the top back wall of the dryer to bring air into the dryer; two fans were placed on the lower front wall above the drying tray as the air outlet. The positioning of the fans was determined using airflow and thermal simulations. The different airflow and thermal simulation results for the various ventilation and circulation positions are shown in Appendix D.

The maximum flow rate of air entering the system was slightly more than 2,000 m³/h which was higher than the minimum flow rate requirement calculated at 1,714 m³/h. Less powerful *Mantech* 220 V fans with an effective diameter of 190 mm and a maximum flow rate of 750 m³/h each were placed on the bottom of the dryer on the front wall below the drying tray. The fan configuration was positioned to create airflow at the top and bottom sections of the sludge bed.

Two *Ebm-Papst* axial S series, 230 V axial circulation fans were mounted across each other on the side walls of the drying chamber above the drying tray. These fans have an effective diameter of 300 mm and are capable of inducing a 2,034 m³/h volumetric air flow rate. Circulation fans and ventilation fans were connected separately to two *Ebm-Papst*, 230V, AC fan speed controllers. Figure 3-4 shows an illustration of the parallel connections for the ventilation system.

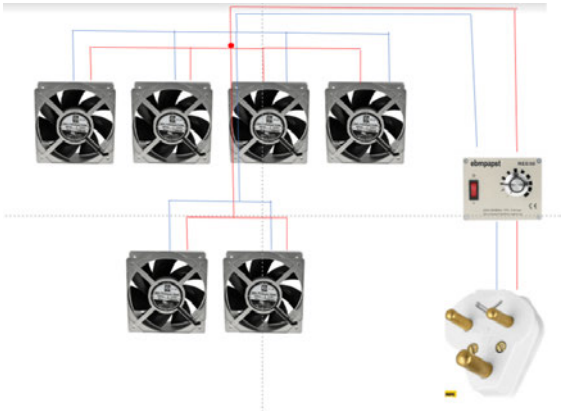

Figure 3-4: Fan electrical connections.

3.2.4. Rake System

The rake system was made up of 5 major components. These components are the blade system, linear actuator, guide rail, blade motor and rake control system. The blade system was used to mix and move the sludge to avoid crust formation. Pillow block 20 mm inside diameter bearings were connected to both ends of the blade shaft and onto the guide rail and linear actuator. The linear actuator and guide rail were connected with a bracket to brace and join the two components together. The linear actuator moved the blade across the drying tray. A mounting and NEMA 34 stepper motor (8-volt high torque stepper motor capable of operating at 12 N·m of torque) was connected on the linear actuator side of the blade shaft. The motor will rotate the blade that was supported by two bearings on either side and mix the sludge product. The blade moves across the drying tray and rotates as it moves.

The operation of the rake was controlled by the rake control system. The rake control system was made up of two motor drivers, two power supplies and an Arduino board. These components were configured to enable the rake to move across the drying tray and change directions along the drying tray after the motor performed a specified number of steps. The rake system had to be positioned at a starting position and thereafter the rake will move automatically across the drying tray in both directions.

The rake system was mounted onto a frame and thereafter mounted to the drying table (i.e., sludge bed support) with two hinges on one side of the table and frame. This frame allows for the rake system to pick up on one side to allow the drying tray to slide in with no obstructions or collisions with the blade. The electronics were mounted in a box outside the dryer. The drying tray was constructed using aluminium angle iron and perforated fine steel mesh with a hole diameter of 1 mm. The tray mesh and frame were riveted together. The rake system and drying tray are shown in Figure 3-5.

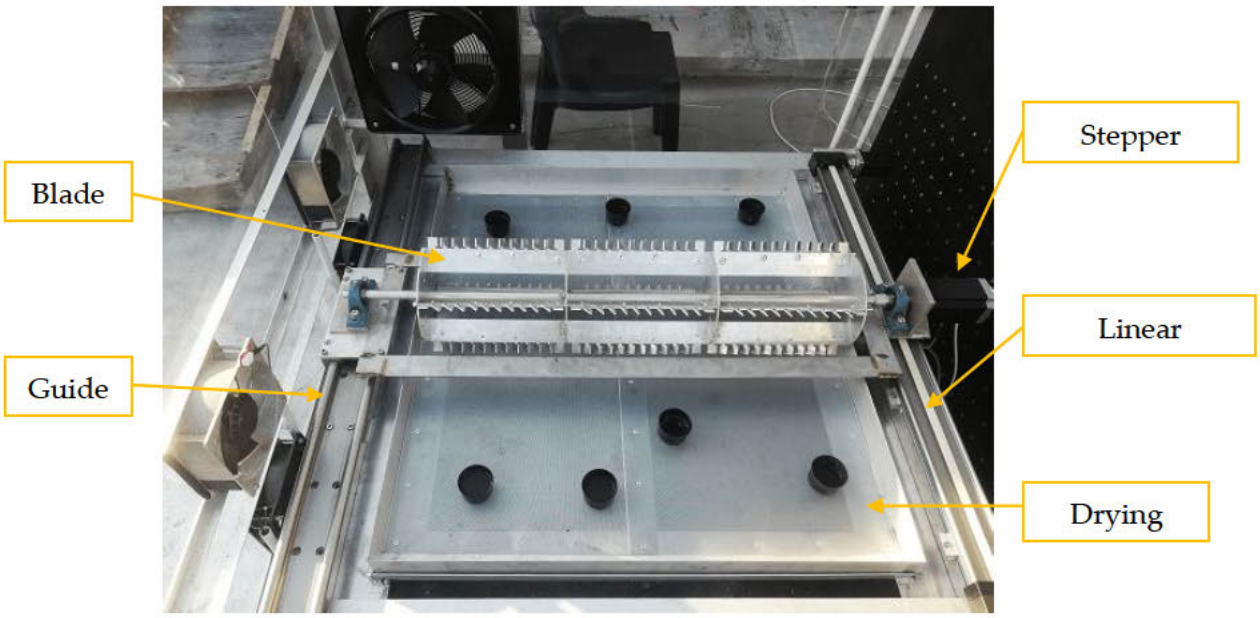

Figure 3-5: Rake system and drying table.

3.2.5. Instrumentation and Control Systems

Temperature and humidity sensors were used to measure temperature and humidity at different points in the dryer. A sensor was positioned on the absorber wall in the air inlet side (referred to as T/H 1). Four sensors were positioned inside the drying chamber (DC): near the roof (T/H 2), near the air entry to the DC from the solar collector (T/H 3), near the floor underneath the drying tray (T/H 4) and the ventilation fans at the air outlet (T/H 5). A sensor was positioned outside the dryer next to the inlet fans to determine the temperature and humidity entering the greenhouse dryer, at the ambient conditions (T/H 6). The positions of the sensors are shown in Figure 3-6.

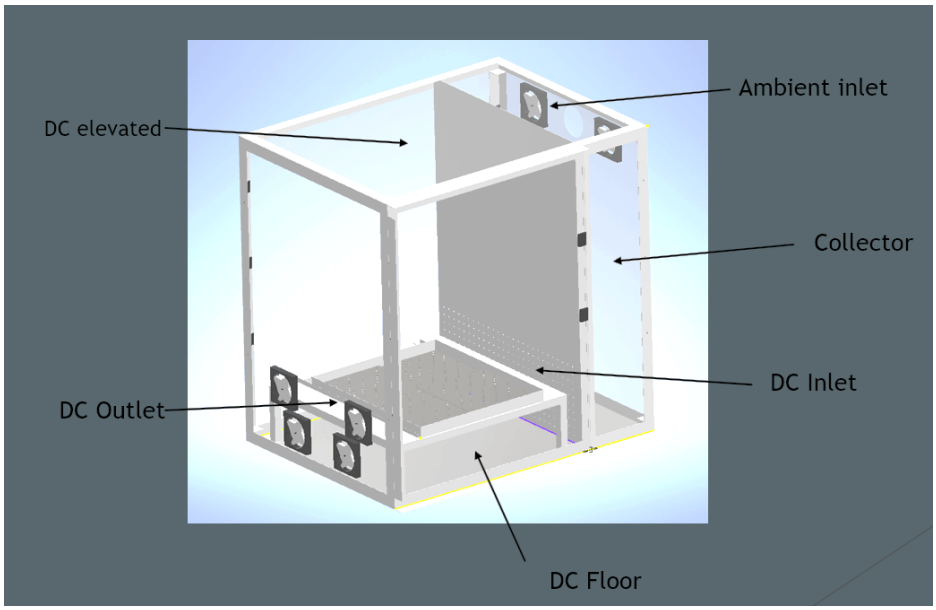

Figure 3-6: Position of the temperature and humidity sensors.

Two electrical boxes housed the electronics for the fans, temperature sensors, motor drivers and power supplies. The ventilation and circulation fan potentiometers were housed in a separate box from the motor drivers and temperature and humidity control system. The potentiometers have 10-speed settings and were used to control the volumetric flow rate of the fans. The material specifications of the dryer from start to finish are shown in Appendix F. The two electrical boxes are shown in Figure 3-7.

Figure 3-7: Electrical control boxes.

3.3. Testing of the Prototype

Testing was conducted to validate the prototype functionality, evaluate the drying performance, improve the operation, and identify opportunities for improvement. The greenhouse dryer utilized temperature and humidity sensors at different positions in the dryer to determine temperature and humidity fluctuations in and around the dryer during the tests. The temperature control system recorded the date, time, temperature and humidity every short interval (10 s) and saved this data as a text file on a memory card. An isolated control system fitted in a portable box was developed to measure and log irradiance readings on a memory card from the pyranometer measurements. The moisture content of the material to dry was measured during the testing in a *Radwag MA 50.R.WH* moisture analyser. The testing procedures and standard operating procedure (SOP) for the moisture analyser can be found in G-1.

The dryer was located on the Chemical Engineering building roof at Howard College campus, University of KwaZulu-Natal (Durban, South Africa), with the coordinates 29.8671° South and 30.9831° East. The back of the greenhouse, where the solar collector was placed, was orientated South and the drying chamber faced North to ensure the drying chamber received a maximum amount of solar radiation per day without the solar collector creating shade. Most of the experiments were conducted in the winter period from August to October between 9 AM and 3 PM during the day. The average ambient temperatures observed were between 25 and 30 °C. The relative humidity observed was between 40 to 60 % on average. Average irradiances recorded were between 500 to 600 W/m² outside the dryer. After 9 AM and before 3 PM the sun irradiance was relatively constant, therefore most of the testing was conducted within this time interval. Data shows temperatures reach the highest in the greenhouse towards the afternoon. Testing was stopped if the wind picked up or in the case of too much cloud coverage, as the tests should be done in consistent weather conditions (sunny conditions without or with low cloud coverage).

3.3.1. Functionality Tests

The functionality tests were conducted to characterize the individual sub-system components' performance (the enclosure, absorber wall, rake system mixing effect, and ventilation and circulation fan speeds).

3.3.1.1. Enclosure temperature tests

A thermocouple was used to determine the temperatures inside the dryer enclosure and the ambient air temperature outside the enclosure (before placing the instrumentation and rake system). The test was conducted on the date of 13-10-2021. The temperature and humidity measurements recorded outside the dryer, inside the dryer with fans off, set to full and set to half capacity are shown in G-2.

3.3.1.2. Ventilation and circulation tests

Tests on the ventilation and circulation fans were conducted for their calibration. During the calibration tests, the airflow velocity induced by each fan was measured using a hot wire anemometer to determine the volumetric flow rate at different fan speed control settings (10-speed settings). The volumetric flow rates were deduced from the product of the airflow speed and the cross-section surface area of the fan The different fan speeds consume different amounts of power.

The power consumption of the fans was determined using a commercial digital watt meter. The power consumption and the fan speeds for the various speed combinations can be found in G-2. Higher fan speeds use more power than slower fan speeds. The ventilation and circulation potentiometer speed settings and volumetric flow rate of air calculated are shown in Table 3-2.

Table 3-2: Ventilation and Circulation flow rates.

Circulation fans (diameter = 300 mm)			
Setting	Speed (m/s)	flow rate (m^3/s)	flow rate (m^3/h)
C0	0	0	0
C3	2.6	0.18	661.28
C6	5	0.35	1271.70
C10	8	0.56	2034.72
Ventilation fans (diameter = 204 mm)			
Setting	Speed (m/s)	flow rate (m^3/s)	flow rate (m^3/h)
V0	0	0	0
V1	2.5	0.08	294.01
V4	3.6	0.11	423.38
V7	6.24	0.20	733.86
V10	8.6	0.28	1011.41
Ventilation fans (diameter = 195 mm)			
Setting	Speed (m/s)	flow rate (m^3/s)	flow rate (m^3/h)
V0	0	0	0
V1	0	0	0
V4	0	0	0
V7	1.0	0.03	100
V10	3.4	0.10	400

3.3.1.3. Absorber wall temperature fluctuation tests

Thermal imaging using a *FLIR One* infrared camera determined the temperature absorber wall reaches during the winter season. Pictures taken with this camera are shown in Appendix G.

3.3.1.4. Rake system and testing instrumentation

Functionality tests of the rake system were conducted to verify the correct operation of the device and to determine mixing effects. Dry sand was initially used to ensure motors were powerful enough to mix and move. Testing instrumentation functionality tests were conducted to ensure temperature sensors were calibrated and displayed correct temperature and humidity values. Results from the functionality of the rake system are discussed in Appendix G.

3.3.1.5. Greenhouse dryer integrated functionality tests

The subsystems were all installed in the greenhouse dryer and the dryer was tested as a whole. The rake system was tested to ensure all the components were working effectively together. Temperature and humidity sensors were calibrated to ensure correct values were recorded. The rake system worked efficiently during dry tests with no feedstock.

3.3.2. Feedstock Tests

The feedstock used in testing was water, wet soil and synthetic sludge.

3.3.2.1. Water evaporation tests

Water tests were conducted between the periods of 13th July 2022 to 5th August 2022. Water was used as feedstock to test the integrated greenhouse dryer prototype to determine the water evaporation rate and the temperature and humidity inside the enclosure. Ventilation and circulation rates were adjusted to determine the best speed setting for the optimal water evaporation rate. Temperature and humidity were measured at the different ventilation speeds to link these parameters to the evaporation performance of the greenhouse.

During the tests, water was placed in 7 round metal containers and placed at different points on the drying table to determine how much water evaporated. The mass of both the metal containers and water weighed initially 100 grams. Ventilation fans and circulation fan speeds were adjusted during testing. Circulation speeds were set at one speed for the day and ventilation speeds were adjusted every 30 minutes. The next day the circulation fan was changed and the same procedure was repeated. The mass of the crucibles and water were measured after each change of ventilation speed. To prevent thermal perturbations from the system after taking out the crucibles from the greenhouse for their weighing, only 2 containers' mass was measured at hourly intervals. Table 3-3 summarizes the basic information from the water evaporation tests.

Table 3-3: Water evaporation testing specifications.

Specifications	**Amount**	***Unit***
Diameter	55	*mm*
Height	40	*mm*
Ventilation flowrate	294 (V1) 423 (V4) 733 (V7) 1011 (V10)	*m³/h*
Circulation flowrate	0 (C0) 660 (C3) 1271 (C6) 2024 (C10)	*m³/h*
Initial mass of crucible and water	100	*g*
Drying time	4–5	*h*

The testing setup and crucibles are shown in Figure 3-8.

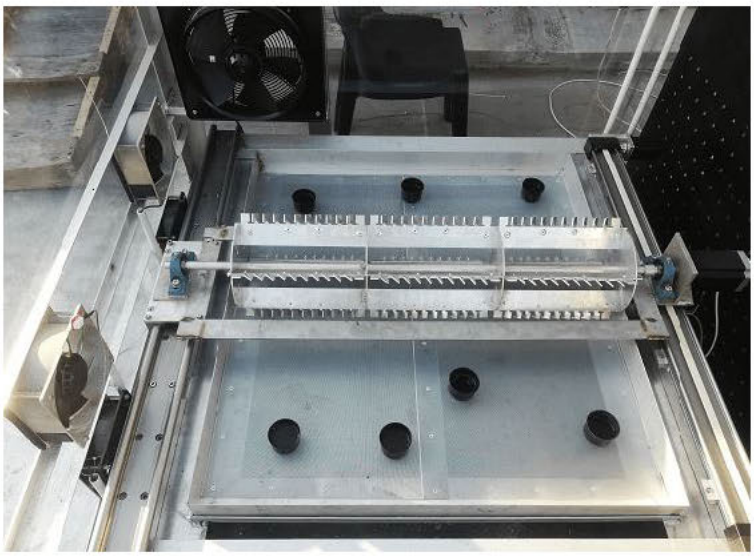

Figure 3-8: Water test drying setup.

3.3.2.2. Wet soil tests

Wet soil was used as a drying product to determine the rake system's effectiveness and the drying performance of the greenhouse dryer. A 1.4 kg sample of wet soil (75 % moisture content) was first used in soil testing to determine how well the drying tray handles high moisture content material. Tests were conducted with 1.4 kg wet soil with and without the rake system in operation.

Thereafter, a 15 kg mass of wet soil (70 % moisture content) was spread onto the drying tray and left to dry. This feedstock presented a watery consistency, leading to some amounts of water being drained into the tray below the drying tray when poured onto the drying tray. Results might display inaccurate data due to loose water being drained and not evaporated. Wet soil was spread onto the drying tray and left to dry between the times of 10:00 and 15:00 throughout the day. Figure 3-9 shows a picture of 15 kg of wet soil in the drying tray while the rake system was operating.

Figure 3-9: Wet soil test with 15 kg soil at 70 % moisture content.

The rake system was turned off for the first test and the rake system was used for the second test. Each test was conducted on separate days. For each test, a small amount of sample between 2–5 g was taken at every 1-hour interval from the lower surfaces of the sludge closer to the centre of the drying tray and placed in a moisture analyser to determine the moisture content. The circulation and ventilation rates were set to a constant value, corresponding to the optimal fan speed setting identified during the water tests. The lowest fan speeds resulted in the highest temperature and lowest humidity readings recorded in the dryer. Table 3-4 lists the basic information from the wet soil tests.

Table 3-4: Wet soil testing specifications.

Specifications	**Test 1**	**Test 2**	***Unit***
Area	0.05	0.5	m^2
Thickness	0.2		*mm*
Ventilation flowrate	294 (V1)		m^3/h
Circulation flowrate	508 (C1)		m^3/h
Initial mass of wet soil	1	15	*kg*
Initial moisture content of wet soil	75	70	*%*
Drying time	5		*h*

3.3.2.3. Synthetic sludge tests

Synthetic sludge was developed to test the performance of the dryer. Synthetic sludge was used because of the restrictions of faecal sludge use on the Chemical Engineering building's roof at the UZKN campus, due to the hazards associated with the handling of faecal sludge in a non-controlled environment. A recipe for the production of synthetic sludge from the WASH R&D Centre was followed and was used to make a sample to be tested in the greenhouse dryer. The ingredients and quantities for the synthesis of 10 kg of synthetic sludge are shown in Table 3-5. The dry ingredients were first all mixed and thereafter the miso paste was mixed into the dry ingredients and then polyethene and oil were poured into the mixture. Lastly, water was added and mixed thoroughly until all the ingredients were mixed nicely and formed a porridge-like composition. Thereafter the mixture was placed in a cold room for around 4 hours or overnight to set.

Table 3-5: Ingredient for 10 kg batch of synthetic sludge.

Ingredients	**Quantity (g)**
Water	6731.40
Psyllium husk	360.95
Peanut oil	574.55
Miso paste	360.95
Probiotics	1 capsule
Ground vegetables (dried mushrooms)	50.79
Cellulose paste	126.04
Polyethene glycol	360.95
Calcium phosphate	360.95

For these tests, a mass of around 10 kg of synthetic sludge at 80 % moisture content was dried within a period of a few days.

Table 3-6 summarizes the basic information for the synthetic sludge tests.

Table 3-6: Synthetic sludge testing specifications.

Specifications	**Amount**	***Unit***
Area	0.8–0.9	m^2
Thickness	10	*mm*
Initial mass of wet soil	10	*kg*
Initial moisture content of wet soil	80	*%*
Ventilation flowrate	294 (V1)	m^3/h
Circulation flowrate	506 (C1)	m^3/h
Drying time (1 day)	6	*h*

Specifications	**Amount**	*Unit*
Period	5	*days*

Figure 3-10 shows a picture of the initial sample of a 10 kg sample of synthetic sludge spread onto the drying tray.

Figure 3-10: Synthetic sludge spread on the drying tray inside the dryer.

3.4. Data Treatment and Analysis

3.4.1. Output Parameters

The measured parameters were as follows:

- Temperature (°C).
- Humidity (%).
- Solar irradiance (I).
- Power consumption (W).
- Mass of drying product (kg).
- Moisture content (%).
- Drying time (h).

These parameters can be used to determine the performance parameters of the system together with the effective area exposed to solar irradiance, the surface area of the drying product and the latent heat of vaporisation of water.

3.4.2. Performance Parameter Calculations

The measured parameters were recorded in tabular form and compared. The data acquired from these parameters were used to calculate the performance parameters of the dryer, such as drying rate, moisture removal, solar dryer efficiency and specific energy consumption, using the following formulas:

Equation 1: Moisture removal.

$$\Delta M = (MC_i \times M_i) - (MC_f \times M_f)\ [kg]$$

Where:

ΔM = Mass of moisture removed (kg).

MC_i = Initial moisture content (on wet basis).

MC_f = Final moisture content (on wet basis).

M_i = Initial mass of the sample.

M_f = Final mass of the sample.

Equation 2: Drying rate.

$$DR = \frac{\Delta M}{\Delta t \times A} \; [kg/h/m^2]$$

Where:

A = Effective surface area of the sample (m^2).

Δt = Drying time (h).

Equation 3: Dryer efficiency.

$$\eta = \frac{DR \times \Delta H}{I \times A}$$

Where:

I = Solar irradiance (W/m^2). Note: that the efficiency values were a rough approximation and may be underestimated because GHI was used to calculate the solar irradiance received by the absorber wall, whereas its position was vertical, so it may receive less irradiance than the one estimated by the calculation.

ΔH = Solar irradiance (W/m^2). Note: that the efficiency values were a rough approximation and may be underestimated because GHI was used to calculate the solar irradiance received by the absorber wall, whereas its position was vertical, so it may receive less irradiance than the one estimated by the calculation.

Equation 4: Specific energy consumption (SEC).

$$SEC = \frac{P}{DR} \; [kW{\cdot}h/t]$$

Where:

P = Power consumed in the drying system by the fans, rake system and instrumentation (kW).

3.4.3. Statistics/Uncertainties

Two runs were done at the same operating conditions for water and synthetic sludge tests to ensure data reproducibility, even though the replicates could not be reproduced in identical weather conditions due to the variable nature of the weather between different days. No duplicate soil tests were done during

testing due to time constraints. Temperatures, humidity and solar irradiances were averaged for the duplicate tests of water and standard deviations were calculated using Excel functions for the various recorded variables. Chapter 4 will discuss and analyse the results.

Chapter 4: Results & Discussion

Results obtained from functionality, water, wet soil and synthetic sludge tests are discussed and analysed. Functionality tests of the various subsystems and the greenhouse dryer were conducted to ensure all the individual sub-systems were operating effectively before it was integrated into the prototype. Thereafter the greenhouse dryer was tested with all the systems in place. Feedstock was tested after the conclusion of the functionality tests and all testing data was recorded and analysed in this section.

4.1. Functionality Tests

Functionality tests of the enclosure, ventilation, circulation, rake, drying table, temperature and humidity sensors were conducted individually. A few issues were experienced with the rake system whereby the motor for the blade on the rake was not powerful enough and would jam when force was exerted against the blade movement. Larger motors and drivers were procured and installed, and thereafter the rake system operation worked smoothly. All the sub-systems were integrated after issues with the rake system were resolved. The subsystems performed well during the functionality tests. Temperature and humidity sensors were calibrated and tested.

After the initial functionality tests, the temperature and humidity data were recorded at 5 different points in the dryer. The ambient inlet air enters the dryer and is heated in the collector. This heated air moves over the absorber walls and through the holes into the drying chamber. The heated air was then distributed throughout the dryer. Moist air was removed at the drying chamber outlet. The temperatures recorded in the dryer were relatively higher than the ambient temperature entering the dryer. Duplicate tests were conducted for varying ventilation and circulation speeds therefore the humidity and temperature measurements were averaged over the two days of respective fan speed testing.

Temperatures inside the dryer recorded were significantly higher than ambient temperatures outside. Temperatures recorded in the dryer were at least 4 °C more than the ambient temperatures recorded. All the humidity values recorded inside the dryer were significantly lower than the relative humidity outside the dryer. The humidity recorded in the dryer was more than 10 % less than the humidity recorded outside the dryer. Higher temperatures and lower humidity promote better drying conditions. Lower humidity will prevent moisture build-up within the walls of the dryer and higher temperatures will promote better drying times and efficiencies. Table 4-1 shows the average temperatures and humidity reached for the different ventilation and circulation fan speed settings at the various points inside and outside the dryer.

The collector receives the ambient air first before passing the air into the drying chamber. The collector temperatures recorded were lower than the temperatures recorded inside the drying chamber and the

humidity was mostly higher than the humidity recorded inside the drying chamber. The outlet humidity recorded (DC outlet) sometimes recorded higher humidity values potentially due to moist air being expelled from inside the dryer. The absorber wall separates the collector and the drying chamber. The absorber wall aids in the increase of temperature in the collector and drying chamber sections of the dryer. The drying chamber reaches higher temperatures as the pre-heated air entering the drying chamber is heated further by the surfaces exposed to direct sunlight. The sensor located near the drying chamber roof (DC elevated) reaches the highest temperatures which could be due to the hot air rising.

It was found that higher ventilation fan speeds resulted in a decrease in temperature and a subsequent increase in humidity. Faster ventilation fan speeds moved air into and out of the dryer much quicker allowing less time for the air to heat up inside the dryer. Circulation fans lead to higher temperatures and lower humidity values recorded as compared to no air circulation. However, the increase in the circulation rate decreases temperatures and increases humidity slightly. Ventilation and circulation speed settings V1 and C3 yielded the most optimal results. The highest temperatures and lowest relative humidity were recorded at these speed settings. Therefore, it was seen lower fan speeds result in better temperatures and humidity values being recorded. These speed settings will be used during water tests to determine how the ventilation and circulation fan speeds affect the drying capability of the dryer.

Table 4-1: Testing data recorded during functionality tests.

		Collector		DC elevated		DC outlet		DC floor		DC inlet		Ambient inlet		
	Ventilation	T1	H1	T2	H2	T3	H3	T4	H4	T5	H5	T6	H6	Irradiance
C0	V1	27.8 ±0.4	37.0 ±3.5	36.8 ±3.8	32.9 ±11.7	31.1 ±0.5	32.5 ±1.7	28.6 ±2.9	36.8 ±5.4	31.8 ±0.3	35.9 ±11.2	22.8 ±0.7	49.8 ±12.2	421.1 ±99.5
	V4	26.7 ±2.3	38.7 ±8.1	34.2 ±6.4	39.0 ±20.5	29.1 ±2.4	35.2 ±6.0	27.5 ±0.9	39.5 ±12	29.5 ±2.9	41.8 ±19.8	22.7 ±0.2	51.65 ±16.3	513.0 ±8.3
	V7	26.8 ±0.6	37.2 ±5.9	33.4 ±1.9	35.9 ±14.4	29.0 ±0.1	33.1 ±1.7	28.1 ±0.1	38.0 ±11.0	29.0 ±0.4	40.8 ±17.3	23.9 ±0.6	47.55 ±14.1	539.4 ±6.9
	V10	29.7 ±4.0	33.9 ±0.6	34.8 ±1.0	33.4 ±10.1	31.3 ±3.7	32.1 ±0.3	29.5 ±2.1	35.8 ±7.8	30.4 ±2.7	35.0 ±8.1	27.5 ±6.3	43.1 ±6.4	556.0 ±11.1
C3	V1	29.8 ±3.7	50.6 ±9.3	36.3 ±4.7	36.9 ±7.7	34.1 ±4.7	44.2 ±9.6	33.1 ±4.7	37.7 ±6.4	34.0 ±3.4	40.2 ±5.9	24.1 ±1.3	65.1 ±5.7	561.9 ±19.4
	V4	29.4 ±0.6	50.9 ±2.2	36.2 ±1.2	36.1 ±2.3	33.0 ±1.7	45.3 ±3.5	31.9 ±1.2	38.8 ±2.1	33.0 ±1.4	40.7 ±3.0	23.8 ±0.6	66.4 ±2.1	532.5 ±2.8
	V7	26.9 ±0.6	57.0 ±2.5	32.7 ±0.6	40.3 ±2.1	29.8 ±0.7	52.8 ±2.9	28.8 ±1.0	43.3 ±2.1	29.8 ±1.0	46.2 ±3.2	23.4 ±0.7	68.4 ±4.4	516.9 ±33.2
	V10	27.2 ±0.8	57.2 ±4.5	32.6 ±0.4	41.1 ±1.8	30.2 ±1.3	53.3 ±4.6	28.6 ±0.6	43.8 ±2.3	29.8 ±1.8	47.3 ±4.8	23.7 ±0.8	66.8 ±4.9	499.3 ±74.7
C6	V1	29.4 ±1.2	47.6 ±8.8	34.9 ±3.3	36.0 ±9.3	32.6 ±1.8	42.0 ±11.7	32.3 ±2.2	36.3 ±6.6	32.8 ±2.1	37.0 ±9.9	25.2 ±1.1	64.1 ±8.1	539.4 ±201
	V4	28.3 ±0.2	49.8 ±2.0	33.7 ±0.5	37.5 ±2.3	31.5 ±0.4	46.5 ±1.8	30.5 ±0.2	38.4 ±1.9	31.4 ±0.9	41.0 ±2.1	25.0 ±0.1	66.5 ±4.5	569.7 ±13.8
	V7	27.9 ±0.4	52.4 ±0.2	31.8 ±0.3	41.0 ±0.4	30.4 ±0.3	51.0 ±1.0	29.1 ±0.4	41.4 ±0.9	30.1 ±0.4	44.4 ±0.4	25.0 ±0.4	71.1 ±10.5	499.9 ±83.6

		Collector		DC elevated		DC outlet		DC floor		DC inlet		Ambient inlet		
	Ventilation	T1	H1	T2	H2	T3	H3	T4	H4	T5	H5	T6	H6	Irradiance
	V10	28.6 ±1.0	52.5 ±0.4	31.9 ±0.7	42.0 ±0.3	29.9 ±0.4	54.7 ±2.0	28.9 ±0.1	41.8 ±0.1	29.5 ±0.3	46.8 ±1.1	23.8 ±0.4	81.4 ±11.9	480.6 ±11.9
C10	V1	29.7 ±2.3	41.8 ±2.9	34.4 ±0.2	38.9 ±3.3	31.2 ±0.4	46.3 ±3.5	32.0 ±1.9	37.9 ±4.1	33.2 ±1.5	40.1 ±5.5	23.8 ±0.4	61.3 ±5.1	564.8 ±6.9
	V4	26.4 ±1.8	42.7 ±13.3	31.2 ±3.3	43.3 ±7.1	29.8 ±3.6	47.9 ±1.8	29.2 ±3.2	42.7 ±6.8	30.0 ±4.0	42.7 ±4.0	22.8 ±0.4	66.5 ±7.1	554.0 ±24.9
	V7	26.0 ±0.6	46.3 ±21.1	31.4 ±0.9	45.6 ±0.7	29.0 ±0.1	50.8 ±9.2	28.1 ±0.1	44.8 ±1.4	28.8 ±0.1	50.9 ±3.0	23.3 ±1.4	67.9 ±11.2	579.2 ±112.9
	V10	29.1 ±5.0	49.1 ±21.6	32.6 ±4.4	44.5 ±5.7	30.9 ±4.2	51.1 ±15.0	29.0 ±3.0	43.5 ±3.6	30.3 ±4.0	48.5 ±5.2	26.4 ±6.6	65.1 ±19.8	563.3 ±173.5
Unit		°C	%	°C	%	°C	%	°C	%	°C	%	°C	%	W/m²

4.2. Water Test Results

During the water tests, temperature and humidity inside the greenhouse dryer and the ambient air entering the greenhouse were compared and analysed. The average of the ambient and greenhouse temperatures for each ventilation and circulation flow rate adjustment were compared in Figure 4-1. The temperature and humidity raw data are shown in G-2.

At circulation speed C3 and ventilation speed V1, temperatures averaged around 35 °C in the dryer at an average ambient temperature of around 23 °C. The temperatures recorded for the other fan speed combinations were lower than 35 °C. This was also observed in the functionality tests where the higher temperatures were recorded at fan speeds C3 and V1 at the DC elevated sensor. The change in circulation fans did not have a major impact on temperatures and humidity as compared to the influence the ventilation fans had, but a slight drop in temperature was observed when circulation fan speeds were increased.

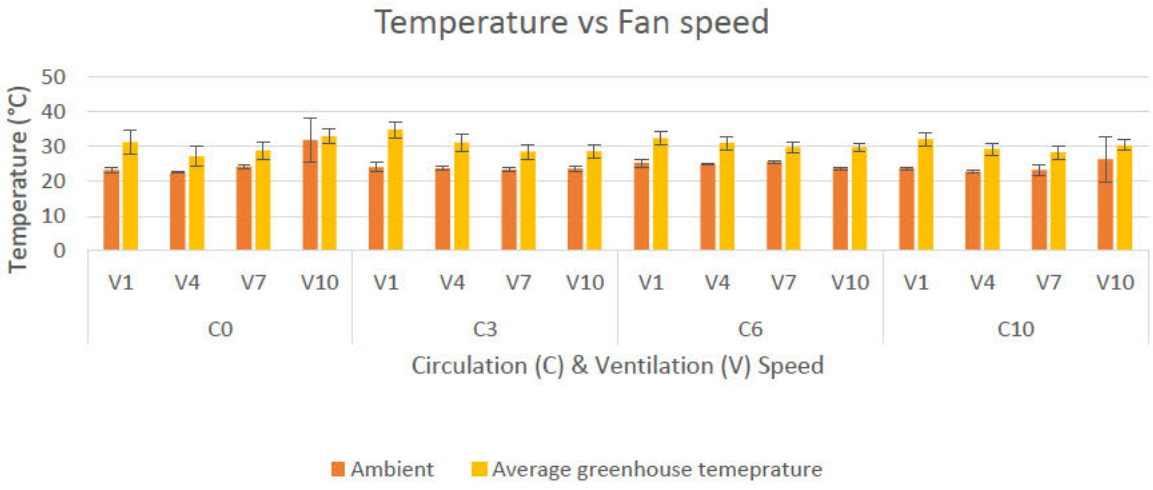

Figure 4-1: Greenhouse temperature for different circulation and ventilation flow rate combinations.

Figure 4-2 shows the average humidity achieved inside and outside the dryer at different circulation and ventilation speeds. The humidity values inside the dryer at the different fan speeds were very close.

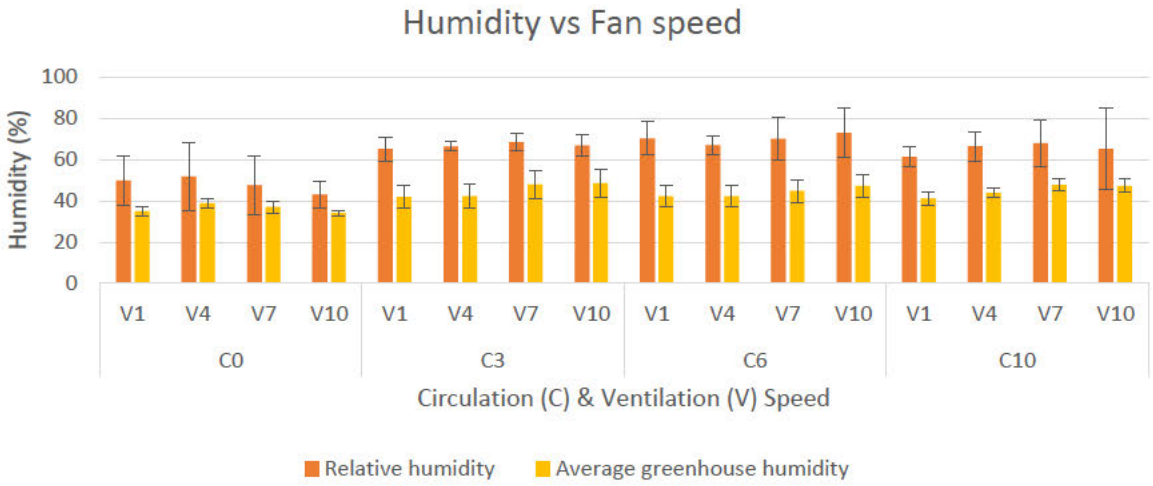

Figure 4-2: Greenhouse humidity for different circulation and ventilation flow rate combinations.

An initial mass of 100 grams of water was placed in 20 grams crucibles. The mass of water and the crucible were measured every 30-minute interval to determine how much water was evaporated in that space. Table G-4 in Appendix G shows the mass of water every 30-minute interval The speeds of the fans were also adjusted every 30 minutes to determine which fan speed combination would yield the highest mass of water evaporated and the lowest power consumption. Tests with selected ventilation and circulation speeds were selected and tests with selected fan speeds were conducted per day. The data recovered for the water evaporation tests for the different ventilation and circulation rates is shown in the tables in Appendix G. The tables show that the best ventilation and circulation rates were the lower fan speed settings which were circulation speed 3 and ventilation speed 1. Performance parameters for the circulation speed 3 are shown in Table 4-2.

Table 4-2: Performance parameters at varying ventilation rates and constant circulation rate (C3) during the water tests.

Circulation speed 3	**V1**	**V4**	**V7**	**V10**	***Unit***
Average irradiance	541.9 ± 19	532.4 ± 2.8	538.9 ± 33	499.3 ± 74	*W/m²*
Average dryer temperature	33.5 ± 2.3	32.7 ± 5.84	29.6 ± 2.1	29.6 ± 2	*°C*
Average dryer humidity	41.9 ± 5.62	42.3 ± 6.88	47.9 ± 6.88	48.5 ± 6.6	*%*
Mass flow rate	0.007	0.003	0.004	0.002	*kg/h*
Drying rate	2.316	1.263	1.895	0.842	*kg/h/m²*
SEC	16667	43333	41250	92500	*kWh/t*
Efficiency	0.208	0.125	0.195	0.019	*%*

From Table 4-2, it was observed the highest drying rate (2.3 kg/h/m²) and drying efficiency (0.208 %) were calculated at ventilation speed V1. The SEC calculated for this ventilation speed was significantly lower than the other fan speed SEC values calculated. At fan speed V1, an SEC of 16,667 kWh/t was calculated as compared to 92,500 kWh/t calculated at fan speed V10. Therefore, it was evident that fan speed V1 leads to the most optimal drying conditions. Lower ventilation fan speeds yield higher efficiency and lower SEC, therefore V1 was selected as the most optimal ventilation speed. Performance parameters for various circulation rates at a ventilation rate of V1 are shown in Table 4-3.

Table 4-3: Performance parameters at varied circulation rates and constant ventilation rate (V1) during the water tests.

Ventilation rate 1	**C0**	**C3**	**C6**	**C10**	***Unit***
Average irradiance	521.75 ± 42.9	541.9 ± 19	547.7 ± 10.9	564.8 ± 2.8	*W/m²*
Average dryer temperature	31.2 ± 3.5	33.5 ± 2.3	32.1 ± 1.8	32.1 ± 1.8	*°C*
Average dryer humidity	35 ± 2.1	41.9 ± 5.62	42.3 ± 5.4	41 ± 3.3	*%*
Mass flow rate	0.003	0.007	0.006	0.0065	*kg/h*
Drying rate	1.26	2.94	2.73	2.74	*kg/h/m²*
SEC	330	16667	28500	49160	*kWh/t*
Efficiency	0.089	0.270	0.198	0.227	*%*

The test at the circulation speed C3 resulted in the largest mass of water evaporated (2.94 kg/h/m²). The reason for this was that the combination of C3 and V1 resulted in the highest temperature rise and humidity reduction, as seen in Figure 4-1 and Figure 4-2. These conditions promote better drying performance. Lower fan speeds also consume less power than higher fan speeds. Figure 4-3 shows a surface chart of the SEC vs the fan speeds and Figure 4-4 shows a surface chart of the dryer efficiency vs the fan speeds. In the chart it can be seen as fan speeds were increased so did the SEC value and as ventilation fan speeds were increased efficiencies began to decrease. Lower fan speeds also consume less power than higher fan speeds. Ventilation fan speed settings V1 displayed minimum SEC and maximum efficiency. Circulation fan speed settings C3 and C6 displayed the highest efficiencies of more than 0.2 %.

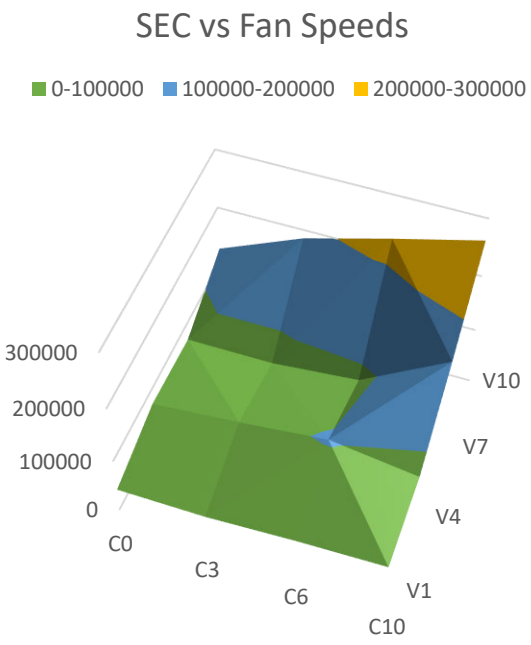

Figure 4-3: Surface chart of SEC vs the fan speeds for selected data from water tests.

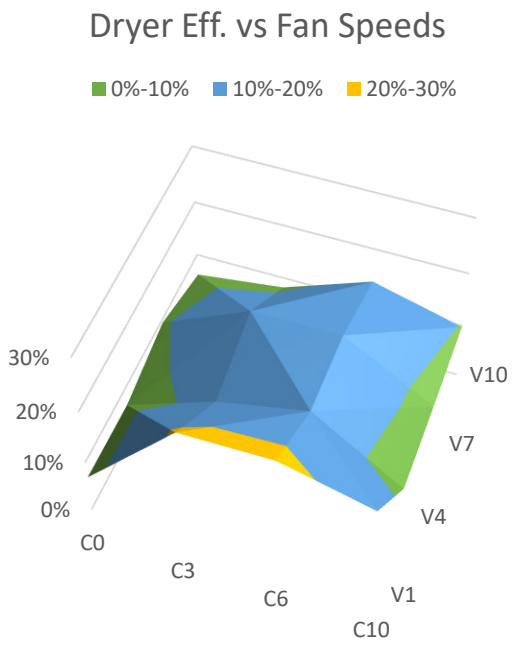

Figure 4-4: Surface chart of dryer efficiency vs fan speeds for selected data from water tests.

After comparing the different test results, it was observed lower fan speed not only elevates temperatures and lower humidity but also consumes less power and promotes more mass of water being evaporated. Temperatures above 30 °C were achieved in the dryer, which was higher as compared to ambient temperatures outside the dryer during water tests. Lower fan speeds resulted in lower SEC values due to less energy being consumed by the fans and higher drying rates being achieved. For instance, C3 yields an SEC of 16,667 kWh/t at V1 as compared to an SEC of 49,160 kWh/t achieved at V10. Therefore, V1 and C1 were the selected fan speeds for the soil and synthetic sludge testing. The rest of the water test results can be found in G-2.

4.3. Wet Soil Drying Tests

Soil tests were conducted with 1.4 and 15 kg of wet soil with and without the rake system.

4.3.1. 1.4 kg Wet Soil Drying Test

A sample of 1.4 kg of wet soil at around 60–65 % moisture content was first dried without the use of the rake system. The dryer handled wet soil well without a large amount of water percolating through the drying tray. Temperatures and humidity recorded are shown in G-2 for both these tests. The drying curve for the tests with and without the rake system is shown in Figure 4-5. With the use of the rake system, a higher moisture content of wet soil was reduced to a lower final moisture content soil in the

same drying time interval. With the use of the rake system, 65 % MC soil was reduced to 21 % in the space of 5 hours and without the use of the rake system, 60 % MC wet soil was reduced to 22 % in the space of 5 hours. Even though the test without the rake system in operation experienced better weather conditions, the test without the rake system performed better at the cost of higher power consumption. The use of the rake system also granulated and mixed the wet soil whereas, without the use of the rake system, a dry cake-like sample of soil was yielded, with the soil sticking onto the bottom of the drying tray.

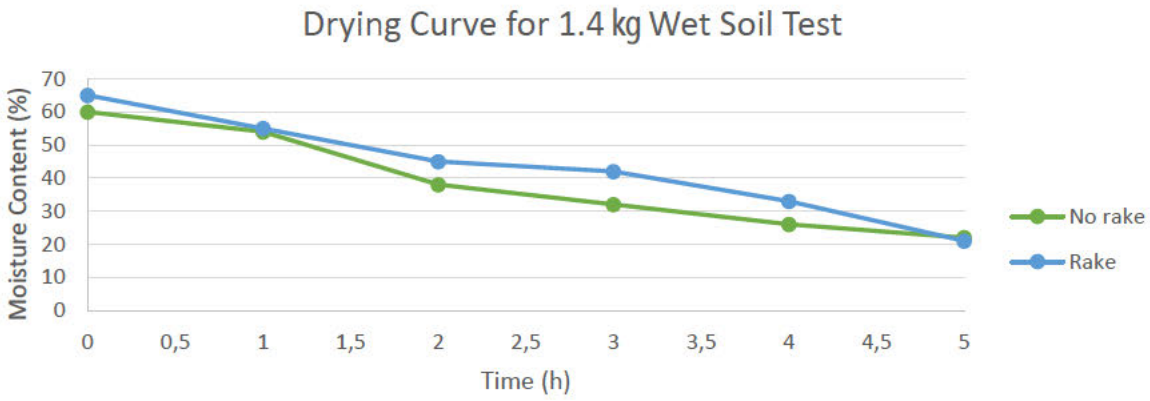

Figure 4-5: Drying curves for 1.4 kg soil tests with and without the rake system.

From the two sets of tests performance calculations of drying rate, SEC and drying efficiencies were determined to compare the performance of the two soil tests. The performance calculations determined for the two 1.4 kg soil tests with and without the rake system in operation are shown in Table 4-4. A drying rate of 1.3 kg/h/m² was calculated for the soil test with the rake system in operation whereas a drying rate of 1.07 kg/h/m² was calculated for the soil test without the rake system. Due to the rake system consuming power, a higher value of SEC was calculated when the rake system was in use. A SEC of 924.63 kWh/t was calculated with the use of the rake system as compared to 608 kWh/t calculated without the use of the rake system.

Table 4-4: Performance parameters for 1.4 kg wet soil test with and without the rake system in operation.

Quantity	**No rake**	**Rake system**	***Unit***
Drying time	5	5	*h*
Average irradiance	648	584	*W/m²*
Average power	170	238	*W*
Initial mass of water	0.81	0.91	*kg*
Mass of solids	0.59	0.49	*kg*
Final mass of water	0.17	0.13	*kg*
Average dryer temperature	40.58	38.1	*°C*

Quantity	No rake	Rake system	*Unit*
Average dryer humidity	32.87	38.97	*%*
Mass flow rate	0.13	0.16	*kg/h*
Drying rate	1.07	1.30	*kg/h/m²*
SEC	608.93	924.63	*kWh/t*
Efficiency	4.41	5.93	*%*

The use of the rake system contributes to a higher SEC but also achieves a higher efficiency and drying rate. The use of the rake system does consume more energy but ensures homogenous drying of the wet soil sample by mixing and moving moist soil from the lower to the top layers. This results in less moist soil settling in the bottom of the tray and ensures a more consistent moisture content of the final dry product. The rake system granulates the soil and prevents large amounts of wet sand from accumulating and sticking on the bottom of the drying tray.

4.3.2. 15 kg Wet Soil Drying Test

The drying curves for the soil tests with 15 kg of 70 % moisture content wet soil with and without the rake system in operation are shown in Figure 4-6. From the drying curves, we can see that drying with the rake system leads to higher drying rates than without the rake in the initial stage (first 2 hours). After 5 hours of the experiment, both cases yielded approximately the same final moisture content.

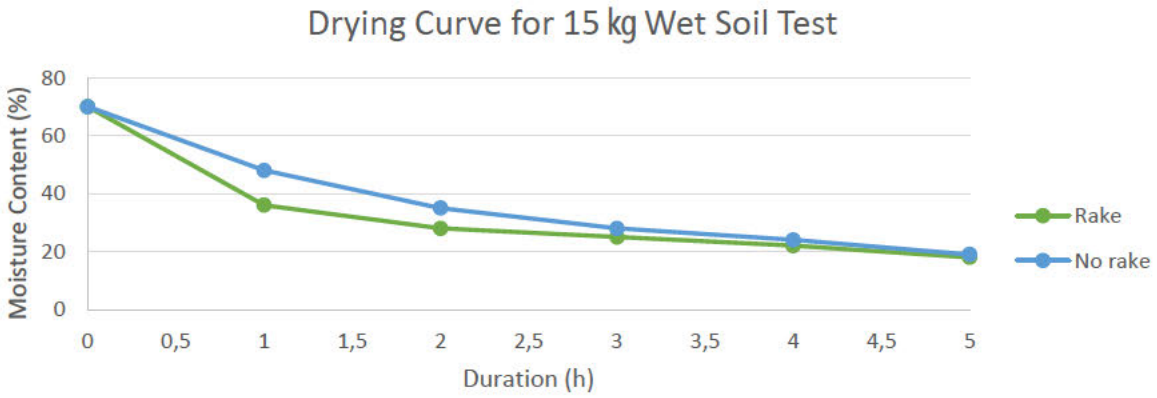

Figure 4-6: Drying curve for 15 kg soil tests with and without rake system operating.

Figure 4-7 shows the drying rate vs time for the 15 kg soil test with and without the rake system. During the first hour, the constant rate period occurred. After the first hour, the falling period was observed. The falling rate period was observed because there was a limitation in the mass transfer of moisture from the core to the surface of the sludge. After the 2nd hour of testing the second falling rate period was observed. Thereafter there was very little change in the drying rate after the 5th hour of testing and

it can be assumed the equilibrium moisture content was reached suggesting that the drying process has stopped.

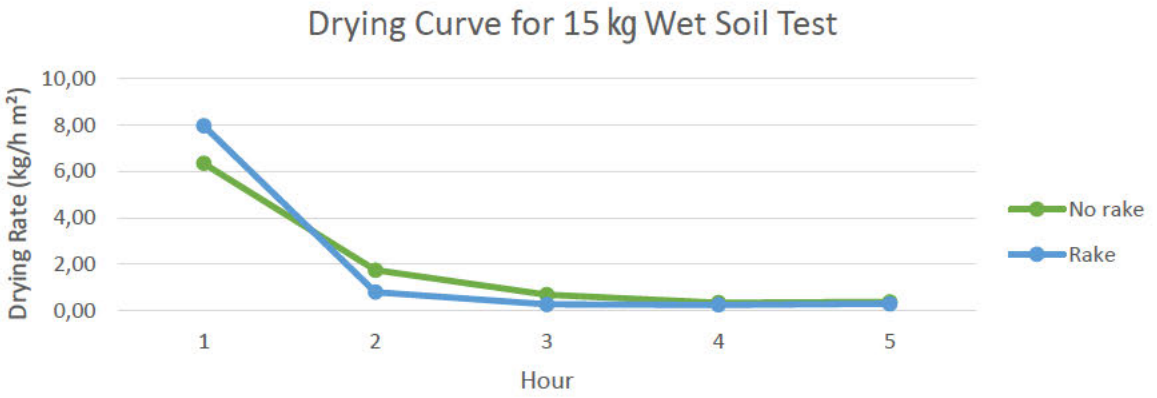

Figure 4-7: Drying rate vs time for 15 kg soil tests with and without rake system operating.

The moisture content and drying rate were also compared against each other in the form of a Krischer curve (i.e., drying rate versus moisture content) in Figure 4-8. The drying rate decreases because the drying process occurs at the falling rate period. The Krishner curve makes it clear the falling rate period. The drying rates are higher for the test with the rake system in operation during the first falling rate period, whereas the drying rates between the two cases were similar during the second falling rate period when the moisture content was less than 30 %.

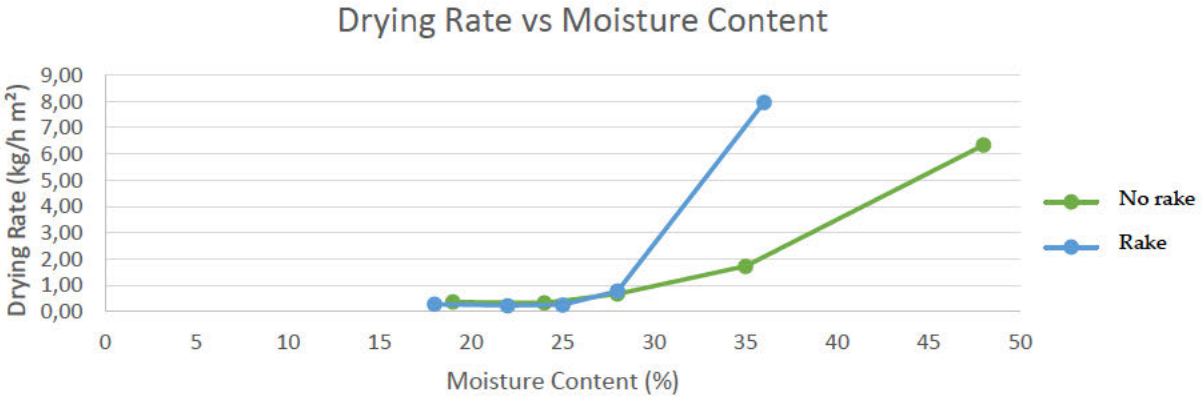

Figure 4-8: Krischer curve for 15 kg soil tests with and without the rake system in operation.

The drying performance parameters calculations with and without the rake system for 15 kg of wet soil are shown in Table 4-5. The detailed data information is shown in G-2.

Table 4-5: Performance parameters for 15 kg wet soil test with and without the rake system in operation.

	No rake	**Rake system**	***Units***
Drying time	5	5	*h*
Average irradiance	619	582	*W/m²*
Average power	170	238	*W*
Initial mass of water	10.5	10.5	*kg*
Mass of solids	4.5	4.5	*kg*
Final mass of water	1.06	0.988	*kg*
Average dryer temperature	40	38	*°C*
Average dryer humidity	31	28	*%*
Mass flow rate	1.89	1.90	*kg/h*
Drying rate	2.95	2.97	*kg/h/ m²*
SEC	90	123.54	*kWh/t*
Efficiency	50.83	72.95	*%*

Even though slightly better weather conditions were experienced with the test without the use of the rake system, better efficiencies and drying rates were achieved with the rake system in operation. Within the space of 5 hours, the dryer was able to reduce 70 % moisture content soil to an equilibrium moisture content of 18 %. The SEC with the rake system was slightly higher due to more power used. The rake system granulates the sludge and prevents crust formation. The result of using the rake yields more particles of dry sand and prevents larger amounts of sand from sticking to the bottom of the tray. Therefore, even though the rake system consumes more energy, considerably higher efficiency was achieved and more homogenous drying should occur due to the mixing effect.

The specific energy consumption with the rake system operating was 123.54 kWh/t whereas the SEC without the rake system was approximately 90 kWh/t. With the rake system in operation, a drying efficiency of 72.95 % was calculated as compared to 50.83 % calculated without the use of the rake system. The results suggest that the rake system was more efficient even though more energy was consumed. The rake system also provides a better granular sample to handle instead of a larger bulky dry sample. Therefore, the rake system proved to be an efficient tool in promoting homogenous and uniform drying conditions. The rake system improves the drying performance of the greenhouse solar dryer. Dryer efficiencies of over 70 % were determined during soil tests. The soil was much easier to handle as compared to faecal sludge in the dryer. Soil does not stick and clog the dryer as much as synthetic sludge or real faecal sludge would.

4.4. Test 3 (Synthetic sludge)

Testing of synthetic sludge was conducted from the 5th to the 9th of September 2022. A second test was done between the dates of the 14th and 15th of September 2022. The initial moisture content of the synthetic sludge was 80 % for both tests. Testing was undertaken between 9 AM and 3 PM. The results and discussion for both tests were analysed individually.

4.4.1. Synthetic sludge test 1

During the first day of tests, the greenhouse temperatures did not surpass 40 °C but good amounts of sunshine were observed throughout the day. Nonetheless, testing for the first day of testing was stopped at 2 PM due to cloud cover and conditions becoming very windy. The synthetic sludge moisture content was reduced by 10 % on the first day of drying despite experiencing frequent cloud cover and lots of wind throughout the day. Synthetic sludge was very sticky at a moisture content of 70 % thereby causing a lot of the sludge to stick to the blade from the rake system.

The second day of testing was very cloudy and less windy than the first day. Clouds were present throughout the day with very little sunshine. More than 10 % moisture content was removed from the synthetic sludge in the space of 5 hours. Testing was stopped at 2 PM due to high winds starting to pick up. The synthetic sludge being dried changed from a wet porridge texture to a silicon texture towards the end of the day. The rake system broke the synthetic sludge into smaller pieces and stuck less to the blade. Synthetic sludge of around 58 % moisture content was present at the end of the second day of testing. A large reduction in volume was observed at the end of the second day of testing.

The third day of testing started very cloudy and less windy than the first two days. Clouds dispersed at around 10 AM. After this time, the skies became clear and important sunshine was observed. Temperatures of more than 40 °C were observed in the greenhouse at around noon. The synthetic sludge was reduced into smaller pebbles by the rake system during the day. The synthetic sludge texture became firmer and more compact as the day progressed. The sludge mass decreased throughout the day and synthetic sludge was reduced to 19 % moisture content at the end of the day.

The fourth day of testing offered clear skies and good amounts of solar irradiation. Temperatures of more than 40 degrees were observed after 11 AM. The synthetic sludge texture became crispy and hard as the day progressed. A reduction of moisture content from 18 to 6.5 % moisture content was observed at the end of the day. The final sludge sample mass was drastically less at the end of testing. On the 5th day, the dryer fans and temperature sensors were left to run but very little change in moisture content was observed.

It was observed the equilibrium moisture content was reached after 4 days of testing with mixed weather conditions. The final 2 days provided good weather conditions and the faecal sludge sample was

reduced to very low moisture contents. High moisture content sludge tended to stick onto the blades but as the sludge began to dry the texture began to change and the synthetic sludge became less sticky. The rake system was an effective system to prevent cake formation on the drying tray and ensured that the sludge was distributed and broken down into smaller particles as drying was conducted. The blade mixed and cut the synthetic sludge sample into small granular pieces. Table 4-6 shows the evolution of synthetic sludge in the 4 days of testing.

Table 4-6: Evolution of synthetic sludge in the 4 days of testing during Test 1.

 *Day 1*	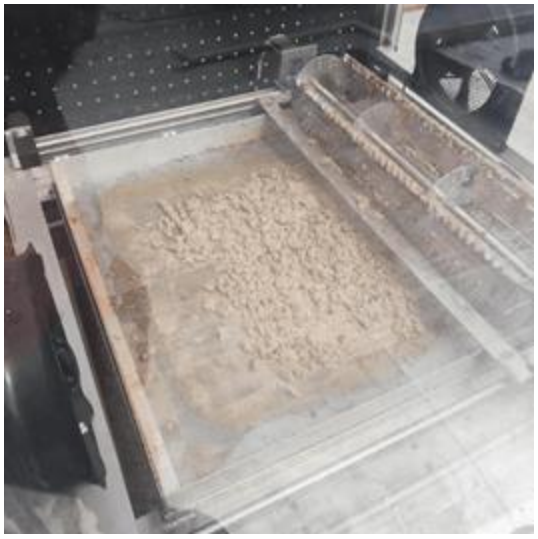 *Day 2*
 *Day 3*	 *Day 4*

The performance data from the four days of testing are shown in Table 4-7.

Table 4-7: Performance data for Test 1 with synthetic faecal sludge.

	Day1	**Day2**	**Day3**	**Day4**	***Unit***
Drying time	5	5	6	6	*h*
Average irradiance	663±86.3	365±190	637±209	798±158	*W/m²*
Average power	238	238	238	238	*W*
Initial mass of water	8.04	4.46	2.43	0.46	*kg*
Mass of solids	1.97	1.97	1.97	1.97	*kg*
Final mass of water	4.46	2.70	0.48	0.14	*kg*
Average ambient temperature	22.5±3.15	23.4±1.7	24.1±0.87	25.9±1.9	*C*
Average ambient humidity	55±6.9	52±5.3	53±2.16	51±2.74	*%*
Average dryer temperature	32.9±2.1	30.5±1.9	34.2±1.8	38±1.8	*°C*
Average dryer humidity	43±2.4	45±2.3	43±1.6	42±4	*°C*
Mass flow rate	0.72	0.35	0.32	0.06	*kg/h*
Drying rate	1.12	0.55	0.51	0.10	*kg/h/m²*
SEC	328.15	668.27	723.19	3674.32	*kWh/t*
Efficiency	20.45	18.28	9.65	1.64	*%*

The drying curve including the solar irradiance measured by the pyranometer for the 4 days of testing is shown in Figure 4-9.

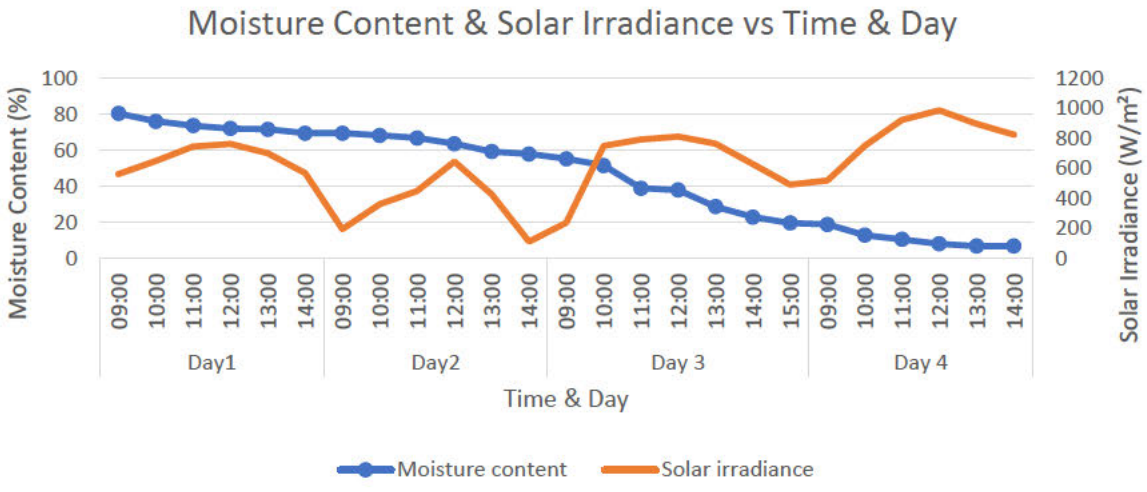

Figure 4-9: Moisture content & irradiance vs time for Test1 with synthetic sludge drying.

From Figure 4-9 we see a drop-in moisture content of around 20 % in two days of testing. On the third day of testing a drastic drop in moisture content, around 30 %, was observed. This was due to better

weather conditions being experienced. The first two days experienced long periods of wind and cloud cover whereas on the 3rd and 4th days of testing clear skies and warmer temperatures were experienced. As drying progressed, the moisture became less abundant and probably more tightly bound to the solid matrix, making it harder to remove and requiring more energy to do so. This resulted in an increase in the SEC and a decrease in drying rate and efficiency as seen in Table 4-7. After day 3, the SEC dramatically increased from around 723 kWh/t to 3,674 kWh/t and the dryer efficiency dropped from 9.65 % to 1.64 %. This was most likely caused by the high level of moisture binding to the solid structure of the sludge.

The drying rate and solar irradiance versus the moisture content for the 4 days of testing are shown in Figure 4-10. At the end of each day, the temperatures began to drop, therefore causing the drying rate to peak during the day and decrease towards the end of the testing day. The drying rate and dryer efficiency were directly proportional. The drying rates and efficiency calculated began to drop when the moisture content of synthetic sludge decreased. At the start of testing when 80 % MC synthetic sludge was presented a peak drying rate of more than 1.8 kg/h was calculated. Drying rates of less than 0.2 kg/h were calculated when the synthetic sludge moisture content was lower than 20 %. The efficiency calculated on the first day was more than 20 % whereas, at the end of the 4th day, the efficiency calculated was around 1.64 %.

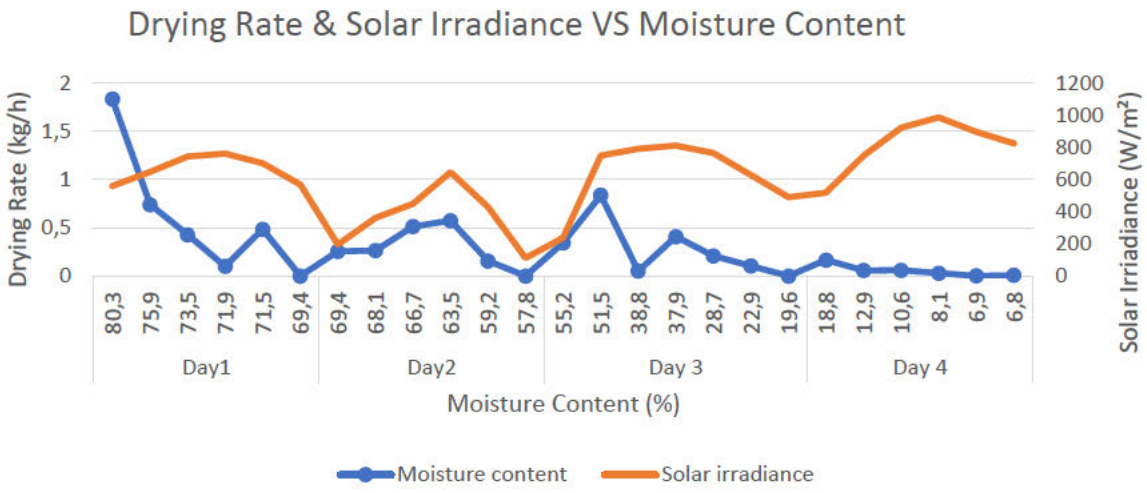

Figure 4-10: Drying rate vs moisture content for the 4 days of drying synthetic sludge.

4.4.2. Synthetic sludge test 2

A second test was conducted the following week on the 14th and 15th of September between 9 AM and 3 PM. These two days offered clear skies and warm conditions throughout the day. The performance data for the first day and second days of synthetic sludge duplicate tests are shown in Table 4-8.

Table 4-8: Performance data for Test 2 with synthetic faecal sludge.

	Day 1	Day 2	*Unit*
Drying time	6	6	*h*
Average irradiance	660	693	*W/m²*
Average power	238	238	*W*
Initial mass of water	7.91	1.80	*kg*
Mass of solids	1.97	1.97	*kg*
Final mass of water	1.82	0.27	*kg*
Average dryer temperature	36.73	42.20	*°C*
Average dryer humidity	45.81	37.88	*%*
Mass flow rate	1.01	0.25	*kg/h*
Drying rate	1.59	0.40	*kg/h/m²*
SEC	231.57	922.73	*kWh/t*
Efficiency	34.14	8.36	*%*

Figure 4-11 shows the drying curve obtained during Test 2.

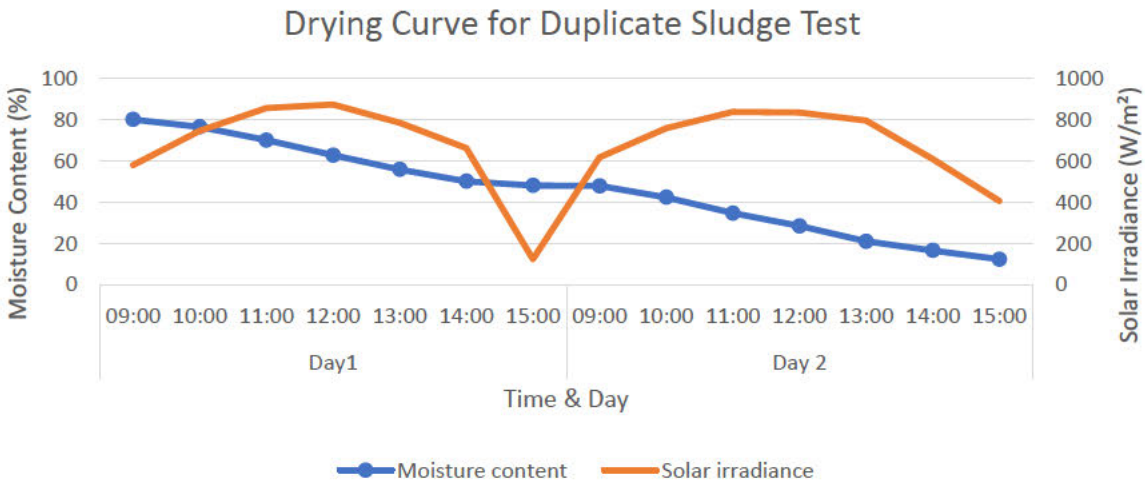

Figure 4-11: Drying curve for duplicate drying test.

Synthetic sludge of 80 % moisture content was reduced to 12 % moisture content in the space of 12 hours of testing. The average drying rate for the first day of testing was approximately 1.01 kg/h. The solar irradiance was significantly higher, approximately 660 W/m², during the first day of testing compared to all the other testing days. The dryer performed better due to very little cloud cover and winds. The dryer achieved more than 30 % dryer efficiency during the first day with a large reduction in moisture content of more than 30 %. The SEC was much lower when the weather conditions were

more favourable as it requires less energy and time to dry synthetic sludge to low moisture content. The SEC calculated on day one was approximately 231 kWh/t.

The second day of testing also led to good results, synthetic sludge of less than 50 % moisture content was reduced to around 12 % in the space of 6 hours. The second day was one of the hottest days of the testing campaign and recorded an average solar irradiance of approximately 693 W/m². The dryer reached temperatures of more than 50 degrees Celsius. The exceptionally high-temperature increase was due to load shedding that was present between 12–2 PM. There was a high increase in temperature due to air remaining in the dryer for a longer period due to fans not operating during load shedding and allowing air to accumulate heat instead of being expelled from inside the dryer to the outside environment. The second day achieved an efficiency of 8.3 % and SEC of around 922 kWh/t. The higher SEC and lower efficiency on the second day were due to less moisture being left to be dried, therefore more power was required to remove the remaining moisture (more bounded).

4.4.3. Evaluation of synthetic sludge tests 1 and 2

The overall performance parameters calculated for Tests 1 and 2 are shown in Table 4-9.

Table 4-9: Overall performance data for Test 1 and Test 2 with synthetic faecal sludge.

Quantity	**Test 1**	**Test 2**	***Unit***
Drying time	22	12	*h*
Initial mass of water	8.02	8.03	*kg*
Mass of solids	1.965	1.97	*kg*
Final mass of water	0.14	0.28	*kg*
Mass flow rate	0.36	0.65	*kg/h*
Drying rate	0.56	1.01	*kg/h/m²*
SEC	655.87	363.67	*kWh/t*
Efficiency	9.6	18.08	*%*

The greenhouse solar dryer was tested with 10 kg of synthetic faecal sludge between the period of 05-08-2022 to 08-08-2022. In the space of 4 days with drying times from 5 to 6 hours per day, synthetic sludge of moisture content of 80 % was reduced to 6.5 % with an average overall drying rate of 0.36 kg/h. The first two days did not offer the best weather conditions but managed to achieve an efficiency of almost 20 % dryer efficiency. Performance drastically decreased the next days due to the drying rate lowering as the remaining moisture was more bound to the solid matrix. The more the sludge moisture content was reduced the more difficult it becomes to dry. Therefore, it must be evaluated the most optimal drying duration without consuming too much power. The overall SEC achieved in the 4 days of test 1 was approximately 655 kWh/t and an overall dryer efficiency of 9.6 %.

A second test with 10 kilograms of synthetic sludge was conducted in the period of 14-08-2022 to 15-08-2022. Synthetic sludge was dried for two days and sludge was reduced from 80 % moisture content to approximately 12 % in the space of 12 hours with an average overall drying rate of approximately 0.65 kg/h. Excellent weather was present during these two days and the efficiencies calculated were much lower than the first synthetic sludge test. After one day of testing, SEC began to rise and dryer efficiency began to drop drastically. On the second day of testing the dryer performance was considerably lower than the first day. Similar to the first test after every consecutive day of the test the dryer efficiency and rate began to decrease due to moisture becoming more bound when the moisture content was reduced drastically. Feedstock that takes longer to dry will consume more time therefore a lower efficiency will be calculated as the efficiency is inversely proportional to the drying time. The overall efficiency of approximately 18 % and average SEC of 363 kWh/t were calculated over the two days of testing.

Weather conditions were directly proportional to the dryer's performance. Clear skies and high temperatures will promote higher efficiencies and lower power consumption. The solar irradiance values recorded averaged around 600 W/m² over the 4 days of testing and around 675 W/m² recorded on the second sludge test conducted. Three days of testing with good weather was estimated to be enough to dry synthetic sludge of 80 % moisture content to very low moisture content. Sludge drying could be stopped when the moisture content is very low to reduce the drop in the performance of the system. At moisture contents, lower than 30 % moisture is highly bound and therefore will result in lower drying rates and efficiencies.

Literature suggests dryers of similar applications were able to dry sewage sludge at similar performance parameter values. Commercial solar dryers for the drying of sewage sludge utilize around 450 kWh/t on average whereas the faecal sludge greenhouse solar dryer over the space of 2 days dries synthetic sludge to a moisture content of around 12 % with an overall SEC of 363 kWh/t (Alice Sorrenti, 2022). Over the space of 2 days, the greenhouse dryer efficiency calculated was around 18 % and this was calculated during the winter seasons. The results indicate that the greenhouse dryer can be an effective tool for the drying of faecal sludge. The optimisation of the prototype can enable the dryer to outperform commercial solar dryers currently utilized. Chapter 5 will conclude the study and discuss the performance and outcomes that were observed from the results.

Chapter 5: Conclusion

The greenhouse solar dryer was developed and tested to evaluate its performance for faecal sludge drying. The greenhouse dryer reached temperatures of 10 degrees Celsius more than the outside temperature. Temperatures in the collector were lower than the temperatures recorded inside the drying chamber but higher than ambient temperatures entering the collector. Temperatures were further elevated when entering the drying chamber. The highest temperatures were recorded at the elevated sensor (DC elevated) in the drying chamber. Higher temperatures reduced the humidity recorded in the greenhouse dryer. A humidity of less than 40 % was recorded inside the greenhouse dryer whereas the relative humidity outside the dryer was more than 50 %.

Water tests concluded that lower ventilation fan speeds contribute to higher temperatures, lower humidity, higher evaporation rate and lower power consumption. The use of circulation fans led to a better drying performance compared to when the fans were turned off. However, the increase in fan speed resulted in a decrease in drying performance. Therefore, lower circulation speeds resulted in better drying performance. The lowest SEC and highest dryer efficiency were calculated at the lowest test ventilation and circulation fan speed (V1 and C3) with a value of around 16,667 kWh/t and 0.27 % respectively.

The rake system allowed for more homogenous drying of both soil and synthetic sludge and resulted in less feedstock settling and sticking on the bottom of the drying tray. The rake system resulted in higher SEC values calculated but improved the process efficiency and led to higher drying rates. The use of the rake system mixed the soil and sludge frequently resulting in a granular final product as compared to one large dried sample. Higher drying efficiencies, SEC and drying rates were calculated when the rake system was utilized.

During the tests with synthetic sludge, the moisture content was reduced to a 6.5 % moisture content sample in the space of a few days with an efficiency of between 10–20 % and overall SEC of between 365–3,500 kWh/t. The drying rate ranged between 0.1 and 1.6 kg/h/m² calculated during sludge testing. High SEC was calculated after reaching low moisture content, probably due to the little remaining amounts of moisture to remove and an increased moisture boundness with the solid matrix. For the greenhouse to operate at its best, drying should be stopped before the sludge reaches a very low moisture content which results in a high level of moisture boundness, a sharp increase in SEC and a reduction in dryer efficiency.

An overall SEC and dryer efficiency of around 650 kWh/t and 9 % respectively were calculated for synthetic sludge dried over 4 days during the first test. The overall dryer efficiency calculated in the second test was around 20 % and the overall SEC of less than 400 kWh/t. The SEC calculated was significantly lower than conventional thermal dryers with values of around 800 to 1,000 kW/h. The

prototype performed better during days with high temperatures and solar irradiances. Dryer performance was weather-dependent, with wind and clouds negatively affecting drying. Soil tests and synthetic sludge tests have been conducted over the winter period and the dryer was still able to perform efficiently.

Research and testing of the greenhouse solar dryer concluded that solar thermal dryers have the potential to deal with the treatment of faecal sludge which was a major problem in developing countries. Further steps to conclude the study include tests with real faecal sludge, improvement and optimization of the system, and techno-economic analysis.

Chapter 6: Observations & Recommendations

A few challenges were encountered when developing the greenhouse dryer prototype. One of the major challenges was installing the PMMA acrylic sheet onto the aluminium frame of the dryer. 3 mm acrylic sheets were very flexible and brittle. The PMMA obtained many cracks and scratches during installation. The recommendations include using thicker acrylic sheets as 3 mm was too brittle. Acrylic sheets of around 6 mm thickness would be ideal.

Motor drivers seemed to seize when motors were running for more than 20 minutes. This was due to the motor drivers running at their maximum for a long time. More powerful stepper drivers were installed to eliminate overheating of motor drivers. Limit switches could be installed to change the rake system movement direction in the drying tray (alternatively to set the number of steps the stepper motor needs to perform before changing direction). The rake system should also be operated in shorter cycles to reduce power consumption.

From water testing, it was found that lower fan speeds result in higher temperatures and lower humidity. Therefore, smaller DC fans can be installed instead of AC axial fans. The implementation of DC fans will make it easier to implement solar photovoltaic energy into the system by installing solar panels and deep-cycle batteries. All the electronic components were capable of operating with a DC configuration except the potentiometer switches. The installation of a solar PV system will ensure less power usage from the grid and power the system during load shedding. This affects the efficiency of the dryer as humidity in the dryer increases above ambient humidity due to fan operations being paused. Higher humidity makes it more difficult to dry and causes perspiration instead of evaporation. Less vapour will exit the dryer as the fans were turned off during load shedding.

Temperature sensors experienced interference when the rake system was powered. Indeed, the motor drivers caused interference as they pulsed power to the stepper motor. Therefore, the temperature sensor control system must be mounted in its separate electrical box to eliminate that issue.

Shiny surfaces tend to reflect sunlight whereas black surfaces absorb solar thermal energy. Therefore, components in the dryer should be painted or sprayed black to achieve higher temperatures reached inside the dryer. Electrical components should be shiny to prevent overheating and seizing of electronics.

The odour was smelt at the outlet of the dryer during synthetic sludge testing. It would be safer to install filters at the exit when using faecal sludge to ensure no harmful chemicals (e.g., sulphide hydrogen) were released into the outside environment and minimize bad odour around the dryer.

References

A. Murray Muspratt, T. C. N. H. J. L. S. J. R., 2014. *Fuel potential of faecal sludge: calorific value results from Uganda, Ghana and Senegal.* s.l.:IWA Publishing.

Abraham, M. M., 2016. *The Energy Resource Institute.* [Online] Available at: https://www.teriin.org/opinion/improvement-faecal-sludge-management-realising-goal-sustainable-sanitation-goa
[Accessed 04 05 2020].

Ahmad Siouti, A. B. A., 2019. Evaluation of Solar Energy Potential for the Red. *Natural Resources,* Volume 10, pp. 96-114.

Ali I., A. L. E. H. B. M. K. E. K. L., 2016. Solar convective drying in thin layers and modelling of municipal waste at three temperatures. *Applied Thermodynamics,* 73(1), pp. 41-47.

Alice Sorrenti, S. F. C. F. T. G. V. M. t., 2022. Enhanced Sewage Sludge Drying with a Modified Solar Greenhouse. *Collection Water and Wastewater Treatment Technologies,* 4(2), pp. 407-409.

Amyx, S., 2019. *Why most of sunlight can not be converted to solar energy.* [Online] Available at: https://scottamyx.com/2019/04/30/why-most-sun-light-cannot-be-converted-into-electricity/ [Accessed 6 4 2020].

Andritz, S., n.d. *Drying technologies for sewege sludge.* [Online] Available at: https://www.andritz.com/resource/blob/13600/75c56d2056bfb401e599a0130086dbd1/se-downloads-drying-technologies-for-sewage-sludge-web-en-data.pdf
[Accessed 29 3 2020].

Ataollah Khanlari, A. S. ,. F. A. ,. C. Ş. ,. A. D. T. ,. A. G., 2020. Drying municipal sewage sludge with v-groove triple-pass and quadruple-pass solar air heaters along with testing of a solar absorber drying chamber. *Science of The Total Environment,* Volume 709.

Belloulid, M. O., Hamdi, H., Mandi, L. & Ouazzani, N., 2017. Solar Greenhouse Drying of Wastewater Sludges Under Arid Climate. *Waste Biomass Valorization,* Volume 8, pp. 193-202.

Bennamoun L., F. L. L. A., 2014. Modeling and simulation of heat and mass transfer. *Drying Technologies,* 32(1), pp. 13-22.

Bradford F Mills, J. S., 2008. Profits or preferences? Assessing the adoption of residential solar thermal. *Energy Policy,* pp. 4145-4154.

Brdjanovic, D. Z. F. M. P. G. H. H. C. Ć. J. T. Y., 2015. *eSOS® – emergency sanitation operation system.* 5 pg 156-164 ed. s.l.:J.Water Sanit.

Bux M., B. R. Q. S. P. J., 2002. VOLUME REDUCTION AND BIOLOGICAL STABILIZATION. *Drying technology,* 20(4), pp. 829-837.

Caramori, S. R. F. A. R. C. S. B. R. B. E. &. B., 2016. *Solar Energy Conversion.* Ferrera: s.n.

Deng W., L. X. Y. J. W. F. C. Y. C. K., 2011. Moisture distribution in sludges. *Journal of Enviromental Sciences,* 23(5), p. 875–880.

Devahastin, A. S. M. &. S., 2013. *Fundamental Principle of Drying.* s.l.:Department of Mechanical engineering University of Singapore.

Dexiao Ma, G. J. W. A. L., 2021. Reinforced contact between sludge and hot wall for enhancing conductive drying by applying external load: Heat and mass transfer analysis. *Process Safety and Environmental Protection,* Volume 154, pp. 372-378.

Dr. Santiago Septien Stringel, M. T. M. M. A. S. D. F. I., 2019. *Drying of Faecal Sludge using,* Gezina: Water research commission.

Ekechukwu, O. N. B., 1999. *Review of Solar-Energy Drying Systems II: An Overview of Solar Drying Technology. Energy Conversion and Management, 40, pp.615-655.* s.l.:s.n.

Energy Efficiency & Renewable Energy, 2023. *Concentrating Solar-Thermal Power Basics.* [Online] Available at: https://www.energy.gov/eere/solar/concentrating-solar-thermal-power-basics#:~:text=CSP%20technologies%20use%20mirrors%20to,an%20engine%20to%20generate%20electricity. [Accessed 08 02 2023].

Energy Efficiency & Renewable Energy, 2023. *How does solar work.* [Online] Available at: https://www.energy.gov/eere/solar/how-does-solar-work#:~:text=When%20the%20sun%20shines%20onto,cell%2C%20causing%20electricity%20to%20flow. [Accessed 08 February 2023].

Erbay Z., I. F., 2010. A review of thin layer drying of foods: theory, modeling, and experimental. *Critical Review of Food Science,* 50(5), pp. 441-464.

Eva Kocbek, H. A. G. C. M. H. I. M. B. L. D. B., 2020. Microwave treatment of municipal sewage sludge: Evaluation of the drying performance and energy demand of a pilot-scale microwave drying system. *Science of total enviroment,* Volume 742.

Fytili, D. &. Z. A., 2008. *Utilization of sewage sludge in EU application of old and new methods: a review.* 116-140 ed. s.l.:Renewable and Sustainable Energy Reviews 12(1).

Gcep, 2006. *An Assessment of Solar Energy Conversions Technology and Research Oppertunities.* s.l.:s.n.

Getahun, S. ,. S. S. ,. M. J. ,. S. T. M. ,. B., 2020. Drying Charecteristics of faecal sludge from different on-site sanitation facilities. *Journal of Environmental Management,* p. 261.

GROSS, T. S. C., 2007. Thermal Drying of Sewage Sludge. *Water and Environment Journal ,* 7(3), pp. 255 - 261.

Hsuan-Yu Chen, C.-C. C., 2022. An Empirical Equation for Wet-Bulb Temperature Using Air Temperature and Relative Humidity. *Atmosphere,* Volume 13.

Huang L.X., M. A., 2005. Development of a new innovative conceptual design for horizontal spray dryer via mathematical modelling. *Drying Technology*, Volume 23, pp. 1169-1187.

Hyndman, B., 2020. Heating, ventilation, and air conditioning. *Clinical Engineering Handbook (Second Edition)*, Issue 2, pp. 662-666.

I., S., 2011. *THE SOLAR DRYING PLANT IN MALLORCA: THE DRYING PROCESS IN WASTE MANAGEMENT*,. Palma de Mallorca, Spain., s.n.

Jarvis, A. H. A. E., 2019. *Global Solar Atlas.* [Online] Available at: https://globalsolaratlas.info/download/south-africa [Accessed 07 04 2020].

Kevin R. Mallon, F. A. a. B. F., 2017. Analysis of On-Board Photovoltaics for a Battery Electric Bus and Their Impact on Battery Lifespan. *Energies*, pp. 9-10.

Koné, D. C. O. O. &. N. K., 2010. Low-cost options for pathogen reduction and ntrient recovery from faecal sludge. *In Wastewater Irrigation and Health. Assessing and Mitigating Risk in Low Income Countries*, pp. 171-178.

KWS Conveying Solutions, 2023. *Storage Hopper with Live Bottom Screw Feeder and Thermal Processors.* [Online]
Available at: https://www.kwsmfg.com/resources/problem-solvers/storage-hopper-live-bottom-screw-feeder-thermal-processors/
[Accessed 16 02 2023].

Li J., C. G. M. A., 2003. Discrete modelling and suggested measurement of heat transfer in gas-solids flows. *Drying Technology*, pp. 979-994.

Linda Strande, M. R. D. B., 2014. *Faecal Sludge Management, Systems approach for implementation and operation.* UK: IWA Publishing.

M.M. Jordan, M. A.-C. M. R. J. R., 2005. Application of sewage sludge in the manufacturing of ceramic tile bodies. *Application of Clay Science*, Volume 30, pp. 219-224.

Mamta Gautam, K. W. G. S. S. S., 2021. Framework for addressing occupational safety of de-sludging operators: A study in two Indian cities. *Journal of enviromental management*, Volume 289.

Marcel Suri,Tomas Cebecauer, 2023. *SOLARGIS.* [Online] Available at: https://solargis.com/maps-and-gis-data/overview [Accessed 13 January 2023].

Mawioo, P. R. A. G. H. H. C. B. D., 2016. *Evaluation of a microwave based reactor for the treatment of blackwater sludge.* pg 548-549 ed. s.l.:Sci.TotalEnviron.

Mayis Kurt, A. A. D. F. S., 2014. Evaluation of solar sludge drying alternatives by costs and area requirements. *Masters thesis, MIDDLE EAST TECHNICAL UNIVERSITY*, pp. 40-60.

Mohamed Khalifa Boutahir, Y. F. M. A. I. Z. a. A. E. A., 2022. Effect of Feature Selection on the Prediction of. *BIG DATA MINING AND ANALYTICS,* 9(4), pp. 309-317.

Montangero, A. &. S. M., 2004. *Faecal Sludge Treatment.* Zurich: Swiss Federal Institute of Aquatic Sciences, Department of.

Mujumdar A.S., W. Z., 2007. THERMAL DRYING TECHNOLOGIES: NEW DEVELOPMENTS AND FUTURE R&D. *5th International Conference on Heat Transfer, Fluid Mechanics and Thermodynamics.*

Niwagaba, C. M. M. S. L., 2014. Faecal sludge quantification,characterisation and treatment objectives.. *aecal Sludge Management – Systems ApproachImplementation and Operation*, pp. 15-42.

Okuna, N. &. Y. A., 2000. *Evaluation of full scale thermal solidification processes implemented in Tokyo lightweight aggregate, slag and brick.* 69-76 ed. s.l.:Water,Science and Technology 41.

Panli Wang, D. M. P. Z. ,. Z. L. ,. P. Q. ,. Q. Z., 2019. Roof solar drying processes for sewage sludge within sandwich-like chamber bed. *Renewable energy,* Volume 136, pp. 1071-1081.

Perry, J., 2007. *Chemical Engineering Handbook.* 8th ed. New York: McGraw Hill.

Phindile Madikizela, S. H. R. K. L. K. W.-J., 2022. Disaster Risk Management, Ventilated Improved Pit Latrines, and Sanitation Challenges in South Africa. *Sustainability,* 14(6934).

Robert Foster, M. G. A. C., 2009. *Solar Energy: Renewable Energy and the Enviroment.* s.l.:CRC press.

Roediger, M., 2011. Medium-Temperature Belt Dryers for Biosolids. *Residuals and Biosolids,* pp. 510-520.

S.Septien, S. B. M. A. S. J. K. C., 2020. Effect of drying on the physical and chemical properties of faecal sludge for its reuse. *Journal of Environmental Chemical Engineering,* 8(1).

Samuel Getahun, S. S. J. M. T. S. I. M., 2020. Drying characteristics of faecal sludge from different on-site sanitation facilities. *Journal of Environmental Management,* Volume 261.

Sapienza, F., 2005. Thermal drying of wastewater solids. *Proceedings Of The Water Enviroment Federation,* pp. 690-700.

Sharma, A. C. C. L. N. V., 2009. Solar-energy drying systems: A review, Renewable and Sustainable Energy Reviews. Volume 13, pp. 1185-1210.

Smith, C., 1995. Revisiting solar power's past. Technology Review. pp. 38-47.

Tchobanoglous, G. B. F. M. I. N. c. &. E. H., 2003. *Wastewate Engineering: Treatment and Reuse.* 4th ed. New York: McGraw-Hill Company.

Turner, I. M. A., 1997. Mathematical modelling and numerical techniques in drying technology, Marcel Dekker Inc. p. 679.

V. L. Mathioudakis, A. G. K. ,. E. A. D. P., 2013. Sewage Sludge Solar Drying: Experiences from the First Pilot-Scale Application in Greece. *Drying technology.*

Visavale, G., 2012. *Solar drying : Fundamentals, Applications and Innovations.* s.l.:Individual Chapter.

Wei Ling, Y. X. ,. C. H. ,. B. Z. ,. J. H. ,. C. Z., 2022. Methods, mechanisms,models and tail gas emissions of convective drying in. *Science of the Total Enviroment*, Volume 845.

Wu Z.H, M. A., 2007. Simulation of the hydrodynamics and drying in a spouted bed dryer. *Drying Technology*, pp. 1-16.

Zhao G., Y. F. L. X. Y. D. G. W. W. L. S. R., 2020. Drying experiment and drying model analysis of dehydrated sludge particles. *Conference Series: Materials Science and Engineering*, p. 768.

Zheng Q., H. Z. L. P. N. L. H. G. Y. Y. Z. L., 2021. Effects of air parameters on sewage sludge drying characteristics and regression analyses of drying model coefficients. *Applied Thermal Engineering*, p. 198.

Appendix A: Psychrometric Chart

The psychrometric chart used in the preliminary calculations in this study is shown in Figure A-1.

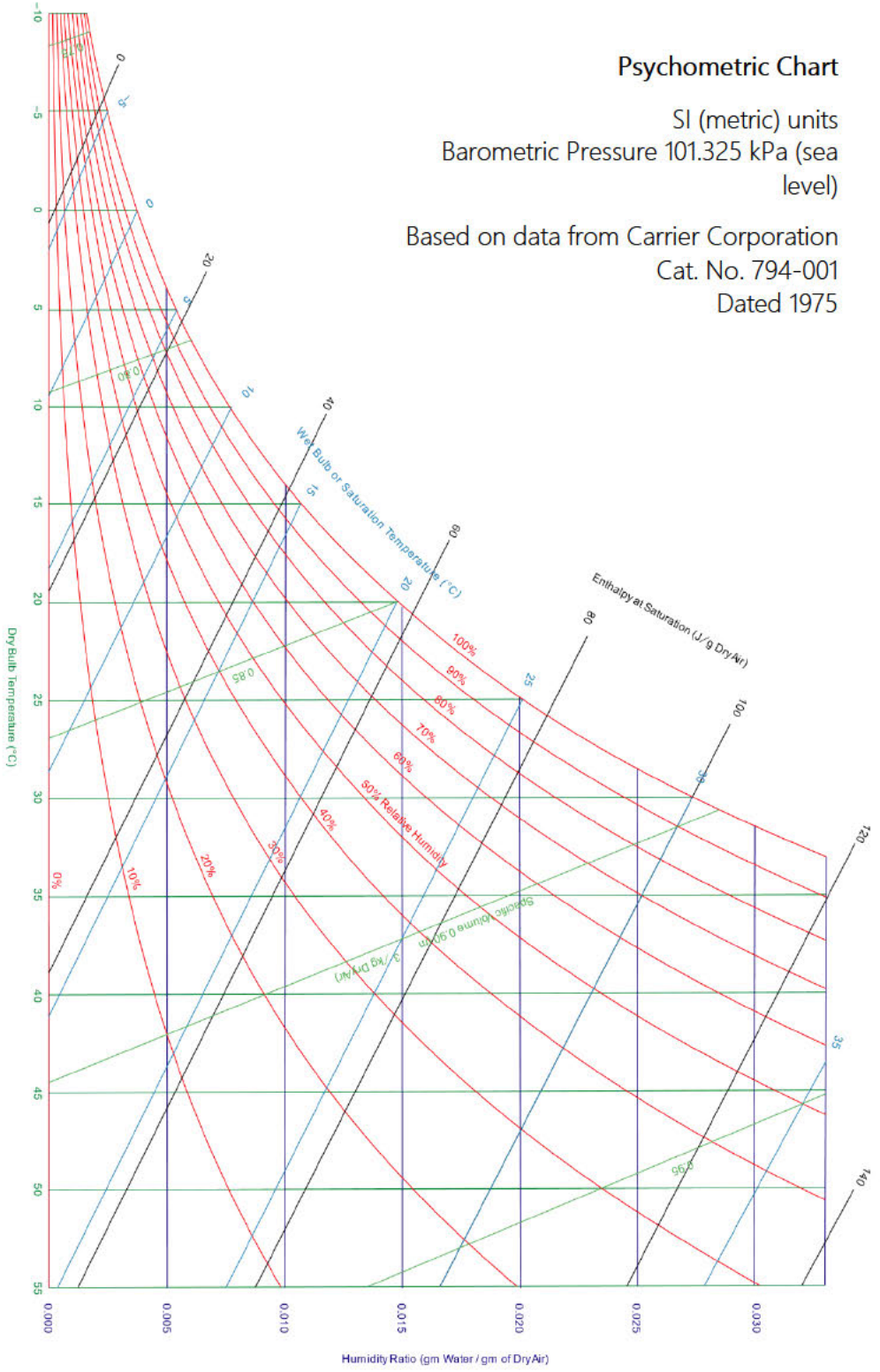

Figure A-1: Psychrometric chart.

Appendix B: Support for the Literature Review

Several thermal drying technologies were used for the treatment of sewage sludge. These technologies are used to treat sludge and produce useful material and energy. The figures below show some of the uses of sewage sludge treatment:

Figure B-1: Treatment of sewage sludge.

Thermal drying technologies include belt dryers (BDS), fluidized bed dryers (FDS) and drum dryers (DDS).

B-1. Belt Dryers

These dryers are used for small to medium evaporation capacity. Belt drying systems granulate sludge in a mixer with a product that has already been dried. The granules are distributed over the belt by feed modules. The even distribution of the sludge mixture creates optimum conditions for the even distribution of drying air. This is necessary for the even drying of the sludge. Below is a figure of a belt-drying plant using waste heat (Andritz, n.d.).

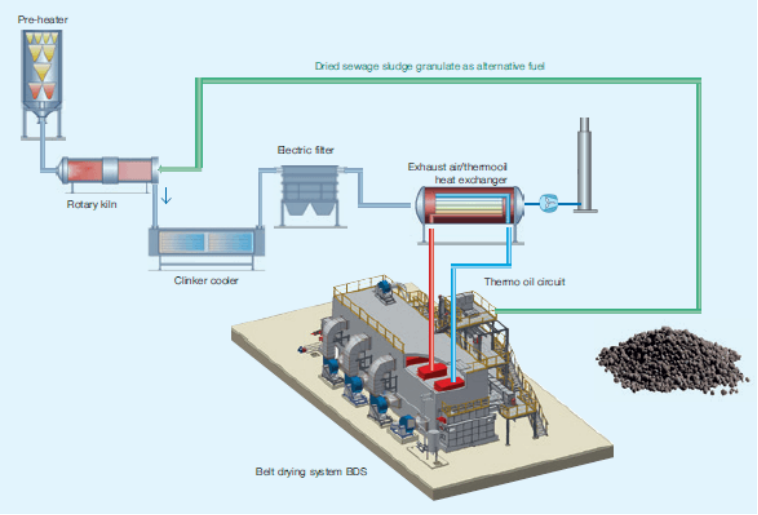

Figure B-2: Belt drying system for sludge (Andritz, n.d.).

B-2. Fluidized Bed Dryers

These dryers accommodate medium to large evaporation capacities. Heat for drying the sewage sludge is taken from the sludge gas produced from the dewatering of sewage sludge. The sludge gas is used to heat fluid bed dryers and achieve efficiencies of more than 90 % in modern incineration plants. The figure below shows a schematic of a fluid bed dryer system for drying sludge (Andritz, n.d.).

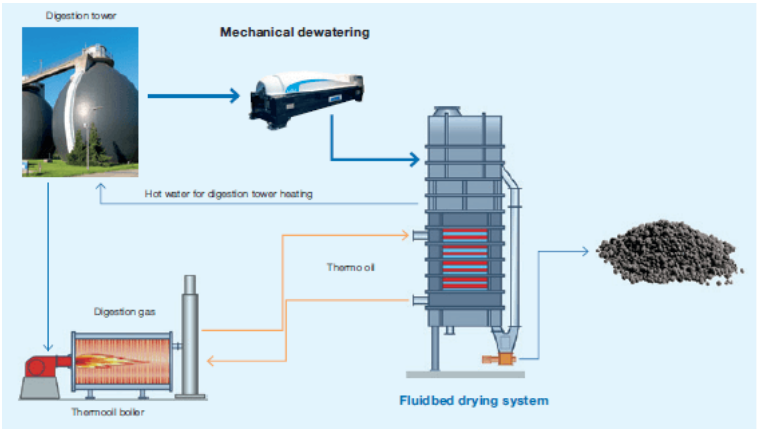

Figure B-3: Fluid bed dryer system for drying sludge.

B-3. Drum Dryers

These are one of the oldest processes for drying sludge. Dewatered sewage sludge is mixed in a mixer to dry the content of approximately 60 % of drying sludge-producing granules. The granules produced are fed to the drum. The hot gas flowing through the drum transports over the granulite sewage sludge and water contained in the sludge is evaporated (Andritz, n.d.).

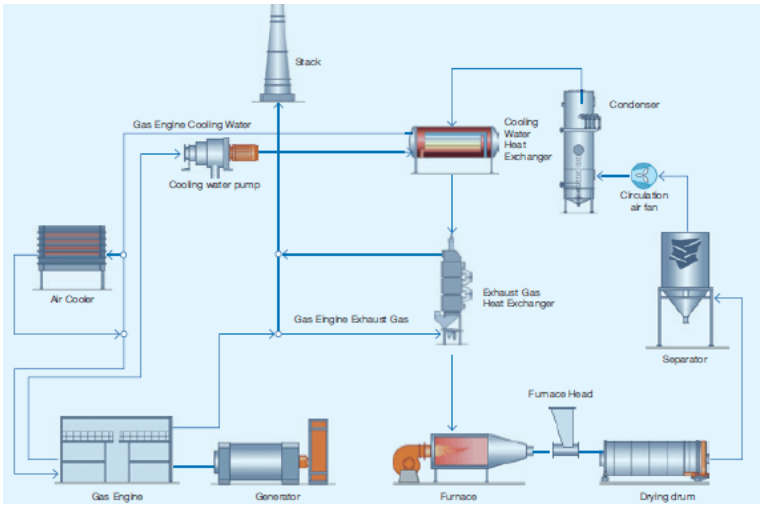

Figure B-4: Drum dryer for drying sludge (Andritz, n.d.).

B-4. Direct-Type Solar Dryers

Direct solar drying involves the spread out of the product to be dried in a thin layer, where it is left until the product has been dried up to desired moisture content. Turning off the product from time to time is effective in accelerating the drying of the moisture trapped under the product. The drying surface of these types of dryers is generally made up of concrete paved floors.

Figure B-5: Example of direct solar drying application.

B-5. Passive Direct-Type Solar Dryers

These types of solar dryers allow for the direct exposure of sunlight to the product, generally crops. This enhances the colour ripening desired in fruits, coffee and the development of roasted beans. There are two types of dryers in the category, these are solar cabinet dryers and greenhouse dryers.

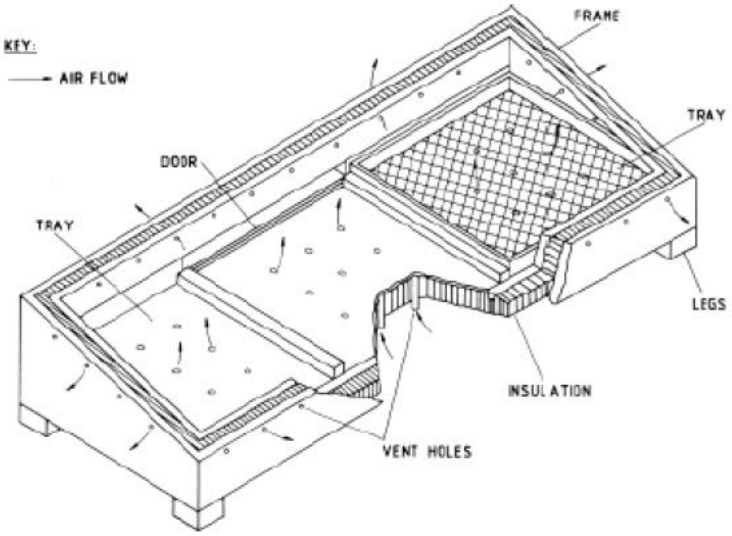

Figure B-6: Composition of a solar cabinet dryer (Ekechukwu, 1999).

B-6. Greenhouse Dryers

These types of dryers are also known as tent dryers and are derived from greenhouses. These dryers are designed with vents of appropriate size and positioning to provide controlled airflow. Figure B-7 below shows the controlled airflow in a simple greenhouse dryer example:

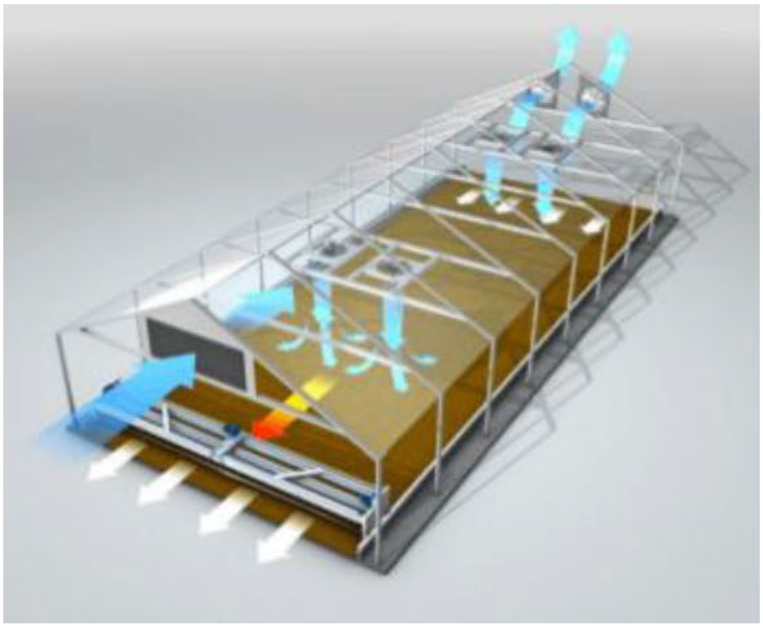

Figure B-7: Typical example of airflow in a solar dryer (Ekechukwu, 1999).

B-7. Active Direct Solar Dryers

Direct-type active solar dryers are like passive systems but are designed with an integrated solar energy collection unit. There are 3 identifiable active direct solar dryers absorption type, storage type and greenhouse dryers. The figure below shows an example of some typical active direct solar dryers:

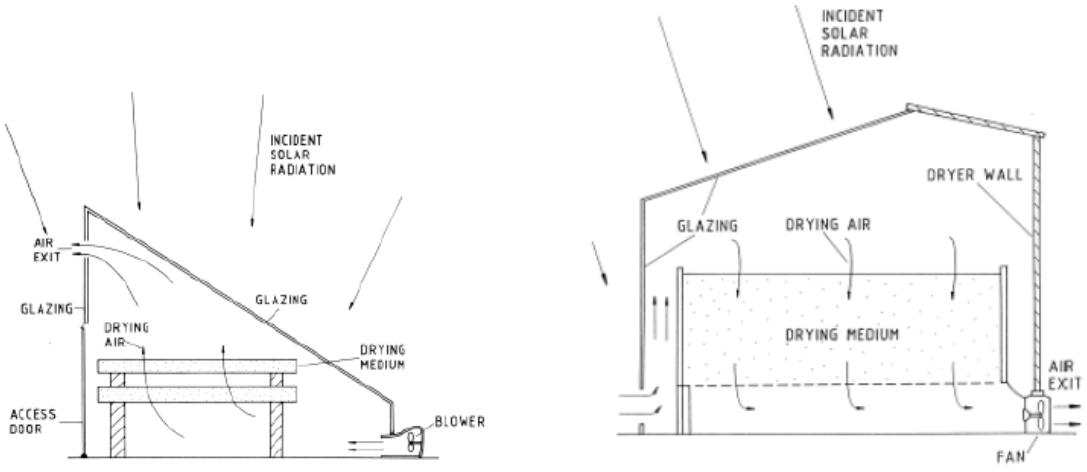

Figure B-8: A forced convection greenhouse dryer and a forced convection transparent roof solar barn (Ekechukwu, 1999).

B-8. Indirect-Type Solar Dryers

Differ from direct drying concerning heat transfer and vapour removal. Products in indirect solar dryers are located on trays or shelves inside a drying cabinet and a separate unit known as a solar collector is used to heat the air entering the cabinet. The heated air is allowed to flow over the product providing heat for the evaporation of moisture by convection heat transfer between the hot air and the wet product. Due to the difference in moisture concentration between dry air and the air in the drying cabinet. The working principle of indirect dryers is shown in Figure B-9.

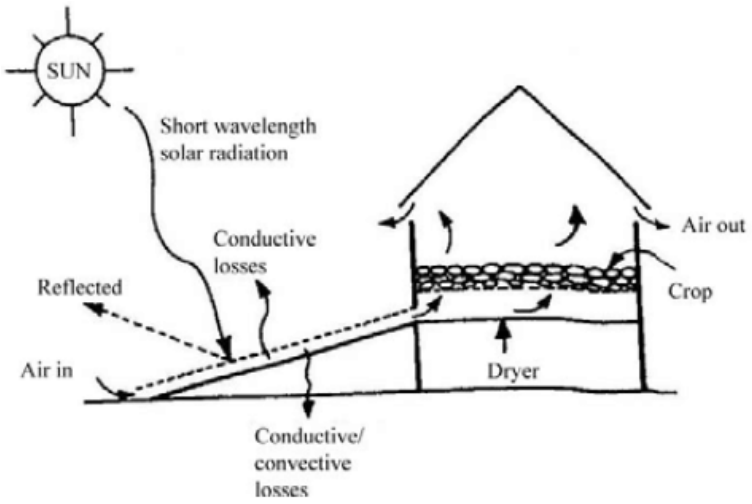

Figure B-9: Working principle of indirect solar dryers (Sharma, 2009).

B-9. Passive Indirect Solar Dryers

These are indirect solar dryers with natural convection of air for drying. To increase the volume of drying more than one try can be used to dry the product. Trays can be placed on vertical racks with sufficient space between trays. This creates the chimney which is the chimney effect which is generated from the resistance of the air created by the packing of the trays below and above each other. This effect increases the vertical flow of air as a result of the density difference between the air in the cabinet and the atmosphere (Visavale, 2012). The below figure shows you a simple design of a passive indirect solar dryer.

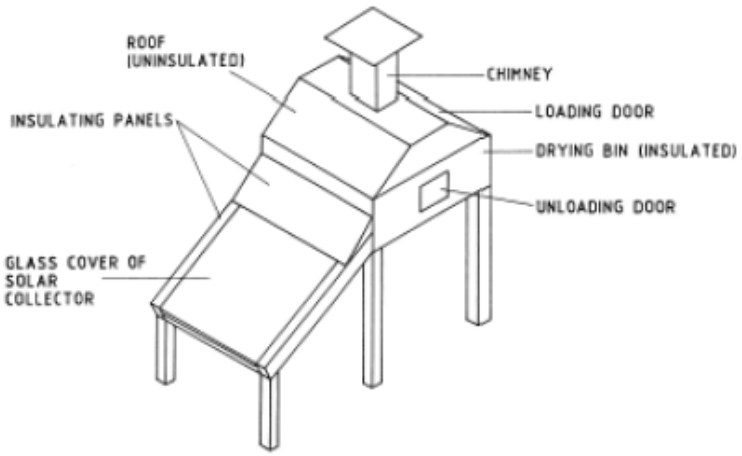

Figure B-10: A distributed-type natural circulation solar maize dryer (Ekechukwu, 1999).

B-10. Active Indirect Solar Dryers

These dryers have a separate collector and drying unit and generally comprise four basic components. These four components are a solar air heater, a drying chamber, ducting and a fan for air circulation. With control in flow rate, high temperatures can be achieved with these systems due to the separate air heating unit. To maximize the efficiency of energy, certain designs employ the recirculation of drying air, which ensures low exhaust temperatures of air. Below is an example of active indirect solar dryers.

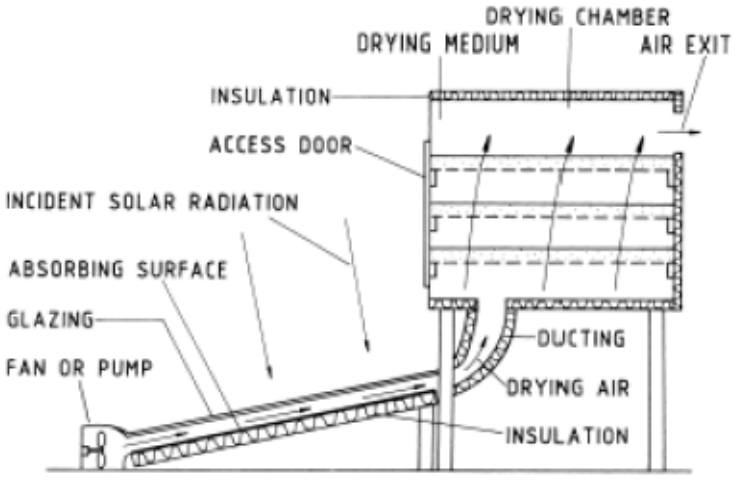

Figure B-11: Active Indirect solar dryer (Ekechukwu, 1999).

B-11. Passive Hybrid Solar Dryer

These types of dryers have the same structural features as indirect and direct-type dryers. These features include a solar air heater, a separate drying chamber and a chimney.

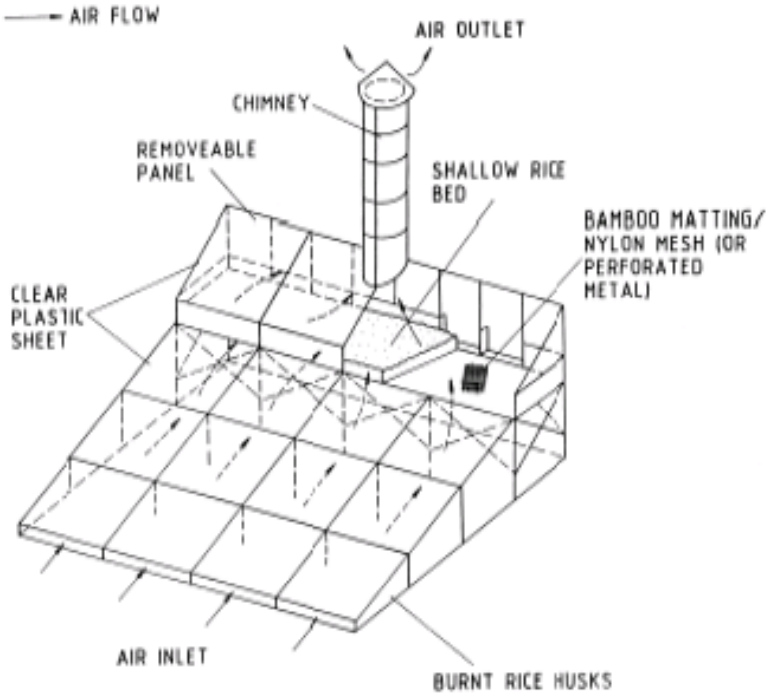

Figure B-12: Working principle of a hybrid solar dryer (Ekechukwu, 1999).

B-12. Active Hybrid Solar Dryer

These types of dryers incorporate solar energy together with an auxiliary source of energy and can be operated in combination or single mode with either energy source. These dryers are generally medium to large installations. The features of an active hybrid solar dryer are shown in the figure below:

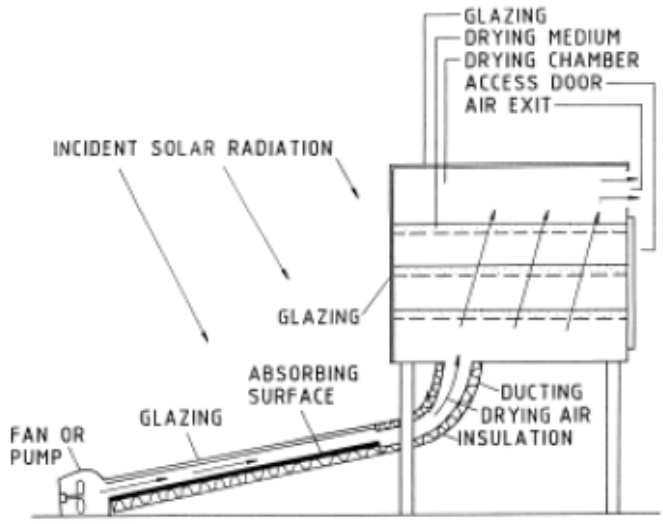

Figure B-13: Features of a typical mixed mode active solar dryer (Ekechukwu, 1999).

Appendix C: Thermal Drying Modelling

C-1. The Mathematical Model for Thermal Drying

Thermal dehydration processes are highly energy intensive and are found in most of the industrial sector. It is therefore important to understand the behaviour of a system before designing further. With the use of simulation software, a system can be modelled and by subjecting the model to computational fluid dynamic parameters, heat and mass transfer phenomenon and thermodynamics, a mathematical model is created. Mathematical modelling is an essential tool in simulating the performance and success of a product before it is manufactured.Modelling specifies key parameters simulating real scenarios based on scientific principles and data to determine the reliability and success of the product. Using mathematical and scientific principles modelling software allows the user to re-create a scenario based on ideal conditions. Model-based control is becoming very popular to ensure good thermal efficiency, safe operation and product quality (Wu Z.H, 2007). Below are some of the mathematical modelling techniques for the drying process:

- **Computational Fluid Dynamics (CFD) model**: These models attempt to simulate the interaction of liquids and gases where the surfaces are defined by boundary conditions. These are comprehensive models for engineering problems. Governing equations, boundary conditions and initial equations are applied to these types of models. Examples of applications of CFDs are the modelling of spray, fluid and spouted bed drying (Huang L.X., 2005).
- **Discrete Element model**: These models use numerical techniques to simulate the behaviour of a population of independent particles. The tracking motion of individual particles is accurate in description, dynamics and particulate phase change. Discrete Element models are generally expensive in computation. Examples of application are particle mixing in a drum, and particle dynamics in fluids and spray beds (Li J., 2003).
- **Finite Element Analysis**: These models use numerical techniques to simulate the behaviour of a population of independent particles. Often used in modelling moisture transfer in wet solids. No need for additional equations to assure continuity across common boundaries. Easy to handle complex geometries, mesh gradation and mixed boundary conditions. These models are easy to program and don't come at expensive computational costs depending on the mesh sizing and fundamental equations used. Examples of applications are rice drying, grain drying and thin-layer drying (Turner, 1997).

The modelling of dryers generally has two sub-models. These are the drying model, which deals with the drying characteristics of the material being dried and the equipment model which deals with the way the material is handled in the equipment. Equipment modelling deals with the heat and mass transfer rates and the residence time the material stays in the dryer. Both these models require a considerable amount of empirical data such as drying kinetics over parameter ranges and the behaviour of the material under a range of parameters that the dryer operates under (Mujumdar A.S., 2007).

Appendix D: CFD Simulations

D-1. Air Flow Direction

Various simulations of different ventilation layouts are undertaken to determine the best flow pattern. Inlet extractor fans positioned on the top of the dryer were determined as the best position for air to enter the dryer. The air entering the dryer will contact the aluminium wall which is exposed to sunlight. Air is heated as it moves down the wall. The faecal sludge is located closer to the bottom of the dryer therefore Atmospheric pressure inlet is modelled on the bottom holes of the absorber wall to direct hot air directly over the faecal sludge. Extractor fans at the outlet were mounted on the middle and bottom sections of the back wall of the drying chamber (DC). Circulation fans were situated above the drying tray on the side walls to create better distribution of air over the drying tray and throughout the dryer.

Air enters the dryer at the inlet and moves down the aluminium wall to the inlet into the drying chamber. Air enters both the top and bottom sections of the drying chamber. The air entering the bottom section of the dryer comes will come into contact with the bottom surface of the faecal sludge through the fine tray mesh. The air flows directly over the faecal sludge in the top section of the drying chamber. The fans allow for air to circulate within the top section of the drying chamber.

Thermal dehydration processes are highly energy intensive and are found in most of the industrial sector. It was therefore important to understand the behaviour of a system before designing further. Simulation software is a design tool used for the optimization and improvement of technologies. Simulations are based on physical models. Using mathematical and scientific principles, modelling software allows users to calculate thermal and airflow results for the performance of the different dryers. Steady-state thermal analysis and airflow simulations were conducted to determine the performance of different greenhouse dryer designs. The airflow rate was determined through calculations shown in Appendix E.

The following conditions were applied to the solar dryer models:

- Energy.
- Radiation on.
- Gravity.
- Transient model.
- K-Epsilon.
- 25 °C operating temperature.
- Solar calculator for Durban latitude and longitude.
- PMMA material applied to dryer walls.
- Aluminium material applied to the floor, table, tray and absorber wall (heat flux).
- Intake fan.
- Pressure inlet – Atmospheric pressure.
- Mass flow outlet for at to enter DC at flow rate 1 kg/s.
- Mass flow outlet for air exiting DC at 1 kg/s.

The position of ventilation and circulation equipment plays an essential role in the construction of a dryer. Inlets and outlets must be placed in locations that provide a suitable airflow path. The objective of this was to determine the best-suited position of ventilation and circulation for the optimum airflow path. Air must flow across the faecal sludge to promote uniform drying and maximize drying rates. The ventilation and circulation fan positions were determined by computational fluid dynamics simulations conducted using ANSYS mechanical software. Figure D-1 and Figure D-2 show the best airflow stream patterns simulated within the dryer enclosure.

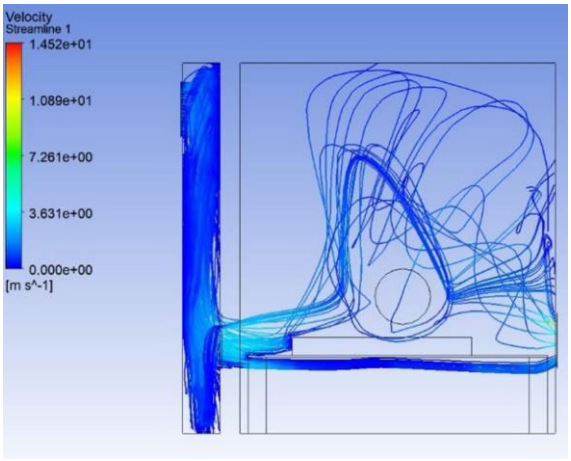

Figure D-1: Velocity air stream within the dryer.

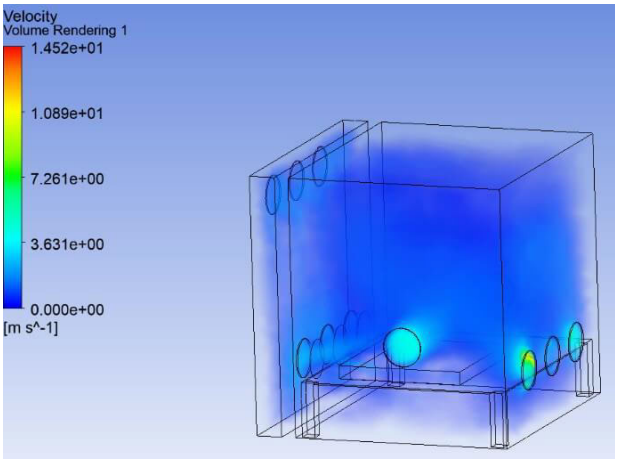

Figure D-2: Volume of air stream within the dryer.

Thermal dehydration processes are highly energy intensive and are found in most of the industrial sector. It is therefore important to understand the behaviour of a system before designing further. Simulation software is a design tool used for the optimization and improvement of technologies. Simulations are based on physical models. Using mathematical and scientific principles, modelling software allows users to calculate thermal and airflow results for the performance of the different dryer designs. Literature for thermal modelling of dryer systems is shown in Appendix C.

D-2. Temperature Fluctuations

A thermal simulation was conducted to determine an approximate temperature the air and dryer enclosure could reach. Steady-state thermal analysis was conducted to determine the temperature fluctuations. Simulation results for the thermal simulation are shown in Figure D-3. The greenhouse dryer was estimated to reach temperatures of more than 40 °C. The absorber wall was modelled in the simulation therefore an approximate effect of the temperature fluctuations the absorber will have in the dryer can be observed.

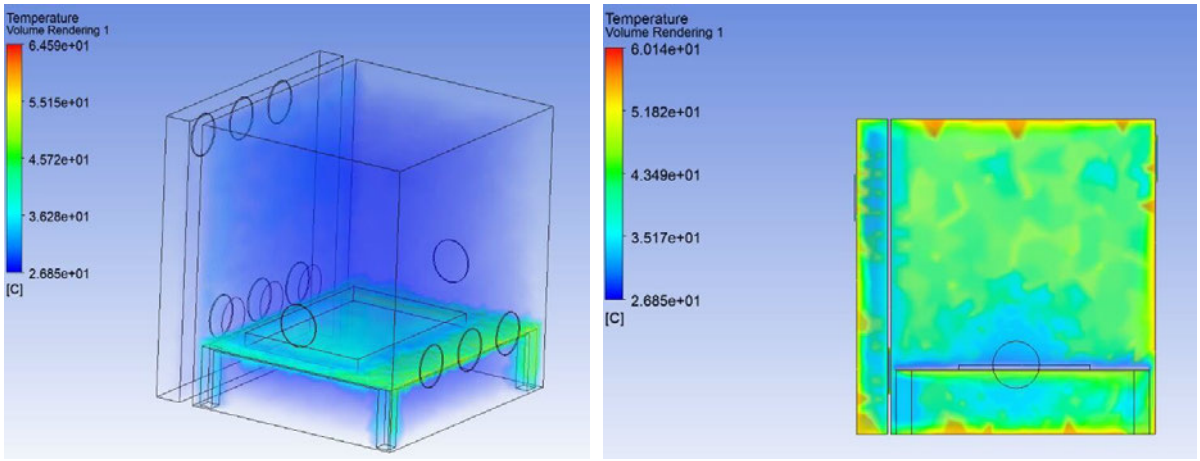

Figure D-3: Air temperature distribution over table and drying tray (left) and air temperature fluctuations inside the greenhouse enclosure during operation (right).

Thermal analysis of the solar dryer yielded maximum air temperatures of around 40 to 50 °C. This is a realistic temperature for the dryer to reach for effective drying of faecal sludge. The tray, faecal sludge and table are also exposed to solar radiation and therefore also heating passing air in the drying chamber. Figure D-4 shows the temperature distribution of air moving over the faecal sludge on the drying tray.

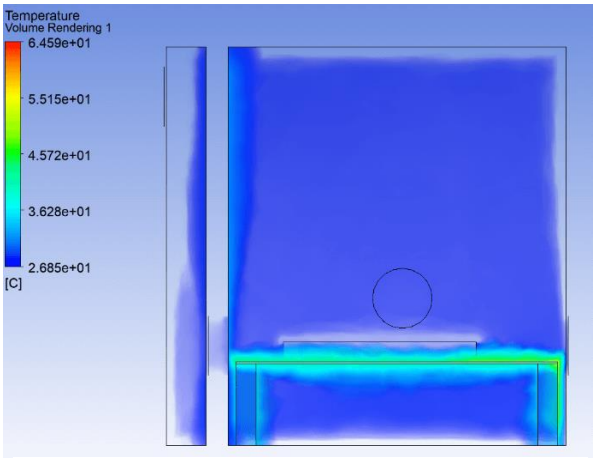

Figure D-4: Temperature of air flowing over faecal sludge.

Concrete and aluminium are used in the modelling of the dryer. Aluminium offers much higher thermal conductivity whereas concrete offers more storage of heat for later use. Simulation results for the various other air flow patterns are illustrated in the figures below:

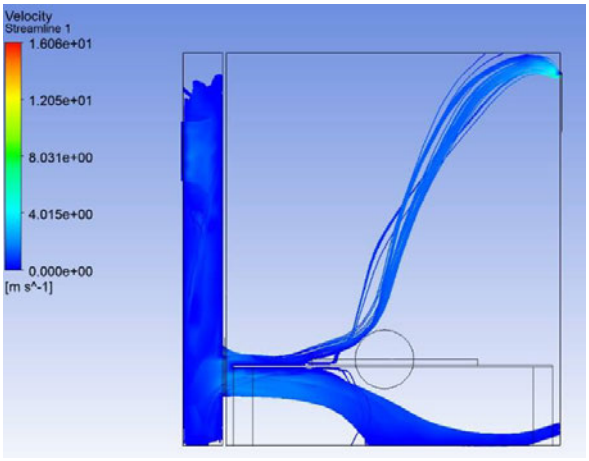

Figure D-5: Airflow pattern result 1.

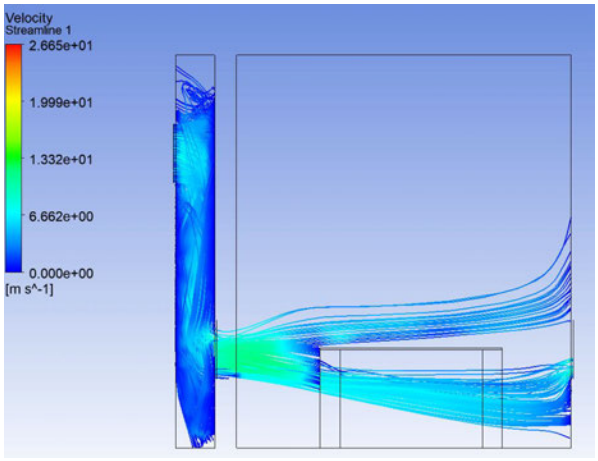

Figure D-6: Airflow pattern result 2.

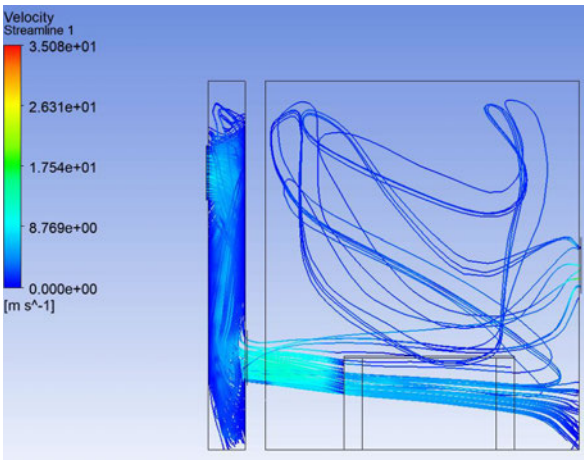

Figure D-7: Airflow pattern result 3.

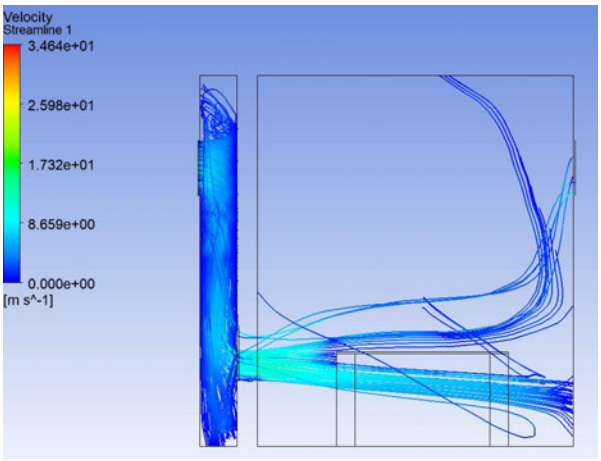

Figure D-8: Airflow pattern result 4.

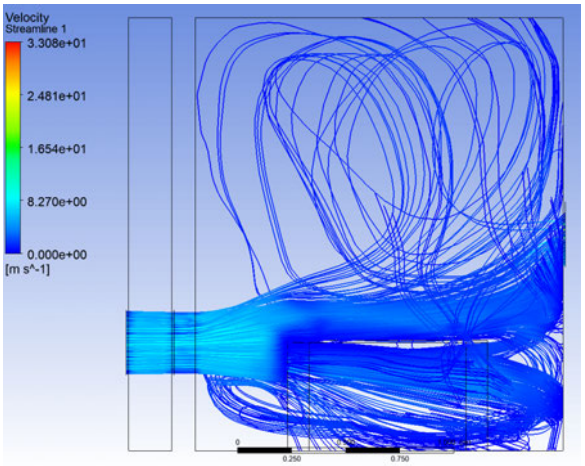

Figure D-9: Airflow pattern result 5.

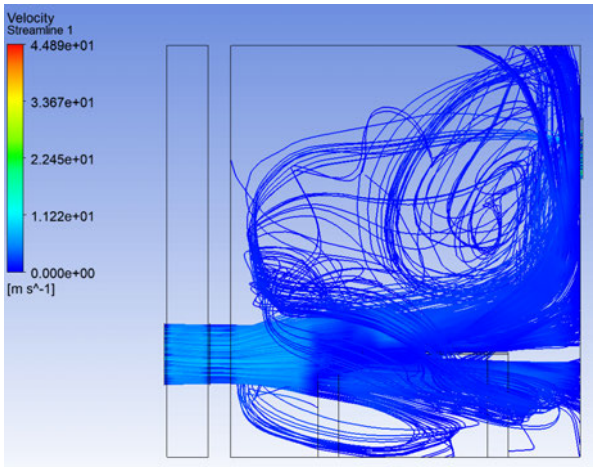

Figure D-10: Airflow pattern result 6.

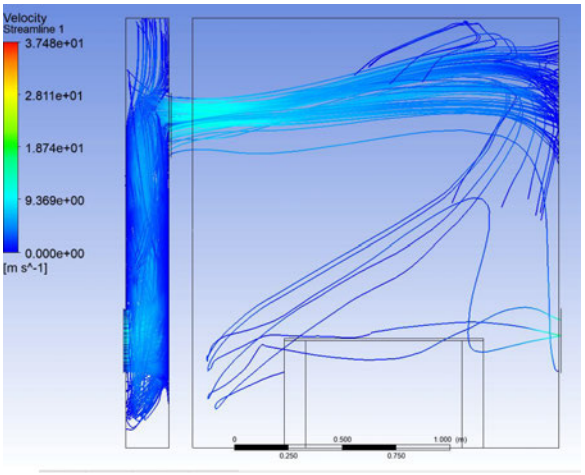

Figure D-11: Airflow pattern result 7.

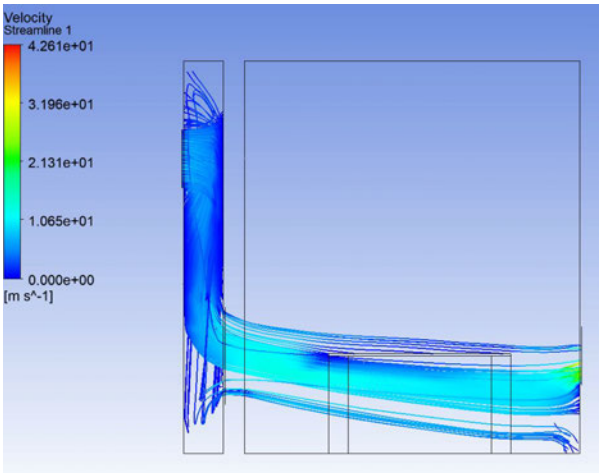

Figure D-12: Airflow pattern result 8.

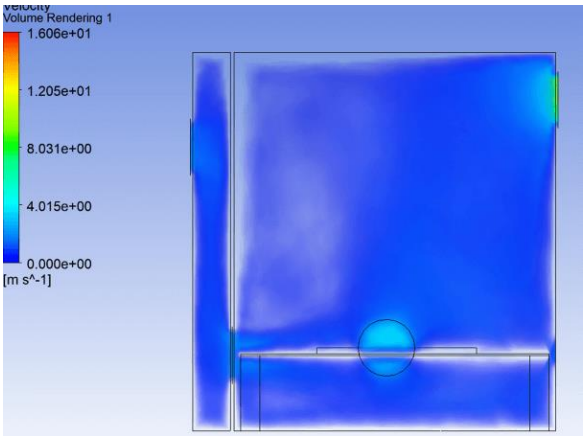

Figure D-13: Air volume rendering result 1.

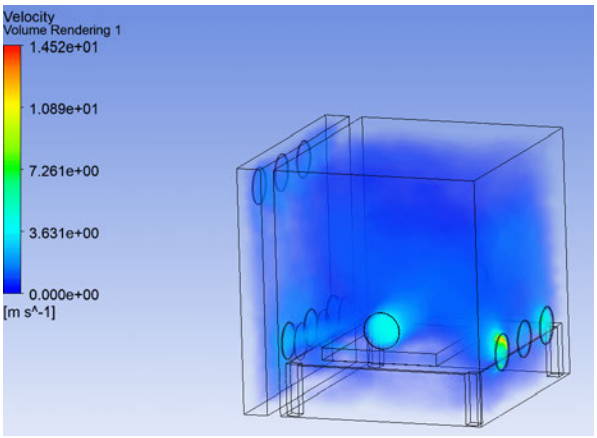

Figure D-14: Air volume rendering result 2.

Appendix E: Design Calculations

E-1. Design Assumptions

Calculations are derived to determine the ventilation power required to dry different volumes of faecal sludge. Theoretical calculations of drying time and relative humidity are important to determine the performance of a greenhouse solar dryer. Table E-1 lists the information required for calculating the ventilation flow rate, drying times and humidity inside a dryer that was located at Howard College.

Table E-1: Design assumptions.

Items	**Assumption**
Ambient Air Temperature (T_{am})	25 °C
Ambient Relative Humidity	70 %
Solar Irradiance (I)	200 W/m² averaged over hours
Initial Moisture Content (M_i)	70 %
Final Moisture Content	20 %
Relative Humidity in the dryer (RH)	80 %
The density of faecal sludge	1200 kg/m³
Initial mass per drying sample (M_p)	40 kg
The heat of vaporization (H)	2260 kJ/kg
Dryer efficiency (n_d)	25 %
Transmittance (n_t)	70

E-1.1. Change in Moisture Content

The water may be contained in a solid in various forms such as moisture or bound form and directly affects the drying. Evaporation of liquid water into vapour requires a large amount of energy (2,260 kJ/kg at 101.3 kPa). The change in moisture content (Δm) is calculated using Equation 5.

Equation 5

$$\Delta m = M_p \left(\frac{M_i - M_f}{100 - M_f} \right)$$

Where:

M_p = Mass of product.

M_i = Initial moisture content.

M_f = Final moisture content.

Using Equation 5 and above assumptions, the moisture content is calculated.

$$\Delta m = 40\left(\frac{70-20}{100-20}\right) = 25\ kg\ of\ water$$

E-1.2. Drying time

The energy in the system was conserved therefore $E_{in} = E_{out}$. The drying time was determined using the following formula:

Equation 6

$$I \times S_{col} \times n_t = \frac{n_d \times \Delta H \times \Delta m}{t_d}$$

Where:

I = Solar irradiance (W/m²).

S_{col} = Surface area of the collector (m²).

n_t = Transmittance efficiency of PMMA.

n_d = Dryer efficiency.

ΔH = Heat of vaporization of water (J/kg).

Δm = Change in moisture content (kg).

t_d = Drying time.

Therefore, the drying time (t_d) can be expressed as:

Equation 7

$$t_d = \frac{n_d \times \Delta H \times \Delta m}{S_{col} \times n_t}$$

Using Equation 7, drying time (t_d) was calculated.

$$t_d = \frac{0.25 \times 2400 \times 10^3 \frac{J}{kg} \times 25}{300 \frac{W}{m^2} \times 4 \times 0.75} = 12500\ seconds = 3.47\ hours$$

E-1.3. Mass flow rate of air

Using a mass balance, the mass flow rate of air can be determined. The addition of the mass flow rate of air entering ($\dot{m}_{wi}$) and the moisture that has evaporated from the faecal sludge ($\dot{m}_a$) per the drying time (t_d)will determine the output flow rate of air ($\dot{m}_{wf}$). The mass balance of water is shown below:

Equation 8

$$\dot{m}_{wi} + \Delta\dot{m} = \dot{m}_{wf}$$

Equation 9

$$\dot{m}_a y_i + \frac{\Delta m}{t_d} = \dot{m}_a y_o$$

Using a Psychometric chart, the following values are determined:

y_i = Humidity ratio at the inlet.

y_o = Humidity ratio at the outlet.

Equation 10

$$\dot{m}_a = \frac{\Delta m}{t_d(y_o - y_i)}$$

To determine the volumetric flow rate of the water and air mixture (V_f) we divide the mass flow rate ($\dot{m}_a$) by its density (p). Therefore, the volume flow rate was:

Equation 11

$$V_f = \frac{\dot{m}_a}{p}$$

E-1.4. Water Activity vs Moisture Content

Figure E-1 shows the water activity versus moisture content in faecal sludge from Urine Diversion Dry Toilets (UDDT) and Ventilated Improved Pit (VIP) Latrine from the eThekwini Municipality:

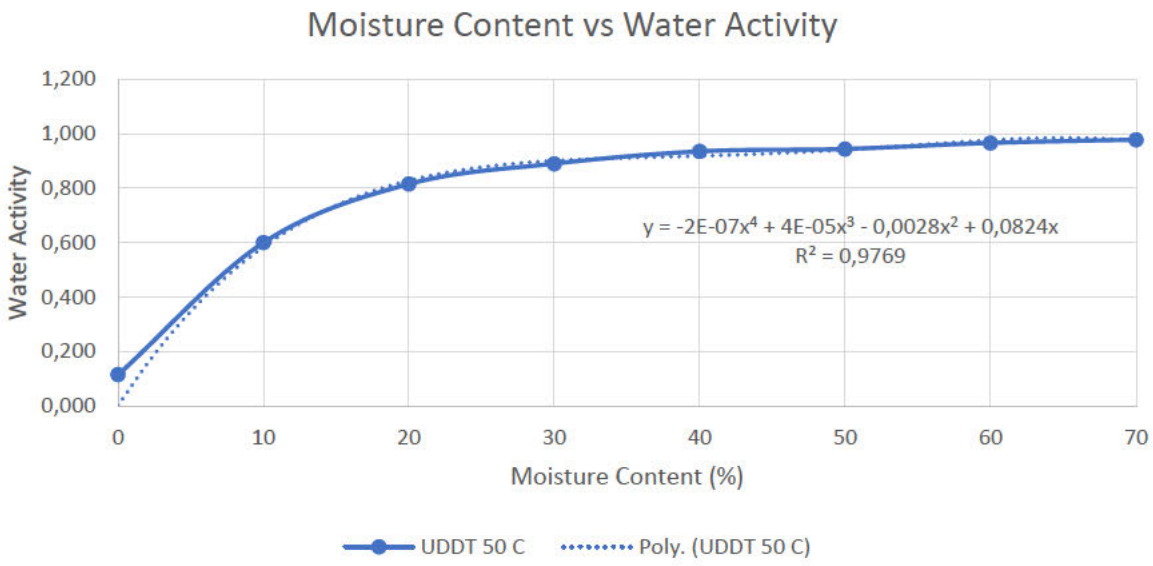

Figure E-1: Moisture content vs water activity.

To determine the mass flow rate of air, the initial humidity ratio of air (y_i) and humidity ratio of air exiting the dryer (y_o) must first be determined. The temperature of the air entering the dryer was assumed to be 25 °C and the relative humidity of air in the outside environment was roughly assumed to be 70 %. The temperature of the air leaving the dryer was also to be set higher at 30 °C and a relative humidity of 80 % inside the dryer. Using a Psychometric chart, the following values are determined:

y_i = humidity ratio at the inlet = 0.00949 kg of water per kg of dry air.

y_o = humidity ratio at the outlet = 0.01033 kg of water per kg of dry air.

Using Equation 10, the mass flow rate of air required to dry a specified mass of faecal sludge was calculated.

$$\dot{m}_a = \frac{\Delta m}{t_d(y_o - y_i)} = \frac{25}{12500(0.01033 - 0.00949)} = 2.38\ kg/s$$

To determine the volumetric flow rate of the water and air mixture we divide the mass flow rate by its density. Equation 11 was used to calculate the volumetric flow rate of air, therefore; the volumetric flow rate was:

$$V_f = \frac{\dot{m}_a}{p} = \frac{2.38}{1.25} = 1.904\ m^3/s = 6854\ m^3/h$$

According to the calculations, a volumetric flow rate of 6,854 m³/h of air was needed to dry 40 kg of faecal sludge or 171 m³/h/kg of sludge.

E-1.5. Rake system calculation

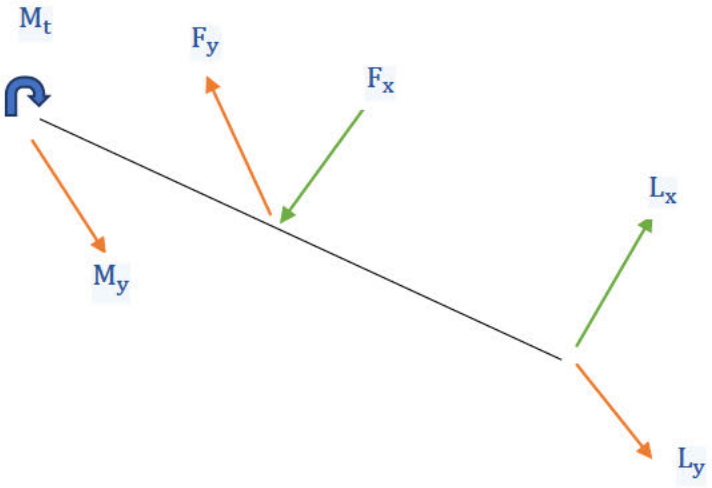

To determine the force required by the linear actuator, the resistance force of faecal sludge must first be assumed. The rake system will experience force resistance from the faecal sludge expressed as a force. This force can help determine the force the linear actuator will require to push through faecal sludge. The resistance force of faecal sludge was determined by the stickiness of the faecal sludge. The overall stickiness of faecal sludge was made up of both cohesive and adhesive forces. Experiments estimate a maximum cohesive force of 110.43 N and max adhesive forces of around 35.6 N. Therefore, F_x = 146.03 N.

Therefore, the sum of forces about the actuator at equilibrium will yield L_x = 140.03 N.

To determine the torque of the motor required for the blade, the yield stress of faecal sludge was required. The maximum yield stress of faecal sludge was estimated to be around 1,000 Pa.

Equation 12

$$\frac{\tau}{r} = \frac{T}{J} = \frac{G\theta}{L}$$

$$J = \frac{\pi d^4}{32} = \frac{\pi \times 0.1^4}{32} = 9.82 \times 10^{-6}\ m^4$$

Using Equation 12 yields:

$$T = \frac{1000 \times 9.82 \times 10^{-6}}{0.05} = 0.1964\ N{\cdot}m$$

Appendix F: Material Specifications of the Greenhouse Dryer

The market review discusses the material selection, material costing, testing Instrumentation and the total cost for the various sub-systems.

F-1. Selection of Material

It was important to identify the various subsystems that make up a component. This allows for better identification of the various applications and purposes of each component making up a product. For the design of a solar dryer, the subsystems determined are the Enclosure, ventilation, absorber wall, rake system and water drainage.

The enclosure was made up of both the drying chamber and the collector which are critical components needed for the drying process. The drying chamber houses the air needed for drying and was the enclosure in which the faecal sludge was to be dried. The collector allows air to enter the dryer and pass through an absorber wall into the drying chamber. Solar dryers utilize both air and sun radiation to dry a product or material. Various types of materials are used in the development of dryers. Greenhouse dryers use transparent material that allows for sunlight to pass into the drying chamber to dry a product. For the drying of faecal sludge, it was important to find materials with good chemical, thermal and mechanical properties. Figure F-1 below shows some of the transparent materials available for the design of a greenhouse solar dryer.

Hard Polymers	Transparency	Stiffness	Toughness	Heat resistance	Processability	ESCR	Scratch resistance	UV stability	Relative cost	Supplier	Brand
GPPS	+++	+++	--	+	+++	--	+	--	€	Styrolution	Styrolution PS
MABS	++	+	++	+	++	++	+	-	€€	Styrolution	Terlux
SAN	+++	+++	+	++	++	++	+	++	€€	Styrolution	Luran
SMMA	+++	++	-	+	+++	+	+	-	€€	Styrolution	NAS
MBS	++	-	++	-	+++	+	+	-	€€€	Styrolution	Zylar
SB Copolymer	+	-	+	-	-	+	-	-	€€	Styrolution	Styrolux
PC	+++	+	+++	+++	-	--	++	++	€€	Sabic IP / Teijin	Lexan / Panlite
HH PC	++	+	+++	+++	-	--	++	++	€€€	Sabic IP	Lexan
PET	++	+	+++	-	--	+++	+	++	€	Artenius	Bright, Shape, Design etc.
PET-G	+++	+	+++	-	--	+++	+	++	€€	Artenius	Xcel
PMMA	+++	+++	-	++	-	-	+++	+++	€€	Evonik	Plexiglas
PEI	+	++	+++	+++	--	+	++	+	€€€€	Sabic IP	Ultem
PES	+	++	+++	+++	--	++	++	-	€€€€	BASF	Ultrason S
PSU	+	++	+++	+++	--	+++	++	-	€€€€	BASF	Ultrason E
PP H	--	--	-	+	++	++	-	+	€	LyondellBasell	Moplen
PP R	-	--	+	+	++	+++	-	+	€	LyondellBasell	Moplen
LDPE	-	--	+++	--	+++	+++	-	+	€	LyondellBasell	Lupolen
PLA-based	+	+	--	-	+	-	+	-	€€€	FKUR	Bio-Flex
Glass	+++	+++	--	+	--	+++	+++	+++			

+++ excellent ++ very good + good - fair -- poor

Figure F-1: Transparent properties of various plastics (Ekechukwu, 1999).

The factors that are most important for the design of a solar dryer are transparency, UV stability, heat resistance and relative cost. Emphasizing these factors will help to determine the most effective polymers for the design of a greenhouse solar dryer. SAN, PC, PETG and PMMA display the best properties. PMMA was selected due to its superior transparency and UV stability properties. PMMA plastic also allows higher frequency and higher energy light to transmit through its surface. Figure F-2 shows the UV properties of the different plastics. PMMA reflects better UV stability than Polycarbonate and polystyrene. PMMA will allow high-energy rays to be transmitted into the greenhouse and offer better UV stability. A low transmittance suggests that the polymer doesn't allow light at that frequency to pass through. In this case, the rays are either absorbed or deflected. This can lead to thermal fluctuations and discolouring of the different plastics.

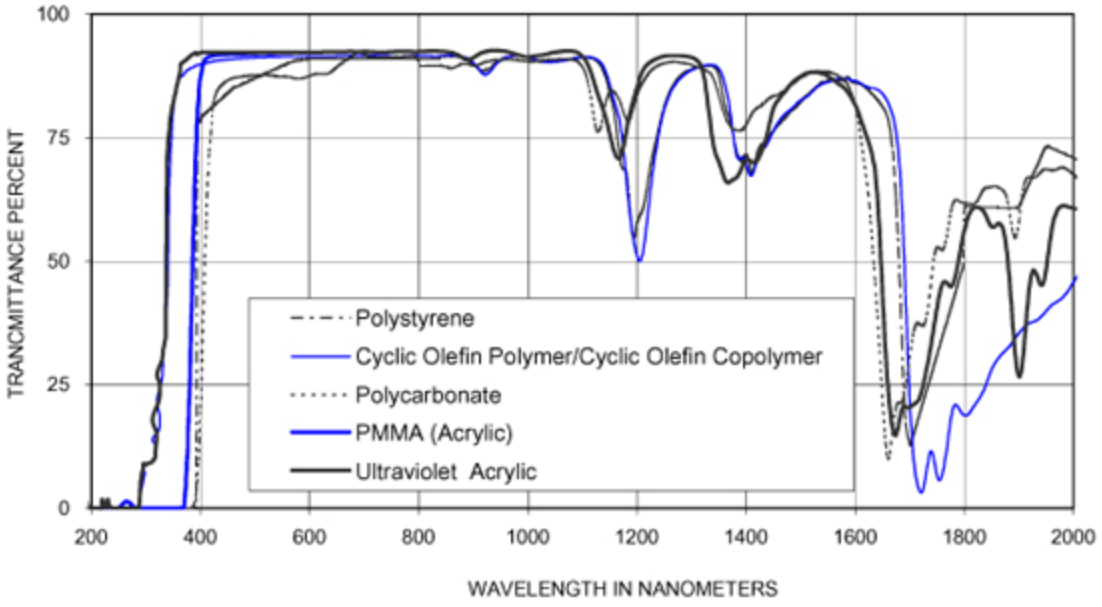

Figure F-2: UV properties of transparent plastic (Ekechukwu, 1999).

Aluminium was selected for the development of the enclosure frame and absorber wall. Aluminium has excellent corrosion resistance and thermal conductivity. Aluminium was also cheaper than stainless steel. The aluminium was painted black to retain heat. Axial fans were selected to develop the ventilation system for the greenhouse solar dryer. The fan positioning was determined using simulation software. Circulation fans were selected for the distribution of air within the drying chamber. These fans will allow air to circulate inside the dryer and maximize contact with faecal sludge inside the collector. A high torque motor, linear actuator, Arduino board, guide rail and motor drivers were selected to design a rake system. Temperature and humidity sensors and an ESP32 module were selected to develop a temperature and humidity control system. The properties of the various materials available and the selected material are shown in Appendix F.

F-1.1. Enclosure

The materials investigated for the enclosure walls are listed below:

F-1.1.1. Polycarbonate (PC)

PC plastics are commonly used in the manufacture of vehicle components, eyewear, medical devices and greenhouses. These plastics exhibit similar properties to glass and unlike glass have better impact resistance. Various colours and shades of PC are commercially available and the material used to produce PC allows for effective transmission of light similar to that of glass. PC has a very good UV stability which prevents degradation of PC when exposed to sunlight over long periods. This plastic was highly heat resistant which was an important criterion in a dryer design. These thermoplastics can withstand temperatures up to 200 °C and have a tensile strength of more than 50 MPA.

F-1.1.2. Poly(methyl methacrylate) (PMMA)

PMMA was also known as acrylic or acrylic glass. Acrylic has many advantages due to its high transparency, excellent light transmission and high resistance to UV light and scratches. Different grades of PMMA allow up to 90 % of light to pass through it and was tough, durable and lightweight thermoplastic. The only big disadvantage of PMMA was its poor impact resistance and its brittle. PMMA was a tough plastic that was prone to crack under excessive load. PMMA has limited heat resistance and can withstand temperatures up to 80 °C. Acrylics have limited chemical resistance and can cause degradation when exposed to organic solvents such as chlorine.

F-1.1.3. Polyethylene Terephthalate Glycol (PETG)

PETG was commonly used to produce plastic bottles, food storage containers and packaging material. Its toughness and feasibility make PETG a viable option when compared to PMMA and PC plastic. PETG provides significant chemical resistance and durability. Similar to PC, PETG has good impact resistance and was easily fabricated (ACME Plastics.com, 2020).

F-1.1.4. Polyetherimide (PEI)

PEI plastics are high-strength, temperature and chemical-resistant plastic. These plastics are commonly used in automotive, electrical, medical and industrial applications. PEI plastics are inherently flame retardant and offer high tensile strength over a wide range of temperatures. PEI was expensive to manufacture and offers less UV stability as compared to PC, PMMA and PETG.

UV light was part of the solar spectrum and was higher energy light rays compared to visible and infrared light. UV light was split into three categories, which are UVA, UVB and UVC. The table below states the wavelength ranges for these three categories and the common effect these rays can have.

Table F-1: UV light categories.

Description	Wavelength range (nm)	Common effect
UVA	320–400	Skin tanning
UVB	280–320	Skin burning
UVC	100–280	Germicidal

UV rays can cause a photochemical effect within a polymer structure and this can lead to the degradation of the polymer structure. Many polymers offer high resistance to UV rays and can easily deal with high-energy rays of short wavelengths. Polymers that offer high transmittance at low wavelengths offer better UV stability. Over long periods polymers will degrade and become weaker. Therefore, it was essential to choose the most UV-stable polymer for the design of a solar dryer.

PMMA acrylic sheet was selected for the enclosure's transparent walls due to its high transparency and good UV stability.

PMMA acrylic sheet

Also known as acrylic or acrylic glass. Acrylic has many advantages due to its high transparency, excellent light transmission and high resistance to UV light and scratches. Different grades of PMMA allow up to 90 % of light to pass through it and is tough, durable and lightweight thermoplastic. The only big disadvantage of PMMA is its poor impact resistance and its brittle. PMMA is a tough plastic that is prone to crack under excessive load. PMMA has limited heat resistance and can withstand temperatures up to 80 °C. Acrylics have limited chemical resistance and can cause degradation when exposed to organic solvents such as chlorine.

From the figure above, PMMA reflects better UV stability than that Polycarbonate and polystyrene. PMMA will allow high-energy rays to be transmitted into the greenhouse and offer better UV stability. A low transmittance suggests that the polymer doesn't allow light at that frequency to pass through.

Aluminium

Aluminium has high corrosion resistance and is widely used in many applications. Many different items are made from aluminium angle, square tubing and sheet. Aluminium also offers good corrosion resistance, and ductility and is relatively cheaper than stainless steel. An aluminium angle is used for the construction of the solar dryer frame that will hold the PMMA sheets in place. Aluminium's corrosion and chemical resistance properties make it an ideal fit for the drying of faecal sludge.

The dryer floor and absorber wall are constructed with aluminium sheet metal. Aluminium has a considerably high thermal conductivity and is much cheaper than metals such as copper and silver which have much higher thermal conductivities but are very expensive.

F-1.2. Absorber Wall

An absorber wall was implemented into the design of a greenhouse solar dryer to either heat air passing through the dryer or store heat for later use. The ambient air passing through the solar dryer can achieve higher temperatures by implementing an absorber wall in the solar dryer. For this application, it was difficult to determine whether a metal wall or thermal mass walls such as concrete or brick would be a better choice. Therefore, a simulation will help in determining which wall would achieve higher air temperatures passing through the drying chamber. The absorber wall should have a black surface to prevent long-wavelength radiation from escaping.

F-1.2.1. Metal absorber wall

Metals are very good conductors and extremely strong. This allows metals to reach high temperatures when exposed to heat. Metals reach higher temperatures than other materials but provide poor storage of thermal energy. Metal can be a very expensive choice for the construction of a solar dryer. This was due to its manufacturing and forming process. Metals have long life spans but are also subjected to corrosion and rusting when exposed to moisture over long periods. Waterproof paints and treatments are applied to prevent surface corrosion on metals. High temperatures can easily be achieved in hot areas and summer seasons. During winter periods and cool places will result in metals reaching very low temperatures. Table F-2 illustrates some of the properties of the various metals.

Table F-2: Properties of metals.

Material	Melting point ^0C	Density Kg/m^3	Specific heat J/ (K kg)	Thermal conductivity W/ (m K)
Aluminum	933	2702	903	237
Copper	1358	8933	385	401
Gold	1336	19300	129	317
Iron	1810	7870	447	80.2
Nickel	1728	8900	444	90.7
Tungsten	3660	19300	132	174
Silver	1235	10500	235	429

F-1.2.2. Concrete absorber wall

Concrete, brick and stone are excellent insulation materials. These materials aren't as strong as metal surfaces but are much cheaper to construct and provide better storage of thermal energy. Concrete materials are very strong but are also brittle. Extreme loads or impacts can cause concrete to break.

During colder periods such as winter and the evening periods, these materials can release stored thermal energy.

Table F-3 shows some of the properties of composite materials.

Table F-3: Stone to concrete properties.

	Material	Specific heat capacity	Thermal conductivity	Density	Effectiveness
	stone	1000	1.8	2300	high
	brick	800	0.73	1700	high
	concrete	1000	1.13	2000	high
	unfired clay bricks	1000	0.21	700	high
	dense concrete block	1000	1.63	2300	high
	gypsum plaster	1000	0.5	1300	high
	aircrete block	1000	0.15	600	medium

An aluminium sheet 3 mm thick was selected for the absorber wall. Aluminium has good thermal conductivity, therefore, making it a suitable choice to heat air entering the dryer. The absorber wall was painted black to retain heat within the direr. Holes of 10 mm diameter are drilled on the bottom of the absorber wall. This will allow air to enter the top of the dryer and allow air to pass over a hot wall and thereafter enter the dryer.

F-1.3. Ventilation

Solar dryers generally tend to build up a lot of moisture within enclosures at high relative humidity. Ventilation was an effective tool in preventing moisture build-up. Ventilation allows dry air to pass into an enclosure from the outside environment. Thermal loads on drying products will result in vapour arising from the wet product which was carried out of the enclosure by the ventilation system. This cycle will drastically reduce the water build-up. The power of the ventilation system will greatly reduce thermal fluctuations and high humidity build-up within the dryer.

The ventilation component within a solar dryer is responsible for the recycling of moist air with dry air from the outdoor environment. The solar dryer includes a ventilation system to remove the evaporated moisture and renew the air inside the enclosure. The ventilation should have enough capacity to avoid the build-up of humidity inside the dryer, as this could slow down the drying process by limiting the ability of air to hold further water vapour molecules and by decreasing the driven force for the mass transfer of the evaporated moisture from the sludge to the environment. The ventilation was made up of 6 axial fans coupled to a variable control switch for fan speed adjustment.

F-1.3.1. Axial fans

AC Axial fans are selected to create forced ventilation induced in the greenhouse dryer. Calculations and simulations determined a 2,000 m³/h flow rate required to effectively dry faecal sludge of various weights. Four fans with a flow rate of 1,002.4 m³/h are selected to be used within the greenhouse dryer. Two fans are mounted on the back wall of the dryer to bring air into the dryer and two fans on the exit are mounted towards the front of the dryer to remove moist air in the drying chamber. Table F-4 lists the technical specifications of the axial ventilation fans.

Figure F-3: Axial fan.

Table F-4: Technical specifications of the axial fan.

Input voltage	220 V AC
Power consumption	80 W
Airflow	1002.4 m³/h
Dimensions	205 × 205 × 75 mm
Fan speed	3000 rpm

These four fans are very expensive therefore a cheaper alternative was used below the outlet ventilation fans to expel air out of the lower drying chamber. The lower chamber fans cost half the cost of the high flow rate fans and produce a maximum flow rate of 750 m³/h.

F-1.3.2. Fan speed controller

A variable switch was selected to control the flow rate of the fans. This switch was essential to determine the best flow rate for the drying of faecal sludge. The best flow rate was calibrated and set according to the temperatures and humidity values yielded by the different flow rates.

Table F-5 lists the technical specifications for the fan potentiometer.

Figure F-4: ebm-papst variable control switch.

Table F-5: Technical specifications of the fan potentiometer.

Supply voltage	230 V AC
Maximum current	5 A
Speed settings	Variable (0–100 % speed)

F-1.4. Circulation Fans

It was essential to get powerful circulation fans to overcome the flow rate of air created by the ventilation fans and allow for the distribution of air over more surfaces within the dryer. The selected fans are the Ebm-Papst axial plate fans. The circulation fans will have a separate speed control switch which was the same type of switch used by the ventilation fans. Figure F-5 shows a picture of the circulation fans used in the construction of the dryer.

Figure F-5: Square-mounted circulation fans.

The specifications of the circulation fans are listed in Table F-6.

Table F-6: Technical specifications of the square-mounted fan.

Air flow rate	2320 m^3/h
Fan speed	1350 rpm
Max current	520 mA
Blade diameter	312 mm
Voltage	230 V AC
Power consumption	110 W

F-1.5. Rake System

The rake system was constructed using a linear actuator, guide rail, pillow block bearings, blade and NEMA 34 stepper motor.

F-1.5.1. Linear Actuator

A linear actuator with a stroke close to 1m was used to move the rake blade across faecal sludge. The linear actuator will need to be powerful to overcome the resistance of faecal sludge when the blade was moving through the tray. A linear actuator was required to move a rotary blade across the faecal sludge. Actuators provide accurate control of a linear system. The drying tray design dimensions are 1,200 × 950 mm therefore a linear actuator of around 1,000 mm stroke length was sufficient if blade diameter was considered. To develop an actuator a carriage, power screw, motor and housing are required. An actuator with a stroke length of 1 m was very expensive if components are purchased and assembled individually therefore, an affordable linear actuator was selected preassembled. An Igus belt-driven electric actuator was selected

Figure F-6: Igus belt-driven linear actuator.

to develop the rake system. The linear actuator is capable of handling 100 N axial loads and 600 N radial loads. Figure F-6 shows the linear actuator used in the construction of the rake system.

F-1.5.2. Guide Rail and Carriage

A guide rail was needed to allow for a horizontal rotary rake to move across the faecal sludge drying tray. The guide rail will work hand in hand with the linear actuator. Pillow block bearings are mounted on the guide rail carriage and the linear actuator moving head. The selected guide rail was an *Igus W-series* guide rail. Figure F-7 shows a picture of the Igus linear guide rail.

Figure F-7: Igus linear guide rail.

Table F-7 shows the technical specifications for the Igus linear guide rail used in the design of the rake system.

Table F-7: Technical specifications of the linear guide rail.

Material	Aluminium and stainless steel
Rail length	1500 mm
Static load rating	12800 N
Rail Width	74 mm

F-1.6. Drying Tray

Aluminium angle, Aluminium sheet and perforated steel wire mesh are selected for the construction of the drying tray.

F-1.6.1. Perforated Steel wire mesh

A finely perforated steel wire mesh was used to hold faecal sludge. The mesh has small air gaps to allow hot air passing the bottom of the drying tray to come into contact with the bottom layer of the faecal sludge and to allow loose water to fall through into the draining tray. Steel and aluminium are very similar materials and are often used together. The perforated sheet has 1 mm holes across its surface and was 2 mm thick.

F-1.6.2. Aluminium angle (76 × 76 × 2 mm)

The drying tray was manufactured using an aluminium angle. The angle was 2 mm thick and the side dimensions of 76 mm on either side. The aluminium was cut into 4 pieces and Tig welded together at the 4 corner edges to make a rectangle frame.

F-1.7. Drainage system

The drainage system was made up of a 1.75 mm thick aluminium sheet cut and bent into a drainage tray. The tray was welded in the corners to ensure that the tray keeps its shape and integrity. The tray was light and flexible and can be easily removed from inside the dryer or positioned in the dryer.

F-2. Testing Instrumentation

The greenhouse dryer will include testing instrumentation to measure and log the temperatures and humidity reached inside the dryer. Included below are the various testing instrumentation for the testing of airflow speed and solar irradiance.

F-2.1. Temperature and Humidity Testing Instrumentation

Temperature and humidity are essential quantities to determine as these variables are used to test and determine the performance of the dryer. High temperatures will promote quicker vaporisation and drying times. Humidity was important to control and investigate as higher humidity will promote vapour build-up which can negatively affect evaporation performance. It was essential to determine the best humidity to achieve and compare these humidity values to the drying time. Achieving Lower humidity in the dryer will promote better drying conditions and time.

F-2.1.1. Temperature and humidity sensors

The temperature and humidity sensors selected are the DHT-22 sensors. The DHT-22 sensors are made up of a humidity sensor and a thermistor. Temperature accuracy was roughly 0.5 °C and humidity accuracy was roughly 5 %. These sensors are low-cost and are compatible with most of the common development boards. These sensors are used often with Arduino boards but due to Arduino boards having limited input and output channels, an ESP32 microcontroller was selected as the best development board for connecting multiple sensors. An illustration of the DHT-22 temperature sensor is shown in Figure F-8.

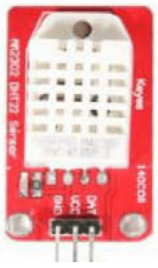

Figure F-8: DHT- 22 temperature and humidity sensor.

The technical specifications of the temperature and humidity sensors are shown in Table F-8.

Table F-8: Technical specifications of the temperature and humidity sensor.

Operating voltage	3.3–5V DC
Max current	2.5 mA
Temperature range	-40–125 °C
Humidity range	0–100 %
Sample rate	0.5 Hz

F-2.1.2. Power module

The various other components selected to determine temperature and humidity values require 5V to 3.3 V supplied power to operate. Therefore, a KEYES MD0111 power module was used to power the Micro SD card holder, microcontroller, temperature/humidity sensors and Arduino board. The input power required was supplied by a 220 VAC to 12 VDC charger. The charger allows you to use the power from a plug point or wall socket that supplies 220 VAC. The WROOM power module is shown in Figure F-9.

Figure F-9: WROOM power module.

The technical specifications of the power module are shown in Table F-9.

Table F-9: Technical specifications of the power module.

Input voltage	6.5–12 V DC or USB power supply
Output voltage	3.3 & 5 V
Maximum output current	700 mA

F-2.1.3. Microcontroller

ESP32 development boards provide easy ways of connecting various input components such as sensors, motors and various other applications. These boards are capable of connecting various components, with the ability to use more than one input channel for various functions. The ESP32 development board was Bluetooth and Wi-Fi integrated and allows users to display performance over a network. This sophisticated device was not limited to one function and can relay multiple functions simultaneously.

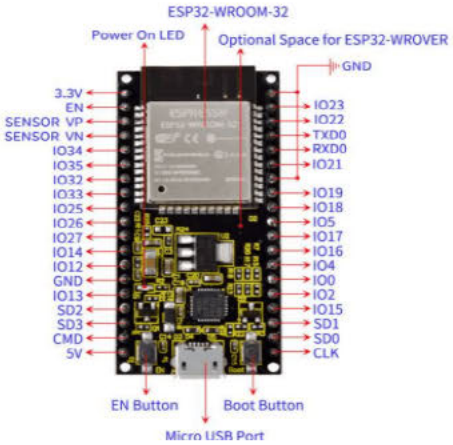

Figure F-10: ESP32 development board.

Technical specifications of the ESP32 microcontroller are shown in Table F-10.

Table F-10: Technical specifications of the microcontroller.

Type	ESP-WROOM-32 module
Operating voltage	DC 5V
Operating current	80 mA (average)
Wi-Fi frequency range	2.4 GHz – 2.5 GHz
Bluetooth	V4.2 BR/EDR
Weight	9.3 g

F-2.1.4. MicroSD card module

A microSD card holder was selected to store all the data the microcontroller receives from the sensor. The microSD card holder together with a microcontroller enables a system to read and write all feedback data from the temperature and humidity sensors in the greenhouse dryer. This specific cardholder requires a 5 V supply and 6 connection pins. The 6 pins include the *GND*, *VCC*, *MOSI*, *MISO*, *SCK* and *CS* pins. *GND* was the ground pin and *VCC* was the power supply. *MOSI*, *MISO* and *SCK* pins form part of the *SPI* (Serial Peripheral Interface) bus. *CS* was the chip select signal pin. This module was easy to install and achieves integration with various other modules. Figure F-11 shows an illustration of the microSD adapter used.

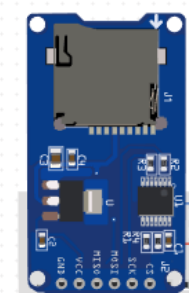

Figure F-11: MicroSD card module.

F-2.2. Air Flow Meters/Anemometer

Airflow meters and Anemometers are used to measure air velocity and air pressure. The fans can operate at different speeds therefore an Anemometer could help to determine the best airflow rates for the removal of moisture within the dryer.

F-3. Costing

The cost of the material for the construction of the greenhouse is shown in Table F-11.

Table F-11: Material costing.

	Comment	Quantities	Subtotal
Enclosure material			
PMMA (Acrylic)	3 m × 2 m × 3 mm	5	R5,755
Aluminium square hollow tubing	38 mm × 1m length	1	R95
Angle iron	1 m × 15 mm × 15 mm	8	R2,000
Hinges	Stainless steel	4	R600
Floor aluminium sheet	3 m × 2 m × 3 mm thick sheet	1	R1,500
Ventilation			
70 W AC axial plate fan	205 × 205 mm	4	R10,000
60 W AC axial fan	180 × 180 mm	8	R1,500
Speed control switch	220 V, 5A	1	R 2,000
Rake system			
1000 mm stroke linear actuator	Electric (150 N axial force)	1	R25,000
Stainless steel hollow tube	20 mm × 1 m	1	R450
Stepper motors	12 V, 110 rpm	1	R850
Linear guide rail	1.5 m length	1	R5,000
Guide carriage	To fit guide rail	1	R2,500
Drying tray			
Steel fine wire mesh	1 mm holes (4 × 500 mm × 500 mm)	1	R1,500
Angle iron	1 m × 15 mm × 15 mm	6	R1,500
Absorber wall			
Aluminium sheet	3 m × 2 m × 3 mm thick sheet	1	R1,500
Paint		1	R300
Drainage system			
Aluminium sheet 0.7 mm thick	2 m × 2 m × 0.5 mm thick	1	R300
Ball valve	tap	1	R80
Circulation fans			
420 W axial circulation plate fan	350 × 350 mm	4	R18,500
Speed control switch	220 V, 5 A	1	R 2,000
Instrumentation			
RS PRO solar power meter	10 W/m² Resolution	1	R8,000
Temperature probe	20–105 °C	1	R3,000
Moisture meter		1	R5,000
Control logic unit		1	R2,500
Total			**R101,130**

Appendix G: Greenhouse Dryer Prototype Testing

G-1. Testing Procedure

The testing methodology of the testing plan includes data treatment, testing uncertainties, and the process of storing and handling data. The microcontroller saves temperature and humidity data to a memory card. The raw data was saved by the microcontroller in a text file, which can then be uploaded to Excel for further analysis. Every 10-second interval, the temperatures and humidity are recorded by the temperature control system. Solar irradiance was recorded on a removable memory card on a separate memory card in Excel format. After a sludge sample was placed in a moisture analyser, the moisture content was manually recorded. Following that, the final data was processed, linked together in tables, and examined. This data was used to create calculations and graphs.

G-1.1. Functionality Testing

The procedure for this phase was carried out as follows:

1. Testing of the various sub-systems individually.
2. Ensure all sub-systems are correctly assembled and working effectively.
3. Ensure all electronics are functional and working correctly.
4. Connecting electronics to power.
5. Calibration of the fans according to the power consumption and fan speeds.
6. Record of temperature and humidity at the various points in the dryer.
7. Thermal imaging camera to determine the temperature of the different surfaces in the dryer.
8. Ensure the sub-systems are working efficiently without any obstacles or problems occurring.
9. Removal of memory card at the end of testing to record temperature and humidity data.
10. Disconnect power from the system.

G-1.2. Tests with Water

The procedure for the water tests was carried out as follows:

1. Water was poured into crucibles until both crucible and water measured a combined mass of 100 grams.
2. Crucibles are placed at assigned positions in the dryer on the drying tray.
3. Fans and temperature and humidity control system was connected to the power.
4. A laptop was used to monitor the temperature and humidity system and ensure data was being recorded correctly.

5. Ventilation and circulation fans are set accordingly and ventilation speeds are adjusted at hourly intervals.
6. Mass of water and crucibles are measured and recorded on hourly intervals.
7. After testing was concluded the dryer electronics are turned off.
8. The Micro SD card was removed and data was stored on a laptop for evaluation.
9. Micro SD card was placed back in electronic boxes.
10. Crucibles are removed from the dryer for further testing.

G-1.3. Tests with Wet Soil

The procedure for this phase was largely similar to the previous phases, and was carried out as follows:

1. Wet soil of determined mass and moisture content was placed on the drying tray in the dryer.
2. A 1-gram sample was removed at the beginning of testing and placed in a moisture analyser and the result was recorded.
3. Fans, rake system and temperature and humidity sensors are powered on. Tests are done with and without the rake system in operation so when the rake system was not in operation rake system plug was removed.
4. The temperature and humidity control system was monitored using a laptop to ensure sensors and the control system were working correctly.
5. A 1-gram sample of soil was removed every hourly interval to determine the amount of moisture removed from the soil.
6. At the end of testing the electronics are turned off and a final sample of soil was removed and placed in the moisture analyser and results were recorded.
7. The microSD card was removed and stored on a laptop.
8. The soil was emptied from the drying tray and the testing rig cleaned.

G-1.4. Tests with Synthetic Sludge

The procedure for this phase was largely similar to the previous phases, and was carried out as follows:

1. Synthetic sludge was dropped on the drying tray in the dryer.
2. The rake system was positioned at its starting position nearer to the door.
3. Electronics were connected and ventilation and circulation fans are both set at speed 1.
4. 1-gram Samples of synthetic sludge were removed every hour and placed in a moisture analyser and moisture content was recorded.
5. Synthetic sludge was left to dry.
6. Micro SD card data was extracted at the end of testing.
7. At the end of testing, sludge was removed from the tray.

8. The rig was inspected and cleaned.

G-1.5. Safe Operating Procedures (SOPs) for Moisture Analyser

The procedure for the operation of the *Radwag MA 50.R.WH* moisture analyser is as follows:

1. Ensure the moisture analyser was calibrated according to the size of the sample. Set temperature and drying time.
2. Once calibrated place the sample steel container in the rig and zero the analyser.
3. Close the analyser door down.
4. Press the start button and wait for the analyser to display ready for the sample.
5. Open the analyser door and place the sample into the sample container.
6. Close the lid and the analyser will begin to dry the product.
7. When the analyser was done with its operation it will set off an alarm and display the final moisture content.
8. The sample can thereafter be disposed of from the sample container.

Note: The sample container will be very hot at the end of the moisture analyser operation therefore care must be taken when handling it.

G-2. Testing Results

The ventilation system was calibrated by measuring the volumetric flow rate of air for the various speed settings on the fan potentiometer with the use of a vain anemometer. The ventilation and circulation speeds are shown in Table G-1.

Table G-1: Ventilation and Circulation calibration.

	Circulation fans (diameter = 300 mm)			**Ventilation fans (diameter = 204 mm)**		
Setting	**Speed**	**Flow rate**	**Flow rate**	**Speed**	**Flow rate**	**Flow rate**
1	2	0.14	508.68	2.5	0.08	294.01
2	2.2	0.15	559.54	2.9	0.09	341.05
3	2.6	0.18	661.28	3.15	0.10	370.46
4	3	0.21	763.02	3.6	0.11	423.38
5	4	0.28	1017.36	4.6	0.15	540.99
6	5	0.35	1271.70	5.5	0.17	646.83
7	6.5	0.45	1653.21	6.24	0.20	733.86
8	7.5	0.52	1907.55	7.1	0.23	835.00
9	7.8	0.55	1983.85	8.15	0.26	958.49
10	8	0.56	2034.72	8.6	0.28	1011.41
Unit	**m/s**	**m^3/s**	**m^3/h**	**m/s**	**m^3/s**	**m^3/h**

The power consumption drawn from the various sub-systems is shown in Table G-2.

Table G-2: Power consumption for the various electrical components.

1. Circulation and ventilation power consumption (W) for the various circulation and ventilation speeds:											
		Ventilation									
		V0	V1	V2	V3	V4	V5	V6	V7	V8	V9	V10
Circulation	C0	0	83	101	120	147	187	210	224	232	240	250
	C1	96	170	190	210	230	265	290	300	310	320	330
	C2	118	182	200	220	245	280	310	325	333	340	350
	C3	138	200	220	240	260	300	330	350	355	360	370
	C4	165	230	250	270	290	330	350	370	380	390	400
	C5	198	260	280	300	320	360	380	400	405	415	420
	C6	220	280	300	320	340	380	405	420	430	440	445
	C7	240	300	320	340	360	400	425	440	450	460	465
	C8	260	320	340	360	380	415	440	455	465	470	480
	C9	280	330	360	380	400	430	460	470	480	485	495
	C10	300	360	380	400	420	450	485	500	510	515	525
2. Temp Control System: 1 W												
3. Rake system: 96 W upon start-up and 93 W running												

Table G-3 shows the temperature difference between the air inside the dryer as compared to the temperature of ambient air outside the dryer and greenhouse dryer temperature tests with ventilation on.

Table G-3: Enclosure temperature tests.

	Outside	**GH temperature, with ventilation**		
Time		**Off**	**Full**	**Half**
09:00	25.5	36.5	33.2	31.2
09:30	34.4	42.9	41.2	40.2
10:00	34.3	43.7	38.3	37.5
10:30	34.4	43.1	38.1	37.6
11:00	32.2	42.9	38.0	38.7
11:30	31.3	42.4	38.5	39.6
12:00	30.0	41.4	37.6	36.8
Unit	**°C**	**°C**	**°C**	**°C**

The absorber walls reached temperatures of around 60 °C on days when ambient temperatures are less than 30 °C. Figure G-1 shows images of the absorber wall and the thermal image that was captured using the FLIR 1 camera.

The rake system was working initially with a smaller motor. When the sand was used the motor began to stall. Therefore, the small NEMA-18

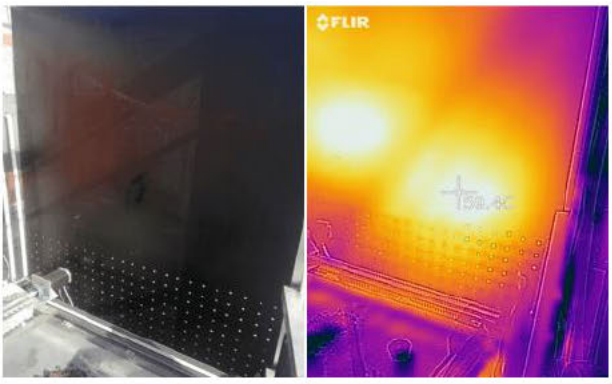

Figure G-1: Thermal imaging taken using a FLIR 1 camera.

was replaced with a NEMA-34 high-torque stepper motor. The rake system was observed to ensure no failure or obstacles affect the rake's operation or components. The system had to be lubricated for the guide rail to travel smoothly.

G-2.1. Water Tests

Table G-4 shows the raw data achieved from tests conducted with C3. Temperatures (T) and humidity (H) for the various positions in the dryer are listed separately. Solar irradiance and the mass of water measured every 30-minute interval are also recorded.

Table G-4: Water tests circulation speed 3 (28-07-2022).

		Collector		DC elevated		DC outlet		DC floor		DC inlet		Ambient inlet				
Vent.	Hour	T1	H1	T2	H2	T3	H3	T4	H4	T5	H5	T6	H6	Irradiance	Mass 1	Mass 2
V0	09:30	30.7	49.3	38.6	33.8	34.3	43.2	27.5	45.9	32.8	43.3	31.4	43.9	383.96	100	100
V1	10:00	33.2	43.1	41.6	29.6	37.1	37.8	31.7	39.5	37.3	35.6	29.1	44.7	460.21	100	100
V1	10:30	27.2	57.1	32.9	42.3	30.8	51.0	29.8	42.2	31.6	44.4	23.2	69.1	575.56	96	98
V4	11:00	29.0	52.4	35.3	37.7	31.9	47.8	31.0	40.2	32.0	42.8	23.4	67.8	530.59	94	97
V7	11:30	26.5	58.8	32.3	41.7	29.3	54.8	28.1	44.7	29.1	48.4	22.9	71.5	540.37	92	95
V10	12:00	26.6	60.4	32.3	42.3	29.2	56.5	28.1	45.4	28.5	50.7	23.1	70.3	552.10	91	94
V1	12:30	32.4	44.0	39.6	31.4	37.4	37.4	36.4	33.1	36.4	36.0	25.0	61.0	548.19	88	92
V4	13:00	29.8	49.3	37.0	34.4	34.1	42.8	32.7	37.3	34.0	38.5	24.2	64.9	534.50	86	91
V7	13:30	27.3	55.2	33.1	38.8	30.3	50.7	29.5	41.8	30.5	43.9	23.9	65.3	493.45	83	89
V10	14:00	27.7	54.0	32.8	39.8	31.1	50.0	29.0	42.1	31.1	43.9	24.3	63.3	446.52	82	88
Unit		°C	%	°C	%	°C	%	°C	%	°C	%	°C	%	W/m²	g	g

Table G-5 shows the performance data calculated from water tests with circulation speed 3.

Table G-5: Performance calculations from C3 test data.

Ventilation	Hour	P.C	ΔM	DR	Efficiency	SEC
V0	09:30	1	0	0	0	0
V1	10:00	200	0	0	0	0
V1	10:30	200	0.0030	2.527	0.212	6917
V4	11:00	260	0.0015	1.263	0.126	24500
V7	11:30	350	0.0020	1.684	0.164	28000
V10	12:00	370	0.0010	0.842	0.081	62500
V1	12:30	200	0.0025	2.106	0.203	8300
V4	13:00	260	0.0015	1.263	0.125	24500
V7	13:30	350	0.0025	2.106	0.225	22400
V10	14:00	370	0.0010	0.842	0.100	92500
Unit		W	kg	kg/h/m²	%	kWh/t

The results from the water tests for the various circulation and ventilation deviations are shown in the Tables below:

Table G-6: Circulation speed 10 vs Ventilation performance parameters (02-08-2022).

		Collector		DC elevated		DC outlet		DC floor		DC inlet		Ambient inlet				
vent.	Hour	T1	H1	T2	H2	T3	H3	T4	H4	T5	H5	T6	H6	Irradiance	mass 1	mass 2
V1	11:30	34,5	37,9	41,6	28,7	36,6	36,1	30	38,4	40,4	29,1	28,8	52,8	569,69	100	100
V1	12:00	31,9	41,7	35,2	34,9	31,5	46,6	33,6	34,2	35,3	34,3	24,5	62,2	565,75	97	98
v1	12:30	31,3	43,8	34,5	36,6	30,9	48,7	33,3	35	34,2	36,2	24,1	64,9	559,92	93	95
V4	13:00	27,7	52,1	33,5	38,3	32,3	46,6	31,4	37,9	32,8	39,8	23	71,5	536,46	90	93
V7	13:30	25,6	61,2	30,7	45,1	28,9	57,3	28,1	43,8	28,8	48,7	22,3	75,8	499,31	88	92
V10	14:00	25,5	64,3	29,5	48,5	27,9	61,7	26,8	46	27,5	52,2	21,7	79,1	440,66	87	91
Unit		**°C**	**%**	**°C**	**%**	**°C**	**%**	**°C**	**%**	**°C**	**%**	**°C**	**%**	**W/m²**	**g**	**g**

Table G-7: Performance parameters calculated for circulation speed 10.

Ventilation	**Hour**	**P.C**	**ΔM**	**DR**	**Efficiency**	**SEC**
V0	11:30	150	0	0	0	0
V1	12:00	300	0.0025	2.11	0.20	113150
V1	12:30	300	0.0035	2.95	0.28	79989
V4	13:00	450	0.0025	2.11	0.21	107292
V7	13:30	500	0.0015	1.27	0.13	166437
V10	14:00	525	0.0010	0.84	0.10	220330
Unit		**W**	**kg**	**kg/h/m²**	**%**	**kWh/t**

Table G-8: Circulation 6 and no circulation testing data (04-08-2022).

C0		Collector		DC elevated		DC outlet		DC floor		DC inlet		Ambient inlet				
vent	Hour	T1	H1	T2	H2	T3	H3	T4	H4	T5	H5	T6	H6	Irradiance	mass 1	mass 2
V0	09:30	30,3	39,6	36,2	39,8	33,8	30,7	32,7	38,6	33,7	43,5	27	53,2	383,96	100	100
V0	10:00	31,5	30,8	39,8	33,8	36,4	33,2	35,2	34,9	37,1	36,9	24,8	58,8	395,65	100	100
V1	10:30	28,1	39,4	34,1	41,2	31,4	33,7	30,6	40,6	32	43,8	23,3	58,4	491,47	99	99
V4	11:00	25,1	44,4	29,6	53,5	27,4	39,4	26,8	47,9	27,4	55,8	22,5	63,2	507,13	98	98
V7	11:30	26,4	41,3	32	46,1	29,1	34,3	28	45,8	28,7	53	24,3	57,5	534,5	96	97
V10	12:00	32,5	34,3	35,5	40,6	33,9	31,9	31	41,3	32,3	40,7	31,9	47,6	548,19	95	96
C 6																
vent	Hour	T1	H1	T2	H2	T3	H3	T4	H4	T5	H5	T6	H6	Irradiance	mass 1	mass 2
V0	12:00	32,4	53,6	36,2	39,7	34,2	50,9	31,4	39,6	33,3	44,6	27,6	56,4	533,8	100	100
V0	12:30	30,3	44,7	36,7	32,8	35,1	38,7	34,3	33,1	36,4	33,5	25,5	66,5	544,28	97	98
V1	13:00	29,9	44,1	36,1	32,7	33,6	37,2	33,8	32,9	34,5	32	25,3	64,4	540,37	93	95
V4	13:30	28,5	48,3	34,3	35,9	32,1	44,3	31,1	36,9	32,3	39,1	24,9	70,2	518,86	90	93
V7	14:00	28,5	51,6	32,6	39,5	31,3	50,1	29,3	41,2	31,1	43,4	25,6	77,5	502,36	87	91
V10	14:30	28,6	52,5	31,9	42	29,9	54,7	28,9	41,8	29,5	46,8	23,8	81,4	480,56	85	89

Unit	**°C**	**%**	**°C**	**%**	**°C**	**%**	**°C**	**%**	**°C**	**%**	**°C**	**%**	**W/m²**	**g**	**g**

Table G-9: Performance Parameters Calculated for No Circulation and Circulation Speed 6.

	No circulation (C0)					**Circulation 6 (C6)**				
Ventilation	**P.C**	**ΔM**	**DR**	**Efficiency**	**SEC**	**P.C**	**ΔM**	**DR**	**Efficiency**	**SEC**
V0	0	0	0	0	0	0	0	0	0	0
V0	1	0	0	0	0	1	0.0025	2.105263	0.1531	200
V1	83	0.0010	0.842105	0.0678	20750	280	0.0035	2.947368	0.2159	5929
V4	120	0.0010	0.842105	0.0657	36750	340	0.0025	2.105263	0.1606	14700
V7	224	0.0015	1.263158	0.0935	37333	440	0.0025	2.105263	0.1659	22400
V10	250	0.0010	0.842105	0.0608	62500	465	0.0020	1.684211	0.1387	31250
Unit	**W**	**kg**	**kg/h/m²**	**%**	**kWh/t**	**W**	**kg**	**kg/h/m²**	**%**	**kWh/t**

Table G-10: Water Test for Circulation Speed 10 (05-08-2022).

		Collector		**DC elevated**		**DC outlet**		**DC floor**		**DC inlet**		**Ambient inlet**		
Ventilation	**Hour**	**T1**	**H1**	**T2**	**H2**	**T3**	**H3**	**T4**	**H4**	**T5**	**H5**	**T6**	**H6**	**Irradiance**
V0	09:30	30.2	39.8	36.1	39.9	33.8	50.9	32.6	38.7	33.7	43.6	26.8	55.8	428.56
V1	10:00	31.5	30.9	39.8	33.8	36.4	43.2	35.2	34.9	37.1	36.9	24.8	69.1	493.45
V1	10:30	28.1	39.7	34.2	41.2	31.4	43.8	30.6	40.8	32.1	44.0	23.5	57.7	569.69
V4	11:00	25.1	33.3	28.8	48.3	27.2	49.2	26.9	47.5	27.2	45.5	22.5	61.5	571.61
V7	11:30	26.4	31.3	32.0	46.1	29.1	44.3	28.0	45.8	28.7	53	24.3	59.9	659.00
V10	12:00	32.6	33.8	35.7	40.5	33.9	40.5	31.1	40.9	33.1	44.8	31.1	51.1	686.00
Unit		**°C**	**%**	**°C**	**%**	**°C**	**%**	**°C**	**%**	**°C**	**%**	**°C**	**%**	**W/m²**

Table G-11: Performance parameters for circulation speed 10.

Mass 1	**Mass 2**	**P,C**	**ΔM**	**DR**	**Efficiency**	**SEC**
100	100	0	0	0	0	0
99	99	300	0.0010	0.842105	0.0676	20750
95	97	300	0.0030	2.526316	0.1755	18333
94	96	450	0.0010	0.842105	0.0583	57500
92	95	500	0.0015	1.263158	0.0759	40000
90	93	525	0.0020	1.684211	0.0972	32500
?	**?**	**W**	**kg**	**kg/h m²**	**%**	**kWh/t**

Table G-12: Water Test for Circulation Speed 0 (No Circulation) (27-08-2022).

		Collector		**DC elevated**		**DC outlet**		**DC floor**		**DC inlet**		**Ambient inlet**		
Ventilation	**Hour**	**T1**	**H1**	**T2**	**H2**	**T3**	**H3**	**T4**	**H4**	**T5**	**H5**	**T6**	**H6**	**Irradiance**
V1	10:00	26.3	34.7	36.6	25.9	28.8	32.9	24.6	33.9	29.3	29.6	21.3	40.4	403.51
V1	10:30	27.5	34.5	39.5	24.6	30.7	31.3	26.5	32.9	31.6	28.0	22.3	41.2	350.73
V4	11:00	28.3	33.0	38.7	24.5	30.8	30.9	28.1	31.0	31.5	27.8	22.8	40.1	518.86
V7	11:30	27.2	33.0	34.7	25.7	28.9	31.9	28.1	30.2	29.3	28.5	23.5	37.6	544.28
V10	12:00	26.8	33.4	34.1	26.3	28.7	32.3	28.0	30.3	28.5	29.2	23.0	38.6	563.83
V1	12:30	30.0	31.5	37.8	25.6	32.7	30.5	29.9	30.1	32.4	28.0	24.1	39.1	552.10
V4	13:00	24.6	37.6	27.3	32.2	25.8	36.9	25.7	33.1	25.9	32.6	21.8	42.3	530.59

		Collector		DC elevated		DC outlet		DC floor		DC inlet		Ambient inlet		
Ventilation	Hour	T1	H1	T2	H2	T3	H3	T4	H4	T5	H5	T6	H6	Irradiance
Unit		°C	%	°C	%	°C	%	°C	%	°C	%	°C	%	W/m²

Table G-13: Performance parameters for water tests with no circulation.

Mass 1	Mass 2	P.C	ΔM	DR	Efficiency	SEC
0.100	0.100	83	0	0	0	0
0.096	0.098	83	0.003	2.5267	0.2613	6917
0.096	0.098	147	0	0	0	0
0.095	0.097	224	0.001	0.8422	0.0561	56000
0.094	0.096	250	0.001	0.8422	0.0541	62500
0.092	0.094	83	0.002	1.6844	0.1106	10375
0.092	0.094	147	0	0	0	0
g	g	W	kg	kg/h m²	%	kWh/t

G-2.2. Soil Tests

Soil tests are conducted between the period of 10th of August 2022 to the 17th of August 2022. Two mass quantities are used for the soil testing. These quantities are 1.4 kg and 15 kg of wet soil at approximately 70 % moisture content. Soil tests are conducted to observe the mixing effect and determine dryer efficiency and performance. The most important quantities to observe were the temperature, humidity, moisture content and power consumption. Water tests are conducted with a set circulation and ventilation speed. Ventilation and circulation speeds were set at speed 1 on the potentiometers. From water tests, it was observed lower fan speeds achieved higher temperatures and humidity. Two different masses of soil are conducted during soil tests. These two masses are 1.4 kg and 15 kg. The soil tests temperatures, humidity, solar irradiance and moisture content for the various days of testing are shown in the Tables below:

Table G-14: Testing data of 1.4 kg soil dried with the rake system, not in operation.

	Collector		DC elevated		DC outlet		DC floor		DC inlet		Ambient inlet			
Hour	T1	H1	T2	H2	T3	H3	T4	H4	T5	H5	T6	H6	Irradiance	MC(%)
10:00	41,4	27,5	40,5	31,3	36	37,1	34,7	42,2	36,3	33,4	25,4	43,5	552,1	60
11:00	43	26,9	43,3	29,6	38,4	34,5	37,3	39,1	39,7	29,9	27,3	42,1	628,34	54
12:00	43,9	27,1	46,5	28,4	40,7	32,6	39,3	37,1	42,8	28,1	27,5	42,8	681,13	38
13:00	43,5	26,9	46,5	28,2	40,8	32,4	39,4	37	43	28	27,6	43	663,53	32
14:00	40,2	30,1	47,3	28,8	40,3	35,2	38,9	38,9	43,5	29,1	26,7	47,1	563,83	26
15:00	35,6	37,1	43,6	31,4	35,2	43,1	35,9	43,4	40	31,7	26	50,7	417,4	22
Unit	°C	%	°C	%	°C	%	°C	%	°C	%	°C	%	W/m²	%

Table G-15: Performance calculations for 1.4 kg soil without the use of the rake system.

P.C	ΔM	ΔM	DR	Efficiency	SEC
170	0	0	0	0	0
170	6	0.0840	0.700	2.228	2023.809
170	16	0.2105	1.754	5.152	807.370
170	6	0.0663	0.552	1.665	2563.081
170	6	0.0623	0.519	1.842	2726.682
170	4	0.0390	0.325	1.560	4351.089
W	**%**	**kg**	**kg/h m²**	**%**	**kWh/t**

Table G-16: Overall performance calculations for 1.4 kg soil without the use of the rake system.

Quantity	Rake	*Unit*
M_{wi}	0.81	*kg*
M_s	0.59	*kg*
M_{wf}	0.17	*kg*
Drying rate	0.13	*kg/h*
Drying rate	1.07	*kg/h/m²*
SEC	2494.41	*kWh/t*
Efficiency	4.41	*%*

Table G-17: Testing data of 1.4 kg soil dried with the rake system in operation (11-08-2022).

	Collector		DC elevated		DC outlet		DC floor		DC inlet		Ambient inlet			
Hour	T1	H1	T2	H2	T3	H3	T4	H4	T5	H5	T6	H6	Irradiance	MC
10:00	40.2	27.5	40.5	31.3	36	37.1	34.7	39.8	36.3	33.4	25.4	43.5	634.21	65
11:00	40.6	31.6	41.4	35.3	36.9	37	35.7	39.7	37.5	36.3	25.7	50.7	677.21	55
12:00	41.4	31.4	43.2	33.8	38.4	44.6	37.2	47.4	39.1	34.6	26.2	51.1	747.60	45
13:00	39.1	35.2	43.4	33.9	38.2	45.3	37.1	47.3	39.8	34	25.7	53.5	731.20	42
14:00	37.4	37.3	43.7	33.5	37.9	46	36.1	48.4	38.5	35.6	25.4	54.7	628.34	33
15:00	32.5	45.5	39.1	37.5	33.8	54	32.7	53.5	34.8	41.4	24.2	57.3	468.03	21
Unit	°C	%	°C	%	°C	%	°C	%	°C	%	°C	%	W/m²	%

Table G-18: Performance calculations for 1.4 kg soil with the use of the rake system.

P.C	ΔM	ΔM	DR	Efficiency	SEC
235	0	0	0	0	0
235	10	0.140	1.17	3.45	1678.57
235	10	0.126	1.05	2.81	1865.08
235	3	0.034	0.28	0.78	6907.70
235	9	0.099	0.82	2.63	2373.78
235	12	0.120	1.00	4.28	1956.41
W	**%**	**kg**	**kg/h m²**	**%**	**kWh/t**

Table G-19: Testing data for 15 kg sample of soil dried without the use of rake system (12-08-2022).

	Collector		DC elevated		DC outlet		DC floor		DC inlet		Ambient inlet			
Hour	T1	H1	T2	H2	T3	H3	T4	H4	T5	H5	T6	H6	Irradiance	MC(%)
10:00	42,3	27,3	40	34,1	36	35,9	34,7	36,43	39,1	31,8	28,2	39,3	569,69	70
11:00	43,4	27,5	42	35,5	37	39,3	36,2	38,8	40,1	32,7	29,5	40,3	702,63	48
12:00	46,1	24,5	46,8	29,1	41,1	29,5	39,9	29,5	42,6	27,9	32,3	33	735,87	35
13:00	45,1	23,3	49,9	25,6	43,3	29,6	41,5	27,5	45	24,1	32,8	32,5	745,55	28
14:00	38,2	26,6	42,5	26,8	38,2	30,9	36,8	30,3	38,9	25,8	30	32,3	516,91	24
15:00	34,8	41	39,6	37,3	33,7	42,8	33,7	45,2	35,2	41,1	24,7	58,2	445,34	19
Unit	**°C**	**%**	**°C**	**%**	**°C**	**%**	**°C**	**%**	**°C**	**%**	**°C**	**%**	**W/m²**	**%**

Table G-20: Performance parameters for 15 kg soil tests without the rake system operating.

P.C	ΔM	ΔM	DR	Efficiency	SEC
0	0	0	0	0	0
170	22	3.3	5.156	78.27	51.52
170	13	1.5	2.376	34.44	111.77
170	7	0.7	1.113	15.92	238.59
170	4	0.4	0.591	12.20	448.95
170	5	0.5	0.709	17.00	374.13
W	**%**	**kg**	**kg/h m²**	**%**	**kWh/t**

Soil tests without the use of a rake system were conducted on the 12th of August 2022 between the times 10 AM and 3 PM. The soil with an initial moisture content of 70 % was placed in the drying tray and circulation and ventilation fan speeds are set to speed 1. The greenhouse dryer managed to reduce soil moisture content by 51 % in the space of 5 hours. The highest temperatures were achieved around 1 PM. Solar irradiance was the highest at around lunchtime. The temperature versus time graph for this day is shown in Figure G-2.

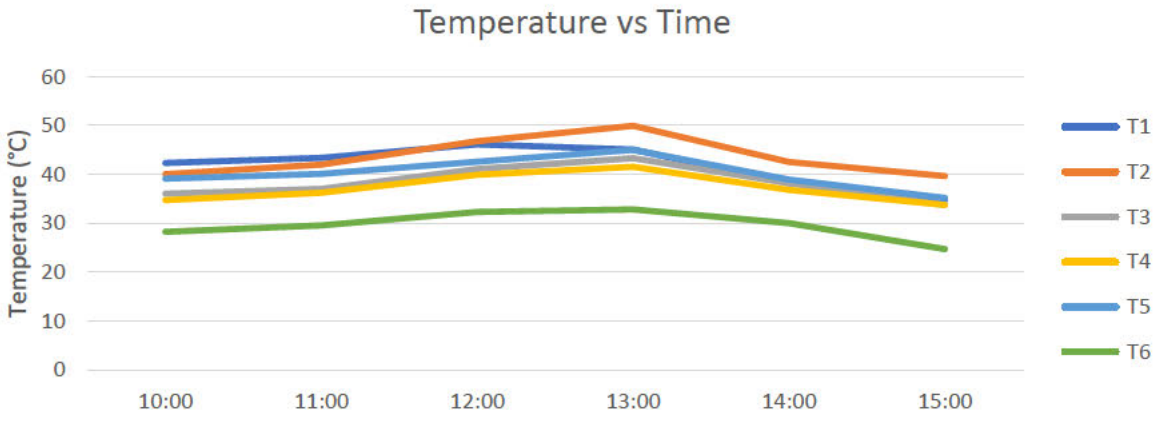

Figure G-2: Graph of Temperature vs Time.

The humidity Inside the direr was slightly lower than the ambient inlet air humidity entering inside the dryer. The graph of humidity vs time is shown in Figure G-3.

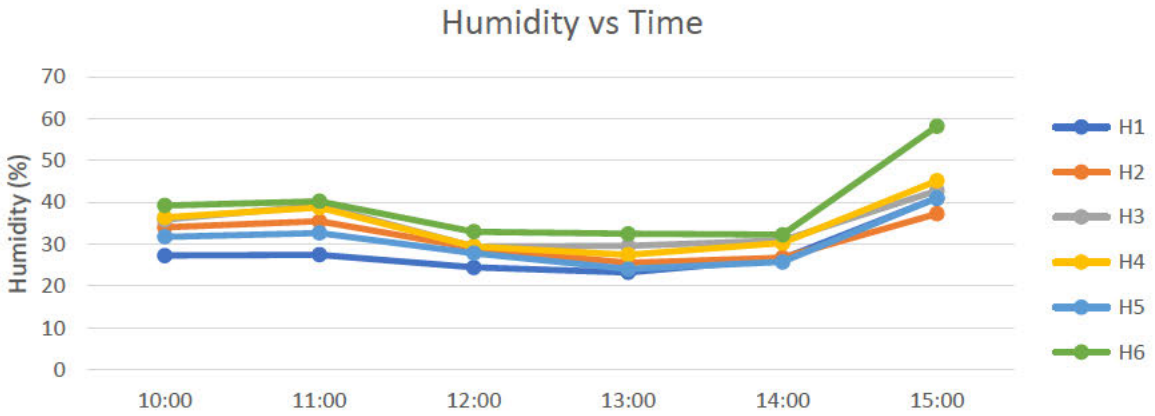

Figure G-3: Graph of Humidity vs Time.

The initial mass of water, the final mass of water, the mass of solid, the drying rate, the drying rate per square meter, Specific Energy Consumption (SEC) and dryer efficiency are shown in Table G-21.

Table G-21: Performance parameters to dry wet soil without the use of the rake system.

Quantity	**Amount**	*Unit*
Drying time	5	*h*
Solar irradiance	619.33	*W/m²*
Power	170	*W*
M_{wi}	10.50	*kg*
M_s	4.50	*kg*
M_{wf}	1.06	*kg*
Drying rate	1.89	*kg/h*
Drying rate	2.95	*kg/h/m²*
SEC	90.00	*kWh/t*
Efficiency	50.83	*%*

The graph of drying rate versus moisture content is shown in Figure G-4.

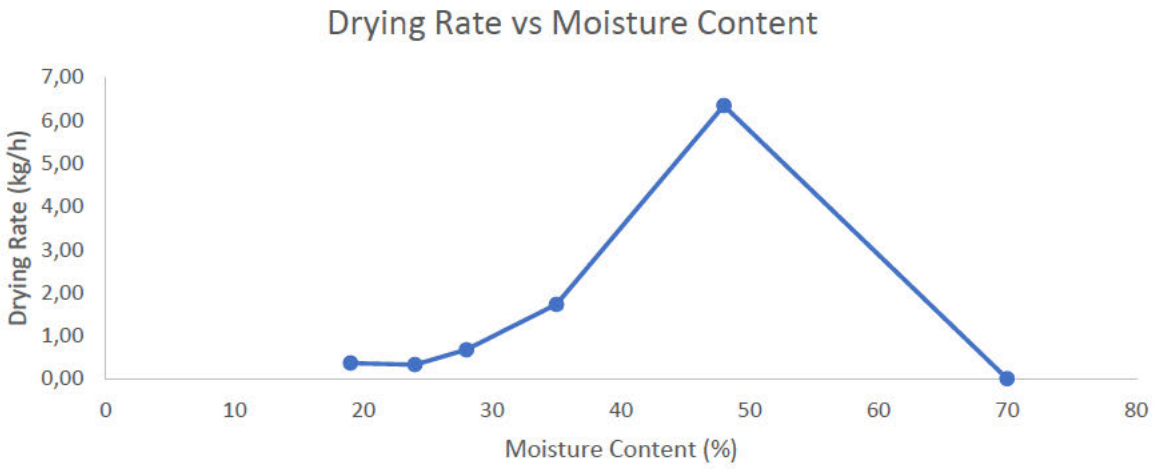

Figure G-4: Graph of DR vs MC for 15 kg wet soil dried with the rake system in operation.

The data captured for the soil tests with the rake system in operation is shown in Table G-22 and Table G-23.

Table G-22: Testing data for 15 kg of wet soil with the rake system in operation (17-08-2022).

	Collector		**DC elevated**		**DC outlet**		**DC floor**		**DC inlet**		**Ambient inlet**			
Hour	T1	H1	T2	H2	T3	H3	T4	H4	T5	H5	T6	H6	Irradiance	MC(%)
10:00	38,6	22,6	38,6	25,2	34,9	29,3	35,7	31,2	37	23,6	26,5	47,8	677,2	70
11:00	39	22,1	38,9	26,2	35,1	31	34,5	33,4	37,5	23,6	29,2	44,7	675,26	36
12:00	40,8	21,4	41,2	24,2	37,2	27,9	36,5	30,8	38,9	22,3	30,5	44,2	591,2	28
13:00	40,5	24,8	43,4	26,7	39	31,8	38,3	34,7	40,5	25	31,8	48,4	401,56	25
14:00	38,5	28,5	43,7	28,3	39,4	33,9	39	37,5	41,5	27,5	31,6	53,3	542,32	22
15:00	36,8	28,1	41,1	27,4	37,2	32,6	36,2	35,4	38,3	27	31	50,9	321,4	18
Unit	**°C**	**%**	**°C**	**%**	**°C**	**%**	**°C**	**%**	**°C**	**%**	**°C**	**%**	**W/m²**	**%**

Table G-23: Calculated performance data for 15 kg wet soil with the use of the rake system (17-08-2022).

Hour	**MC**	**ΔM**	**ΔM**	**DR**	**Efficiency**	**SEC**
10:00	70	0	0	0	0	0
11:00	36	34	5.10	7.97	125.88	46.08
12:00	28	8	0.79	0.78	22.33	470.00
13:00	25	3	0.27	0.25	11.34	1468.75
14:00	22	3	0.27	0.23	8.15	1591.15
15:00	18	4	0.34	0.28	17.78	1304.74
Unit	**%**	**%**	**kg**	**kg/h m²**	**%**	**kWh/t**

The performance data calculated using the measured quantities are shown in Table G-24.

Table G-24: Performance data calculated from soil test with the use of rake system (17-08-2022).

Quantity	**Amount**	*Unit*
Drying time	5	*h*
Solar irradiance	582	*W/m²*
Average power	238	*W*
M_{wi}	10.5	*kg*
M_s	4.5	*kg*
M_{wf}	0.988	*kg*
Drying rate	1.90	*kg/h*
Drying rate	2.97	*kg/h/m²*
SEC	123.54	*kWh/t*
Efficiency	72.95	*%*

The graph of drying rate versus moisture content is shown in Figure G-5.

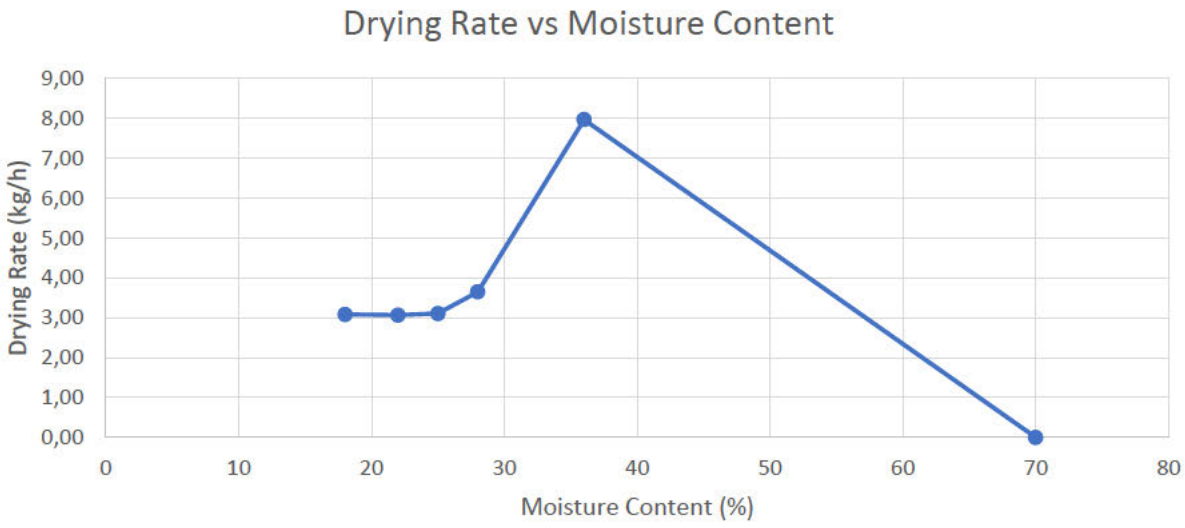

Figure G-5: Drying rate vs moisture content.

G-2.3. Synthetic Sludge

Testing for the first day of testing was stopped at 2 PM due to cloud cover and the roof becoming very windy. Temperatures struggled to surpass 40 °C but good amounts of sunshine are observed throughout the day. The testing data recorded for the first day of synthetic sludge drying tests are shown in Table G-25 and Table G-26.

Table G-25: Day 1 testing data for synthetic sludge (05-09-2022).

	Collector		DC elevated		DC outlet		DC floor		DC inlet		Ambient inlet			
Hour	**T1**	**H1**	**T2**	**H2**	**T3**	**H3**	**T4**	**H4**	**T5**	**H5**	**T6**	**H6**	**Irradiance**	**MC**
09:00	25.8	31.2	26.9	30	24.6	39.1	23.1	40.9	25.8	29.0	16.1	40.9	560	80.3
10:00	34.0	46.7	33.0	50.8	30.8	40.6	29.6	47.6	35.0	43.5	23.2	56.4	647	75.9
11:00	37.3	42.9	36.9	43.4	32.0	43.4	32.7	49.4	38.5	38.3	23.5	57.9	743	73.5
12:00	36.3	43.5	38.6	41.9	32.6	42.5	33.6	46.4	37.7	40.2	24.2	57.1	761	71.9
13:00	34.1	51.7	36.1	47.6	31.6	41.9	32.2	43.4	35.0	43.6	24.1	58.2	700	71.5
14:00	32.7	55.2	37.1	45.3	33.0	37.1	32.3	32.2	38.0	40.3	23.9	58.8	567	69.4
Unit	**°C**	**%**	**°C**	**%**	**°C**	**%**	**°C**	**%**	**°C**	**%**	**°C**	**%**	**W/m²**	**%**

Table G-26: Performance data for day 1 of testing (05-09-2022).

Hour	**MC**	**P,C**	**ΔM**	**ΔM_{db}**	**DR**	**Efficiency**	**SEC**
09:00	80.320	0	4.080	0	0	0	0
10:00	75.913	235	3.150	0.06	1.83	53.614	128.31
11:00	73.520	235	2.776	0.05	0.74	18.840	317.95
12:00	71.909	235	2.559	0.05	0.43	10.618	550.80
13:00	71.500	235	2.508	0.04	0.10	2.723	2335.02
14:00	69.360	235	2.263	0.04	0.48	16.105	486.77
Unit	**%**	**W**	**%**	**kg**	**kg/h**	**%**	**kWh/t**

The testing data for the second day of testing is shown in Table G-27 and Table G-28.

Table G-27: Day 2 testing data for synthetic sludge (06-09-2022).

	Collector		DC elevated		DC outlet		DC floor		DC inlet		Ambient inlet			
Hour	**T1**	**H1**	**T2**	**H2**	**T3**	**H3**	**T4**	**H4**	**T5**	**H5**	**T6**	**H6**	**Irradiance**	**MC (%)**
09:00	37.0	38.4	35.1	43.8	30.0	35.2	26.4	48.2	30.4	52.5	25.9	45.8	194.33	69.360
10:00	30.8	48.1	31.6	54.4	29.0	35.4	29.2	43.3	31.6	48.8	22.5	56.3	360.50	68.100
11:00	27.9	53.2	27.3	51.4	25.1	52.2	25.9	56.1	29.5	50.1	21.9	59.0	448.48	66.680
12:00	36.8	39.7	39.6	39.3	34.5	35.7	34.0	36.1	36.9	35.3	24.1	50.8	643.98	63.520
13:00	32.7	42.4	32.7	42.7	28.3	39.0	29.0	44.0	35.1	35.9	24.6	48.4	426.96	59.189
14:00	25.0	48.4	25.8	49.0	25.1	48.2	25.0	50.6	27.9	47.9	21.4	57.0	112.12	57.827
Unit	**°C**	**%**	**°C**	**%**	**°C**	**%**	**°C**	**%**	**°C**	**%**	**°C**	**%**	**W/m²**	**%**

Table G-28: Performance data for day 2 of 15 kg synthetic sludge testing (06-09-2022).

Hour	**MC**	**P,C**	**ΔM**	**ΔM_{db}**	**DR**	**Efficiency**	**SEC**
09:00	69.360	0	2.26	0	0	0	0
10:00	68.100	235	2.13	0.042	0.254	13.342	925.36
11:00	66.680	235	2.00	0.039	0.263	11.115	892.91
12:00	63.520	235	1.74	0.034	0.512	15.063	458.85
13:00	59.189	235	1.45	0.029	0.573	25.423	410.06
14:00	57.827	235	1.37	0.027	0.156	26.335	1507.43
Unit	**%**	**W**	**%**	**kg**	**kg/h**	**%**	**kWh/t**

The testing data for the third day of testing is shown in Table G-29 and Table G-30.

Table G-29: Day 3 testing data for synthetic sludge (07-09-2022).

	Collector		DC elevated		DC outlet		DC floor		DC inlet		Ambient inlet			
Hour	**T1**	**H1**	**T2**	**H2**	**T3**	**H3**	**T4**	**H4**	**T5**	**H5**	**T6**	**H6**	**Irradiance**	**MC**
09:00	28.8	40.0	27.3	42.8	25.1	43.0	24.1	49.2	24.9	48.8	24.5	50.1	237.30	55.230
10:00	30.0	43.5	30.8	47.1	28.4	44.4	28.8	41.0	32.1	46.7	22.4	54.7	747.60	51.450
11:00	37.3	42.5	38.4	41.7	34.7	34.8	34.0	35.4	39.5	35.2	24.0	54.2	790.61	38.838
12:00	38.2	39.5	41.3	36.7	37.0	35.0	37.5	31.4	41.7	32.8	24.6	52.9	810.16	37.858
13:00	35.9	43.0	40.7	36.1	36.4	43.4	34.9	42.5	39.5	32.8	25.2	52.4	763.24	28.697
14:00	34.4	47.2	39.5	37.7	35.5	44.9	34.4	42.7	37.5	33.8	24.3	55.8	626.39	22.876
15:00	31.5	45.2	37.9	39.2	34.0	47.0	32.8	45.4	35.3	41.4	24.0	56.4	489.52	19.602
Unit	**°C**	**%**	**°C**	**%**	**°C**	**%**	**°C**	**%**	**°C**	**%**	**°C**	**%**	**W/m²**	**%**

Table G-30: Performance calculations for 15 kg synthetic sludge day 3 (07-09-2022).

Hour	**MC**	**P,C**	**ΔM**	**ΔM_{db}**	**DR**	**Efficiency**	**SEC**
09:00	55.23	0	1.23	0	0	0	0
10:00	51.45	235.00	1.06	0.02	0.34	8.67	686.48
11:00	38.84	235.00	0.64	0.01	0.84	20.04	280.86
12:00	37.86	235.00	0.61	0.01	0.05	1.19	4626.39
13:00	28.70	235.00	0.40	0.01	0.41	10.11	576.97
14:00	22.88	235.00	0.30	0.01	0.21	6.31	1126.94
15:00	19.60	235.00	0.24	0	0.10	4.02	3530.02
Unit	**%**	**W**	**%**	**kg**	**kg/h**	**%**	**kWh/t**

The testing data for the fourth day of testing is shown in Table G-31 and Table G-32.

Table G-31: Day 4 (08-09-2022).

	Collector		DC elevated		DC outlet		DC floor		DC inlet		Ambient inlet			
Hour	**T1**	**H1**	**T2**	**H2**	**T3**	**H3**	**T4**	**H4**	**T5**	**H5**	**T6**	**H6**	**Irradiance**	**MC**
09:00	32.4	51.4	33.7	46.0	31.1	51.0	28.9	51.5	31.7	49.5	22.4	56.6	518.32	18.823
10:00	36.5	42.5	37.9	39.3	35.3	47.2	36.7	39.8	35.5	43.6	24.2	52.7	747.60	12.860
11:00	41.0	34.2	41.8	34.8	38.5	46.7	36.7	35.3	39.9	31.6	26.2	50.7	920.35	10.601
12:00	41.0	34.8	44.7	31.6	40.7	41.3	41.5	38.3	43.9	29.2	26.9	48.6	984.30	8.130
13:00	40.4	35.5	44.9	31.8	40.6	41.4	40.4	38.3	40.3	30.7	26.8	49.7	895.35	6.869
14:00	38.6	40.8	45.7	32.6	41.1	42.4	39.0	40.2	41.3	30.5	28.0	51.0	823.42	6.830
15:00	34.6	51.5	41.1	37.4	34.8	46.1	34.6	47.7	41.4	34.7	27.4	54.0	695.68	6.518
Unit	**°C**	**%**	**°C**	**%**	**°C**	**%**	**°C**	**%**	**°C**	**%**	**°C**	**%**	**W/m²**	**%**

Table G-32: performance data for day 4 of testing (08-09-2022).

Hour	MC	P,C	ΔM	ΔM_{ab}	DR	Efficiency	SEC
09:00	18.823	0	0.23	0	0	0	0
10:00	12.86	235	0.15	0.0029	0.17	4.19	1421.91
11:00	10.601	235	0.12	0.0023	0.06	1.18	4113.73
12:00	8.13	235	0.09	0.0017	0.06	1.14	3964.93
13:00	6.869	235	0.07	0.0015	0.03	0.61	8093.84
14:00	6.83	235	0.07	0.0014	0	0.02	265403.96
15:00	6.518	235	0.07	0.0014	0.01	0.19	52032.08
Unit	%	W	%	kg	kg/h	%	kWh/t

The second test was conducted from 14-09-2022 to 15-09-2022. The testing data for the first day of the synthetic sludge duplicate test is shown in Table G-33 and Table G-34.

Table G-33: Day 1 of duplicate synthetic sludge testing data (14-09-2022).

	Collector		DC elevated		DC outlet		DC floor		DC inlet		Ambient inlet			
Hour	T1	H1	T2	H2	T3	H3	T4	H4	T5	H5	T6	H6	Irradiance	MC
09:00	32.8	57.3	32.2	54.6	29.5	56.4	27.3	57.9	30.1	58.9	22.8	58.3	579.47	80.046
10:00	38.1	42.0	37.3	47.1	33.8	47.6	36.8	43.6	41.3	36.8	24.7	54.4	745.65	76.459
11:00	40.5	39.2	35.5	45.1	31.3	47.3	33.1	47.8	41.6	35.1	25.7	54.6	855.13	70.065
12:00	40.7	38.0	41.0	42.4	36.7	49.8	40.6	46.7	44.6	32.4	25.6	54.7	872.72	62.760
13:00	37.7	43.4	41.7	44.6	36.9	49.4	36.0	43.5	44.7	34.4	26.6	54.9	784.75	55.843
14:00	34.8	47.9	39.2	43.8	35.9	50.5	34.8	46.0	43.0	35.1	25.6	56.6	661.58	50.082
15:00	32.7	56.7	40.2	43.0	33.5	48.2	32.9	50.8	36.8	40.1	25.4	58.2	123.94	48.038
Unit	°C	%	°C	%	°C	%	°C	%	°C	%	°C	%	W/m²	%

Table G-34: Calculated performance parameters for day 1 of duplicate testing (14-09-2022).

Hour	MC	P,C	ΔM	ΔM_{ab}	DR	Efficiency	SEC
09:00	80.046	0	4.01	0	0	0	0
10:00	76.459	235	3.25	0.064	1.50	38.21	156.22
11:00	70.065	235	2.34	0.046	1.79	39.59	131.47
12:00	62.760	235	1.69	0.033	1.29	28.02	182.04
13:00	55.843	235	1.26	0.025	0.83	20.00	283.59
14:00	50.082	235	1.00	0.020	0.51	14.74	456.42
15:00	48.038	235	0.92	0.018	0.16	23.72	2365.29
Unit	%	W	%	kg	kg/h	%	kWh/t

Testing data for the second day of the synthetic sludge duplicate are shown in Table G-35 and Table G-36.

Table G-35: Day 2 synthetic sludge duplicate testing data (15-09-2022).

	Collector		DC elevated		DC outlet		DC floor		DC inlet		Ambient inlet			
Hour	**T1**	**H1**	**T2**	**H2**	**T3**	**H3**	**T4**	**H4**	**T5**	**H5**	**T6**	**H6**	**Irradiance**	**MC**
09:00	34.3	55.4	33.7	54.8	31.3	55.1	29.4	56.2	31.2	57.8	24.9	55.1	616.61	47.851
10:00	40.7	39.4	40.3	42.7	37.1	45.7	38.8	44.9	39.2	38.9	27.3	51.8	757.38	42.320
11:00	43.2	36.8	42.1	40.3	38.1	43.1	37.7	48.3	42.8	33.1	28.2	51.2	837.53	34.655
12:00	43.4	35.4	45.6	36.5	41.3	35.1	44.9	35.4	45.7	30.1	29.5	48.0	833.62	28.422
13:00	52.4	29.3	55.0	30.3	46.5	36.1	41.8	34.2	55.4	26.2	41.5	31.0	794.65	20.995
14:00	50.1	30.1	52.0	30.3	44.4	35.1	40.0	34.7	54.3	26.7	40.6	33.4	608.79	16.573
15:00	36.3	43.5	43.9	36.5	38.0	34.5	43.0	32.5	43.0	32.5	28.9	50.4	405.47	12.276
Unit	**°C**	**%**	**°C**	**%**	**°C**	**%**	**°C**	**%**	**°C**	**%**	**°C**	**%**	**W/m²**	**%**

Table G-36: Calculated performance parameters for day 2 of duplicate testing (15-09-2022).

Hour	**MC**	**P,C**	**ΔM**	**ΔM_{ab}**	**DR**	**Efficiency**	**SEC**
09:00	47.851	0	0.92	0	0	0	0
10:00	42.320	235	0.73	0.014	0.36	9.06	648.74
11:00	34.655	235	0.53	0.010	0.40	9.06	586.58
12:00	28.422	235	0.40	0.008	0.26	5.96	895.15
13:00	20.995	235	0.27	0.005	0.26	6.17	908.29
14:00	16.573	235	0.20	0.004	0.13	4.11	1778.05
15:00	12.276	235	0.14	0.003	0.12	5.40	3174.54
Unit	**%**	**W**	**%**	**kg**	**kg/h**	**%**	**kWh/t**

Figure G-6 shows the drying rate versus moisture content for the 2 days of the duplicate synthetic sludge test.

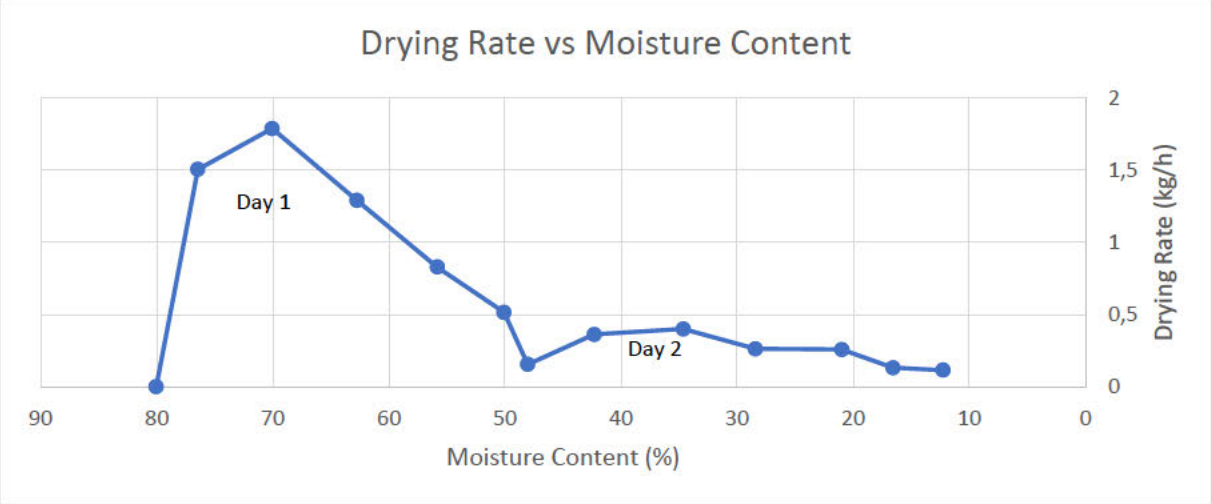

Figure G-6: Drying rate vs moisture content.

H-1. Enclosure Frame

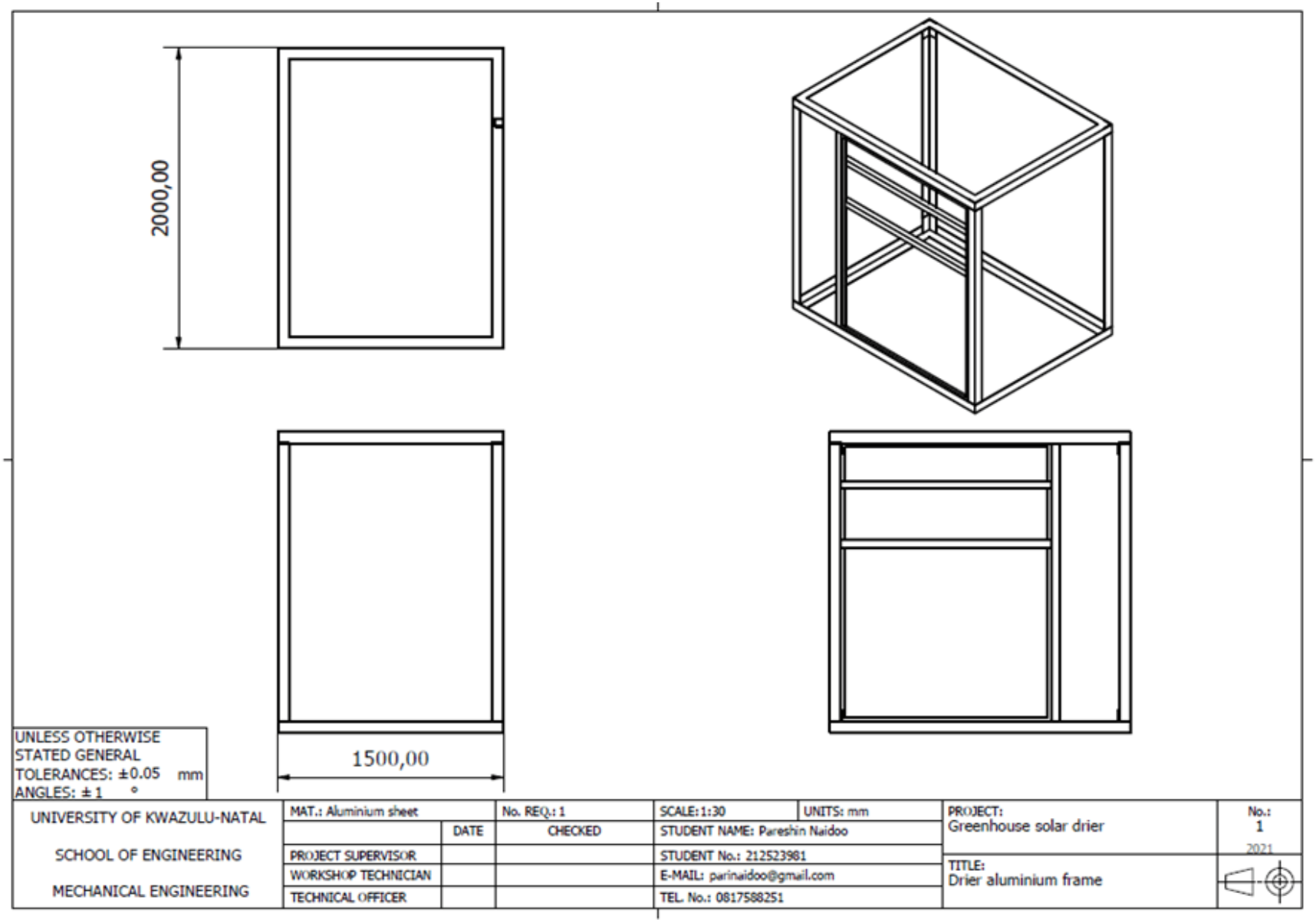
2000,00
1500,00
UNLESS OTHERWISE STATED GENERAL TOLERANCES: ±0.05 mm
ANGLES: ± 1 °
UNIVERSITY OF KWAZULU-NATAL
SCHOOL OF ENGINEERING
MECHANICAL ENGINEERING
MAT.: Aluminium sheet
No. REQ.: 1
SCALE: 1:30
UNITS: mm
DATE
CHECKED
PROJECT SUPERVISOR
WORKSHOP TECHNICIAN
TECHNICAL OFFICER
STUDENT NAME: Pareshin Naidoo
STUDENT No.: 212523981
E-MAIL: parinaidoo@gmail.com
TEL. No.: 0817588251
PROJECT: Greenhouse solar drier
No.: 1
2021
TITLE: Drier aluminium frame

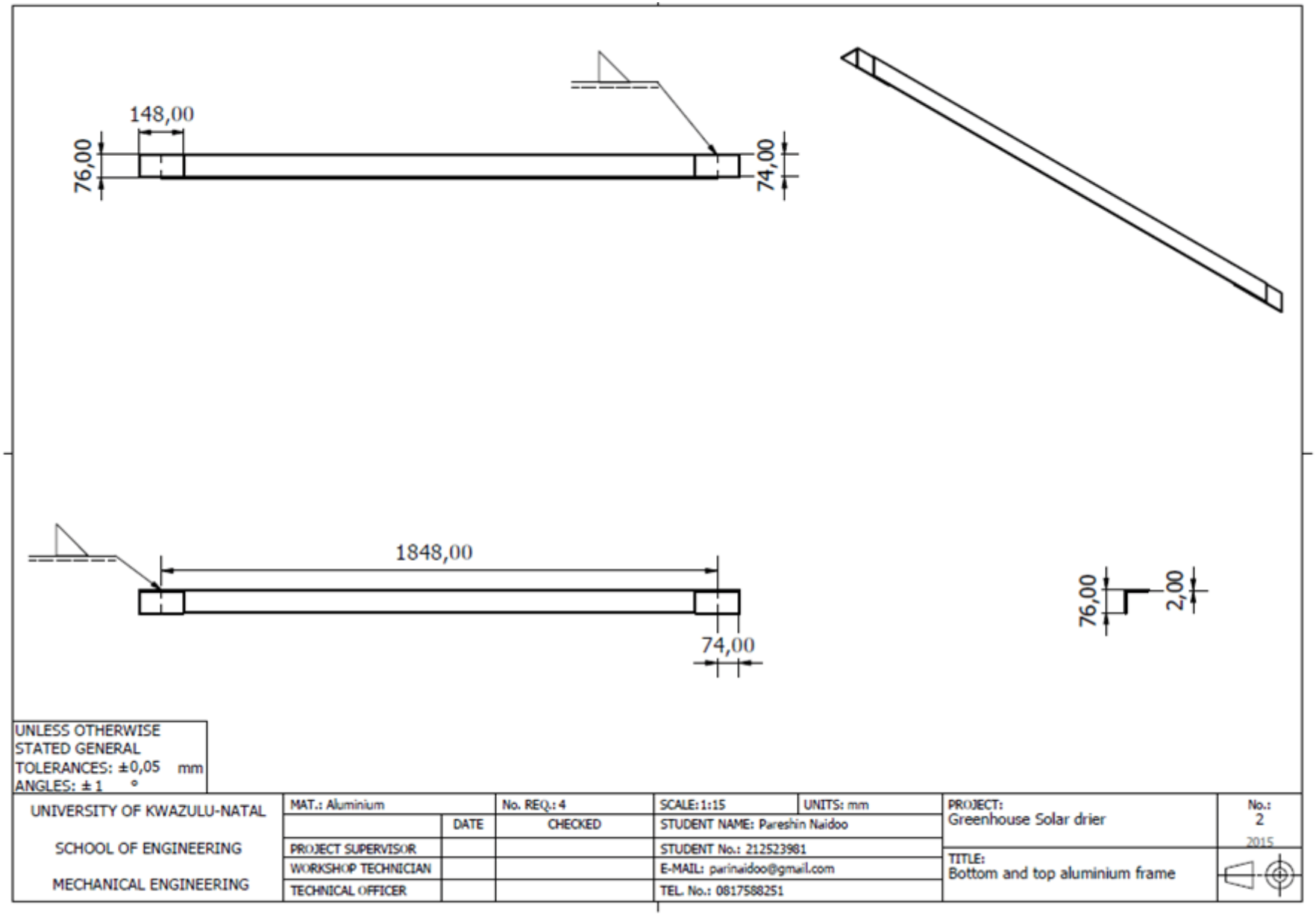

UNLESS OTHERWISE STATED GENERAL TOLERANCES: ±0,05 mm
ANGLES: ± 1 °

UNIVERSITY OF KWAZULU-NATAL SCHOOL OF ENGINEERING MECHANICAL ENGINEERING	MAT.: Aluminium		No. REQ.: 4	SCALE: 1:15 UNITS: mm	PROJECT: Greenhouse Solar drier
		DATE	CHECKED	STUDENT NAME: Pareshin Naidoo	
	PROJECT SUPERVISOR			STUDENT No.: 212523981	TITLE: Bottom and top aluminium frame
	WORKSHOP TECHNICIAN			E-MAIL: parinaidoo@gmail.com	
	TECHNICAL OFFICER			TEL. No.: 0817588251	

No.: 2
2015

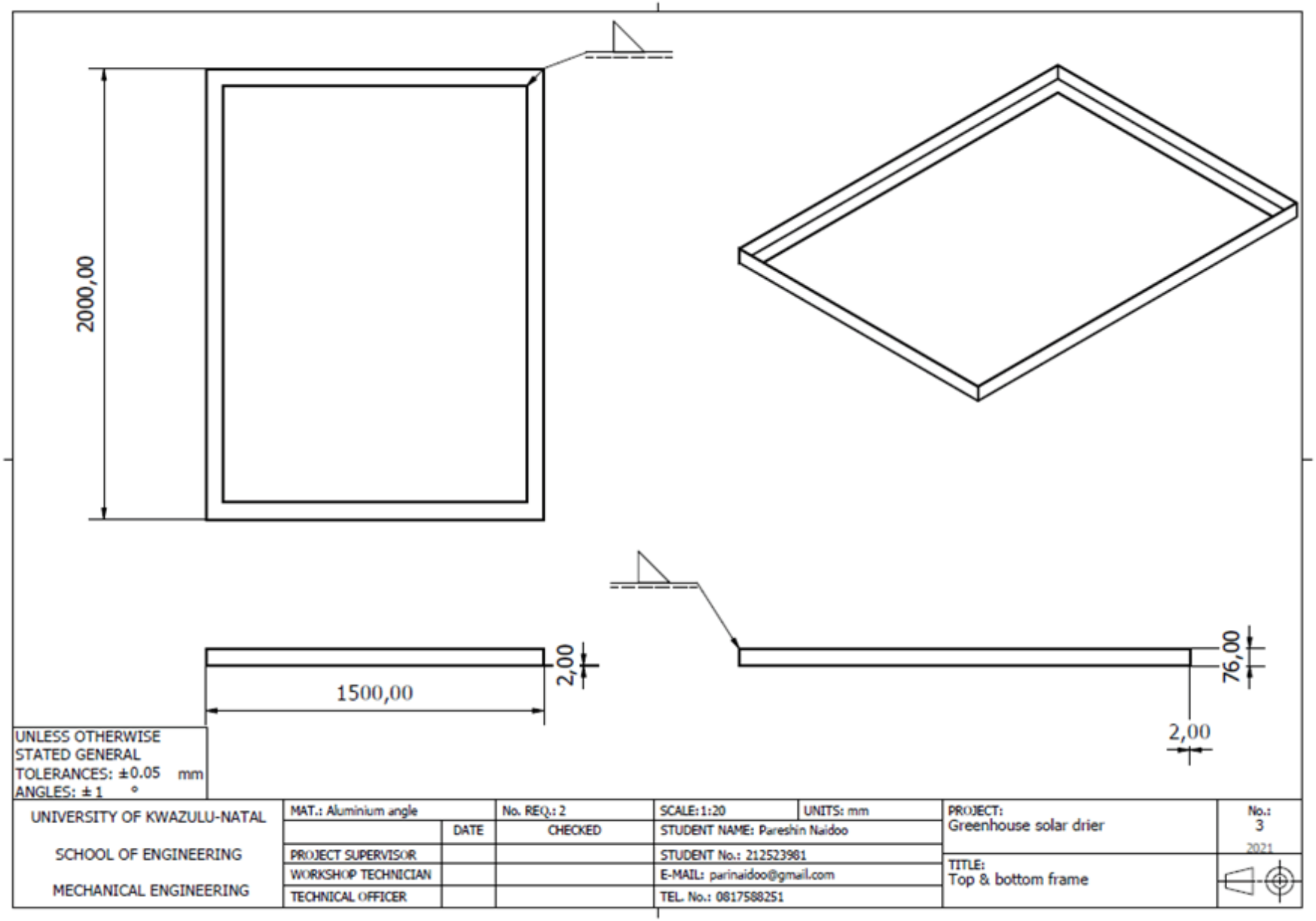
2000,00
1500,00
2,00
76,00
2,00
UNLESS OTHERWISE STATED GENERAL TOLERANCES: ±0.05 mm
ANGLES: ± 1 °
UNIVERSITY OF KWAZULU-NATAL
SCHOOL OF ENGINEERING
MECHANICAL ENGINEERING
MAT.: Aluminium angle
No. REQ.: 2
SCALE: 1:20
UNITS: mm
DATE
CHECKED
PROJECT SUPERVISOR
WORKSHOP TECHNICIAN
TECHNICAL OFFICER
STUDENT NAME: Pareshin Naidoo
STUDENT No.: 212523981
E-MAIL: parinaidoo@gmail.com
TEL. No.: 0817588251
PROJECT:
Greenhouse solar drier
No.:
3
2021
TITLE:
Top & bottom frame

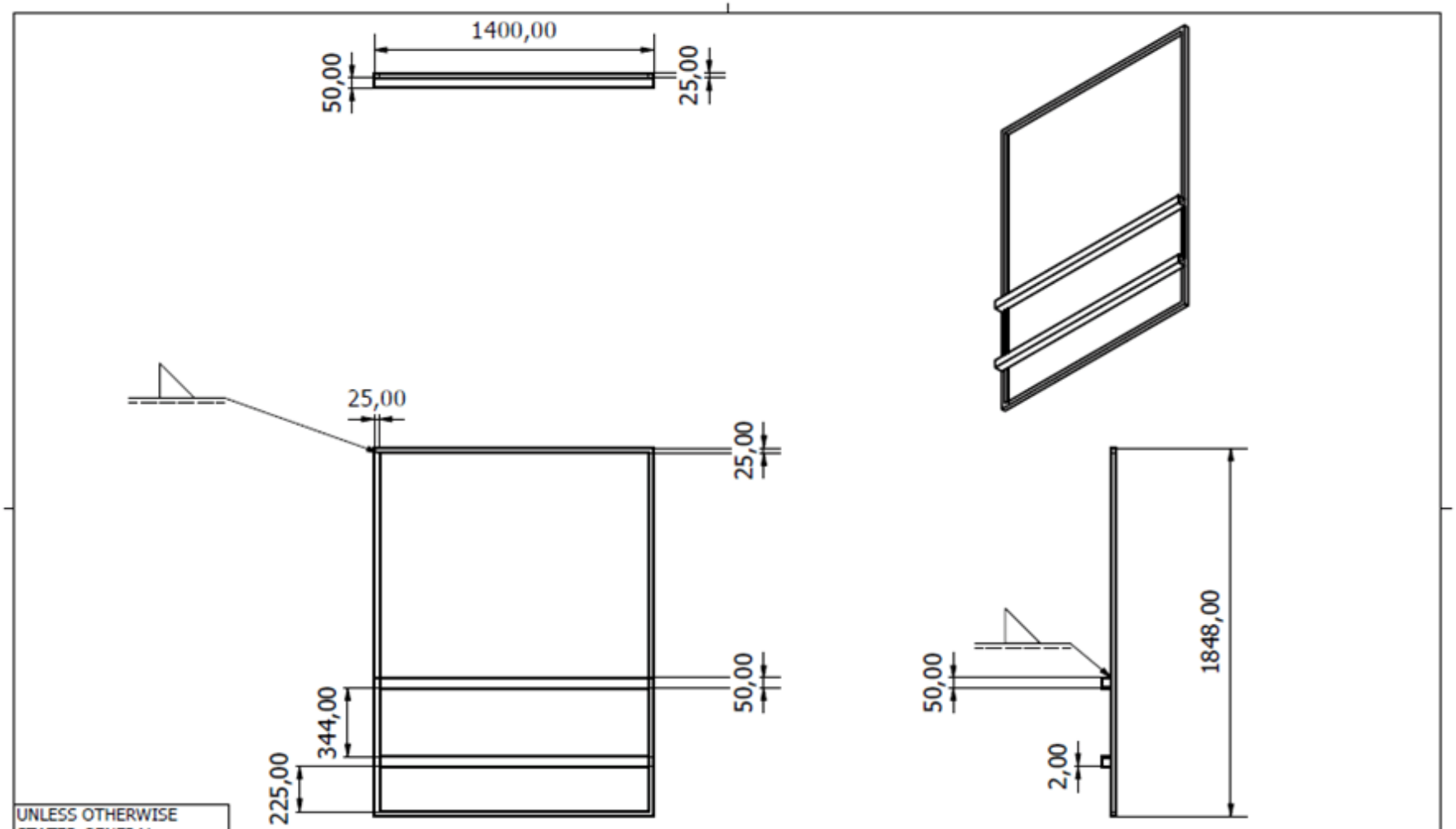

UNLESS OTHERWISE STATED GENERAL TOLERANCES: ±0,05 mm
ANGLES: ± 1 °

UNIVERSITY OF KWAZULU-NATAL	MAT.: Aluminium		No. REQ.: 1	SCALE: 1:25	UNITS: mm	PROJECT: Greenhouse Solar drier
		DATE	CHECKED	STUDENT NAME: Pareshin Naidoo		No.: 4
SCHOOL OF ENGINEERING	PROJECT SUPERVISOR			STUDENT No.: 212523981		2015
	WORKSHOP TECHNICIAN			E-MAIL: parinaidoo@gmail.com		TITLE: Door frame
MECHANICAL ENGINEERING	TECHNICAL OFFICER			TEL. No.: 0817588251		

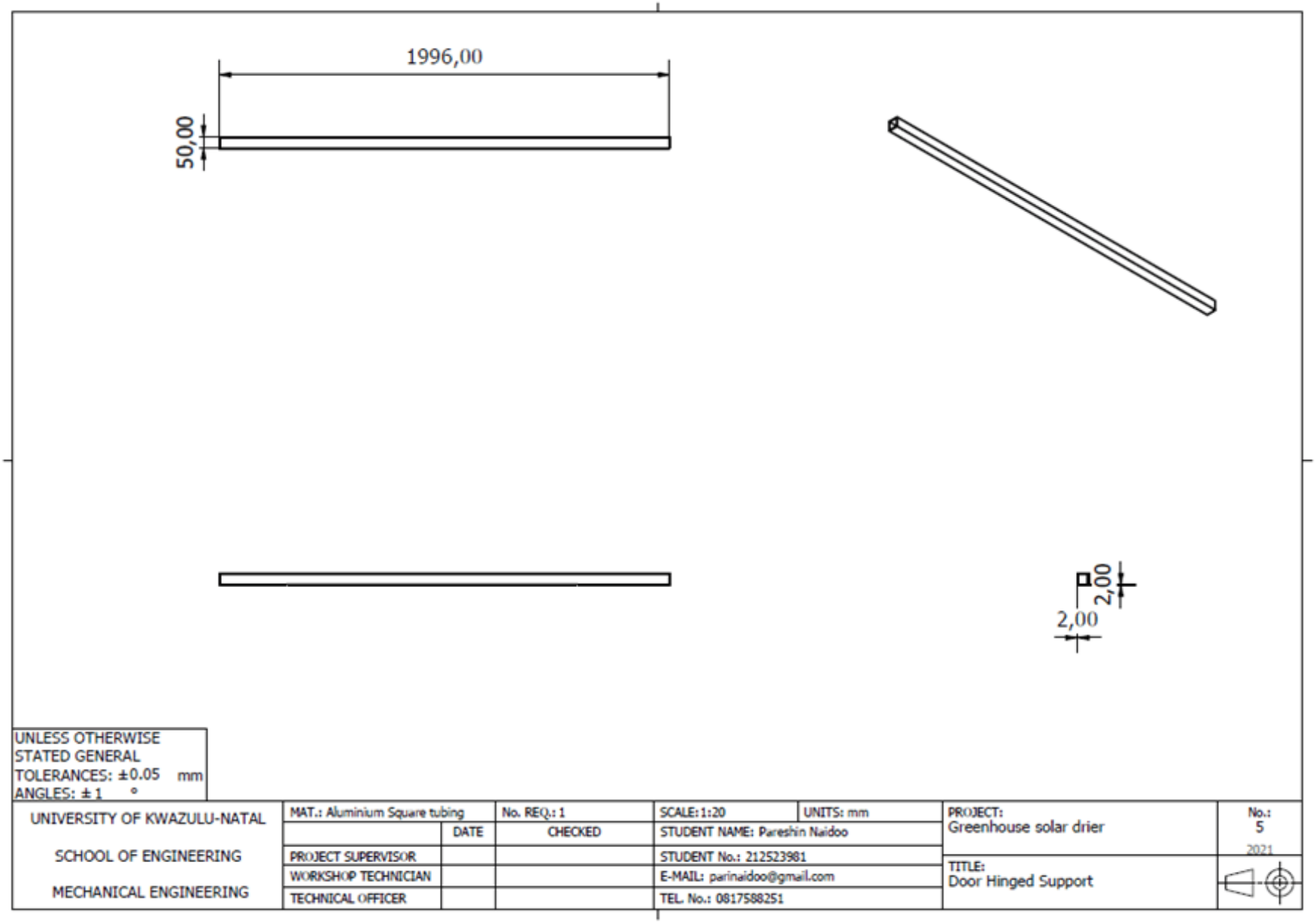

UNLESS OTHERWISE STATED GENERAL TOLERANCES: ±0.05 mm
ANGLES: ± 1 °

UNIVERSITY OF KWAZULU-NATAL	MAT.: Aluminium Square tubing		No. REQ.: 1	SCALE: 1:20	UNITS: mm	PROJECT: Greenhouse solar drier
		DATE	CHECKED	STUDENT NAME: Pareshin Naidoo		No.: 5
SCHOOL OF ENGINEERING	PROJECT SUPERVISOR			STUDENT No.: 212523981		2021
	WORKSHOP TECHNICIAN			E-MAIL: parinaidoo@gmail.com		TITLE: Door Hinged Support
MECHANICAL ENGINEERING	TECHNICAL OFFICER			TEL. No.: 0817588251		

H-2. Absorber Wall

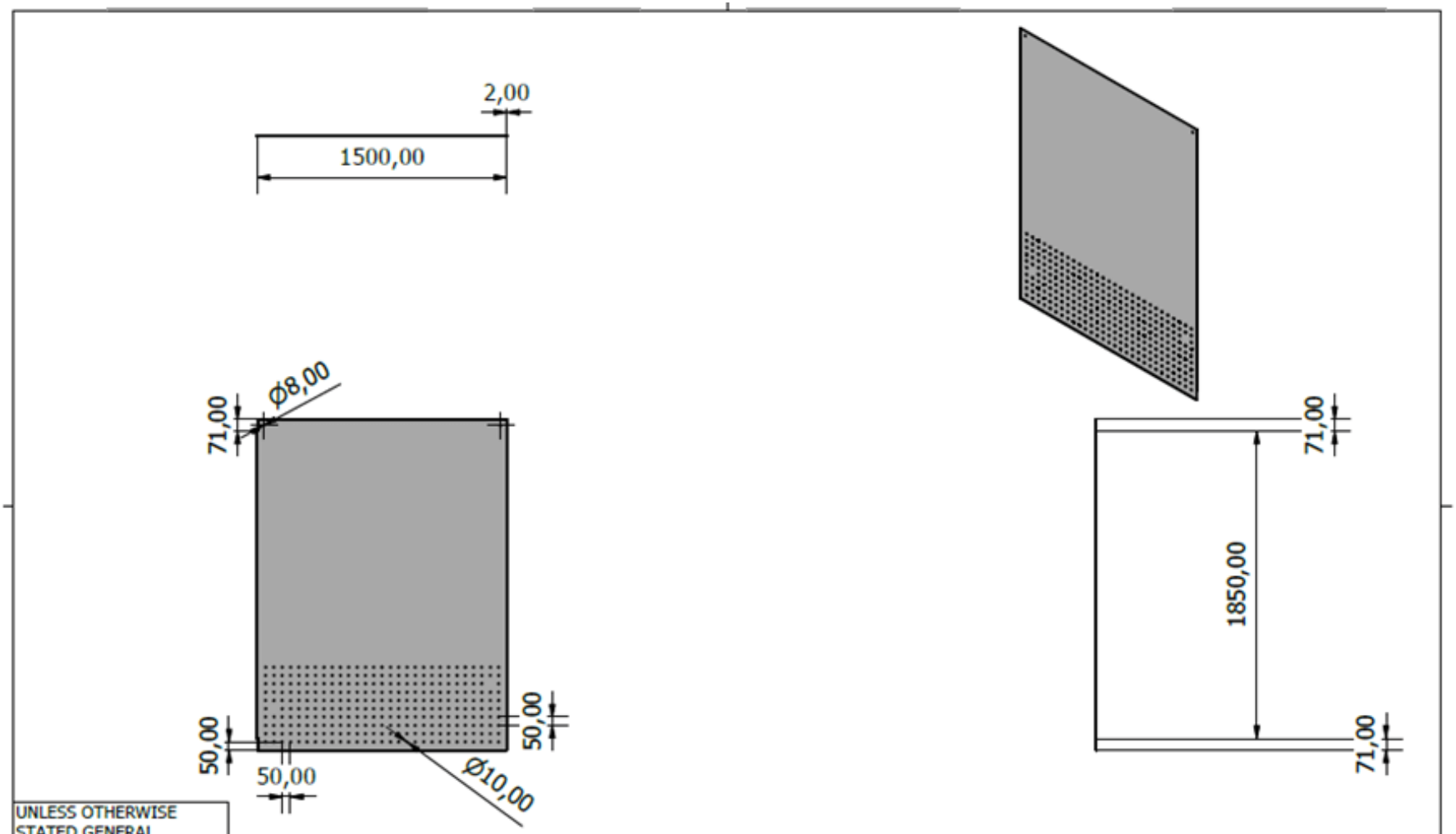

UNLESS OTHERWISE STATED GENERAL TOLERANCES: ±0.05 mm
ANGLES: ± 1 °

UNIVERSITY OF KWAZULU-NATAL	MAT.: Aluminium Sheet		No. REQ.: 1	SCALE:1:30	UNITS: mm	PROJECT: Greenhouse solar drier
		DATE	CHECKED	STUDENT NAME: Pareshin Naidoo		No.: 6
SCHOOL OF ENGINEERING	PROJECT SUPERVISOR			STUDENT No.: 212523981		2021
	WORKSHOP TECHNICIAN			E-MAIL: parinaidoo@gmail.com		TITLE: Absorber wall
MECHANICAL ENGINEERING	TECHNICAL OFFICER			TEL. No.: 0817588251		

H-3. Rake System

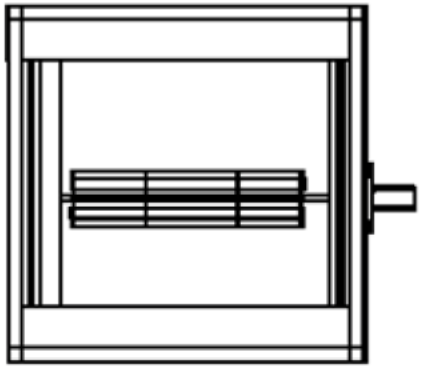

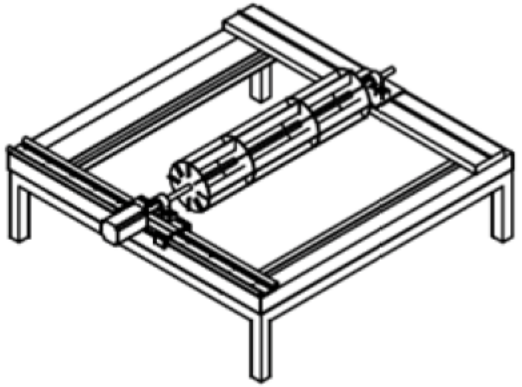

UNLESS OTHERWISE STATED GENERAL TOLERANCES: ±0.05 mm
ANGLES: ± 1 °

UNIVERSITY OF KWAZULU-NATAL	MAT.: Aluminium Sheet		No. REQ.: 1	SCALE: 1:30	UNITS: mm	PROJECT: Greenhouse solar drier	No.: 7
		DATE	CHECKED	STUDENT NAME: Pareshin Naidoo			2021
SCHOOL OF ENGINEERING	PROJECT SUPERVISOR			STUDENT No.: 212523981			
	WORKSHOP TECHNICIAN			E-MAIL: [redacted]		TITLE: Rake system and table support	
MECHANICAL ENGINEERING	TECHNICAL OFFICER			TEL. No.: [redacted]			

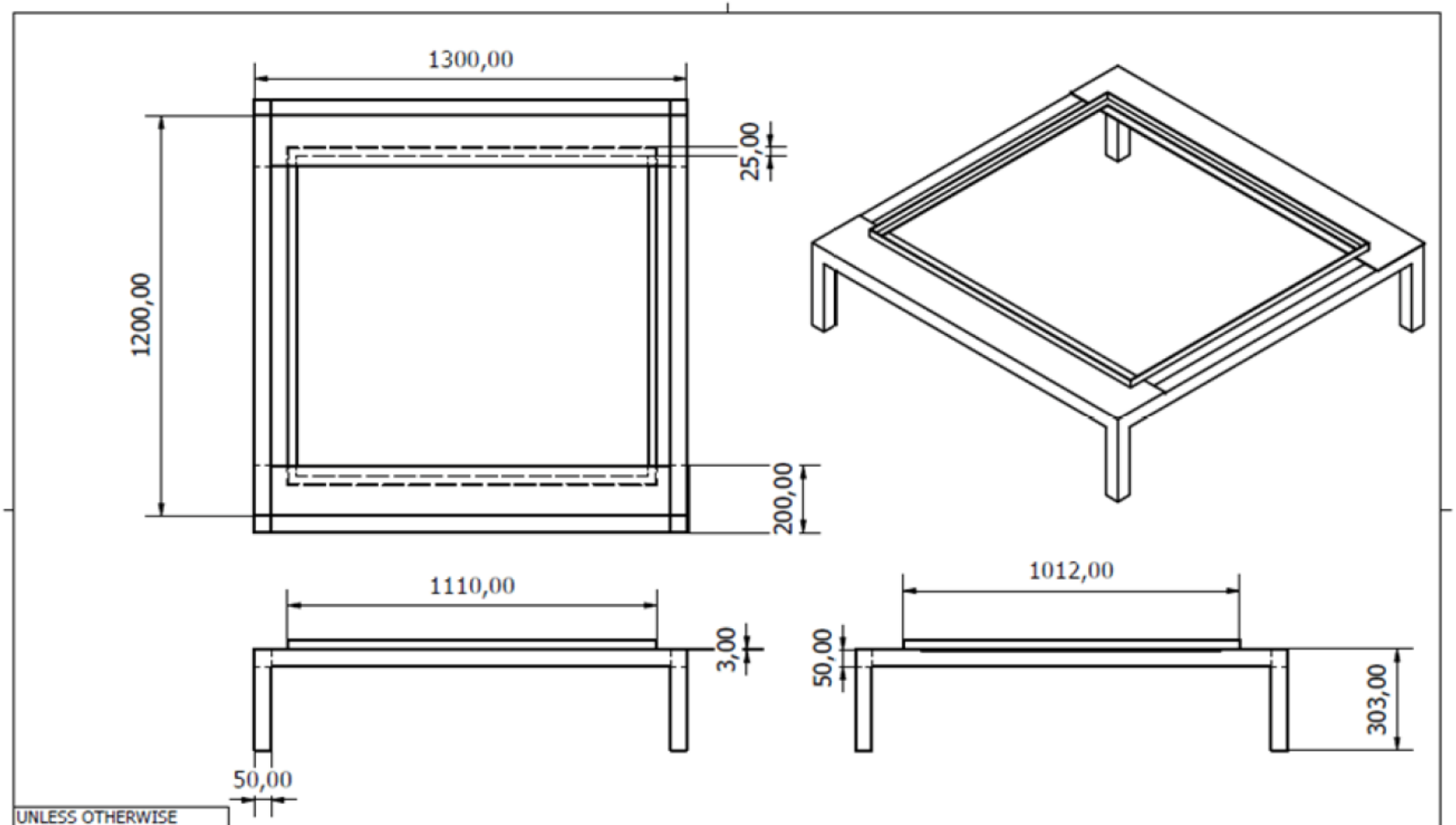
1300,00
25,00
1200,00
200,00
1110,00
3,00
50,00
1012,00
50,00
303,00
UNLESS OTHERWISE STATED GENERAL TOLERANCES: ±0,05 mm
ANGLES: ± 1 °
UNIVERSITY OF KWAZULU-NATAL
SCHOOL OF ENGINEERING
MECHANICAL ENGINEERING
MAT.: Aluminium
No. REQ.: 0817588251
SCALE:1:15
UNITS: mm
DATE
CHECKED
STUDENT NAME: Pareshin Naidoo
PROJECT SUPERVISOR
STUDENT No.: 212523981
WORKSHOP TECHNICIAN
E-MAIL: [redacted]
TECHNICAL OFFICER
TEL. No.: [redacted]
PROJECT:
Greenhouse Solar drier
No.:
8
2015
TITLE:
Drying Table

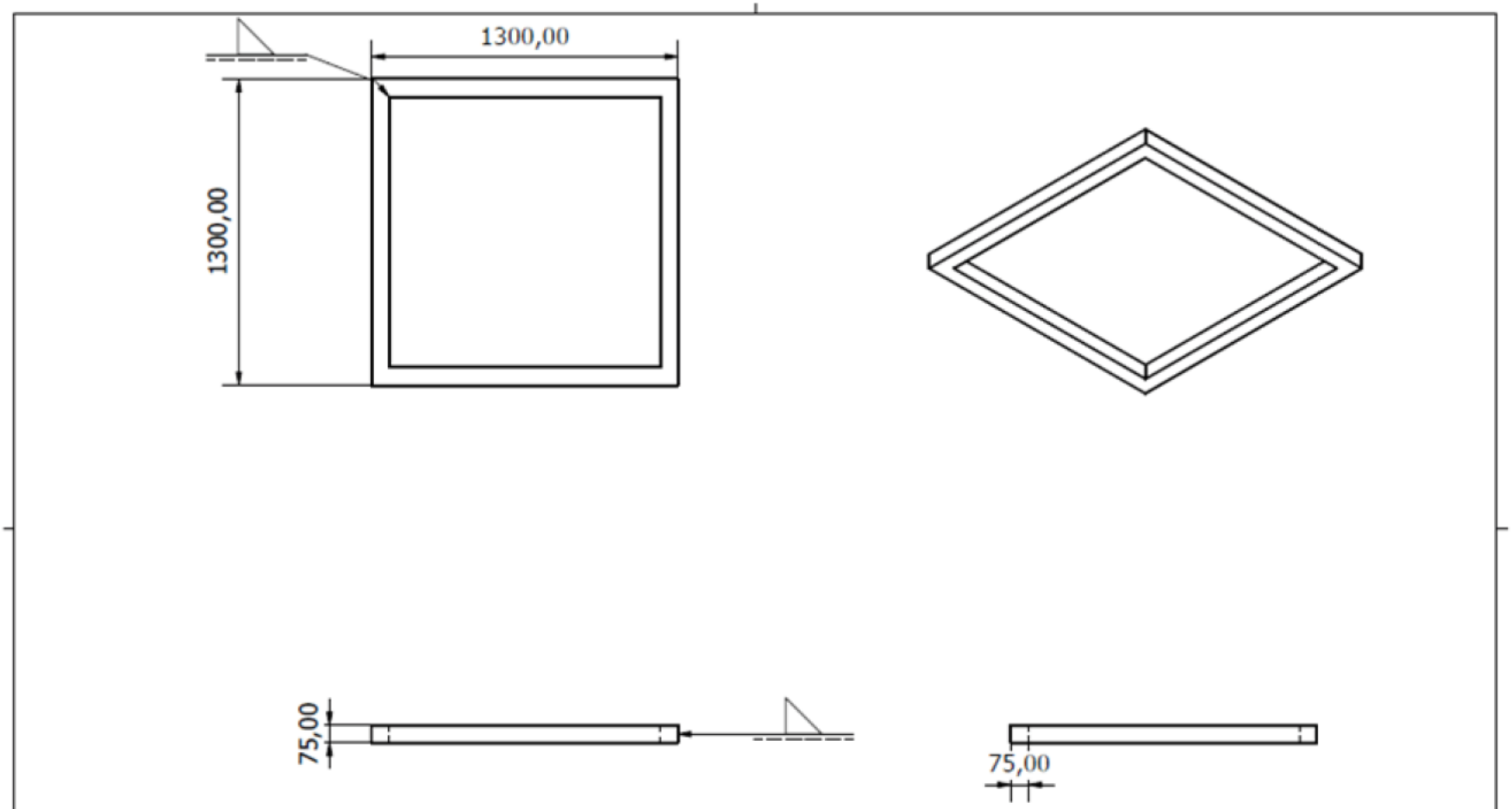

UNLESS OTHERWISE STATED GENERAL TOLERANCES: ±0.05 mm
ANGLES: ± 1 °

UNIVERSITY OF KWAZULU-NATAL	MAT.: Aluminium Sheet		No. REQ.: 1	SCALE:1:30 UNITS: mm	PROJECT: Greenhouse solar drier
		DATE	CHECKED	STUDENT NAME: Pareshin Naidoo	
SCHOOL OF ENGINEERING	PROJECT SUPERVISOR			STUDENT No.: 212523981	
	WORKSHOP TECHNICIAN			E-MAIL: [redacted]	TITLE: Hinged rake system table support
MECHANICAL ENGINEERING	TECHNICAL OFFICER			TEL. No.: [redacted]	

No.: 9
2021

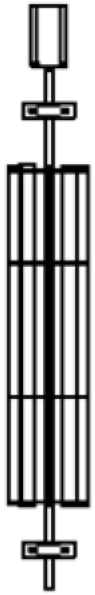

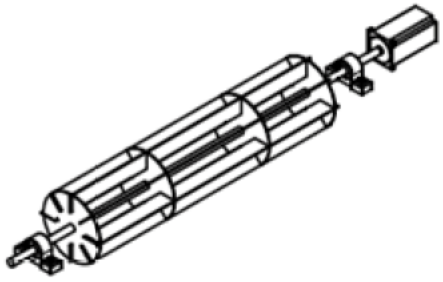

UNLESS OTHERWISE STATED GENERAL TOLERANCES: ±0.05 mm
ANGLES: ± 1 °

UNIVERSITY OF KWAZULU-NATAL	MAT.: Aluminium Sheet		No. REQ.: 1	SCALE: 1:30	UNITS: mm	PROJECT: Greenhouse solar drier	No.: 10
		DATE	CHECKED	STUDENT NAME: Pareshin Naidoo			2021
SCHOOL OF ENGINEERING	PROJECT SUPERVISOR			STUDENT No.: 212523981			
	WORKSHOP TECHNICIAN			E-MAIL: [redacted]		TITLE: Assembly rotary blade	
MECHANICAL ENGINEERING	TECHNICAL OFFICER			TEL. No.: [redacted]			

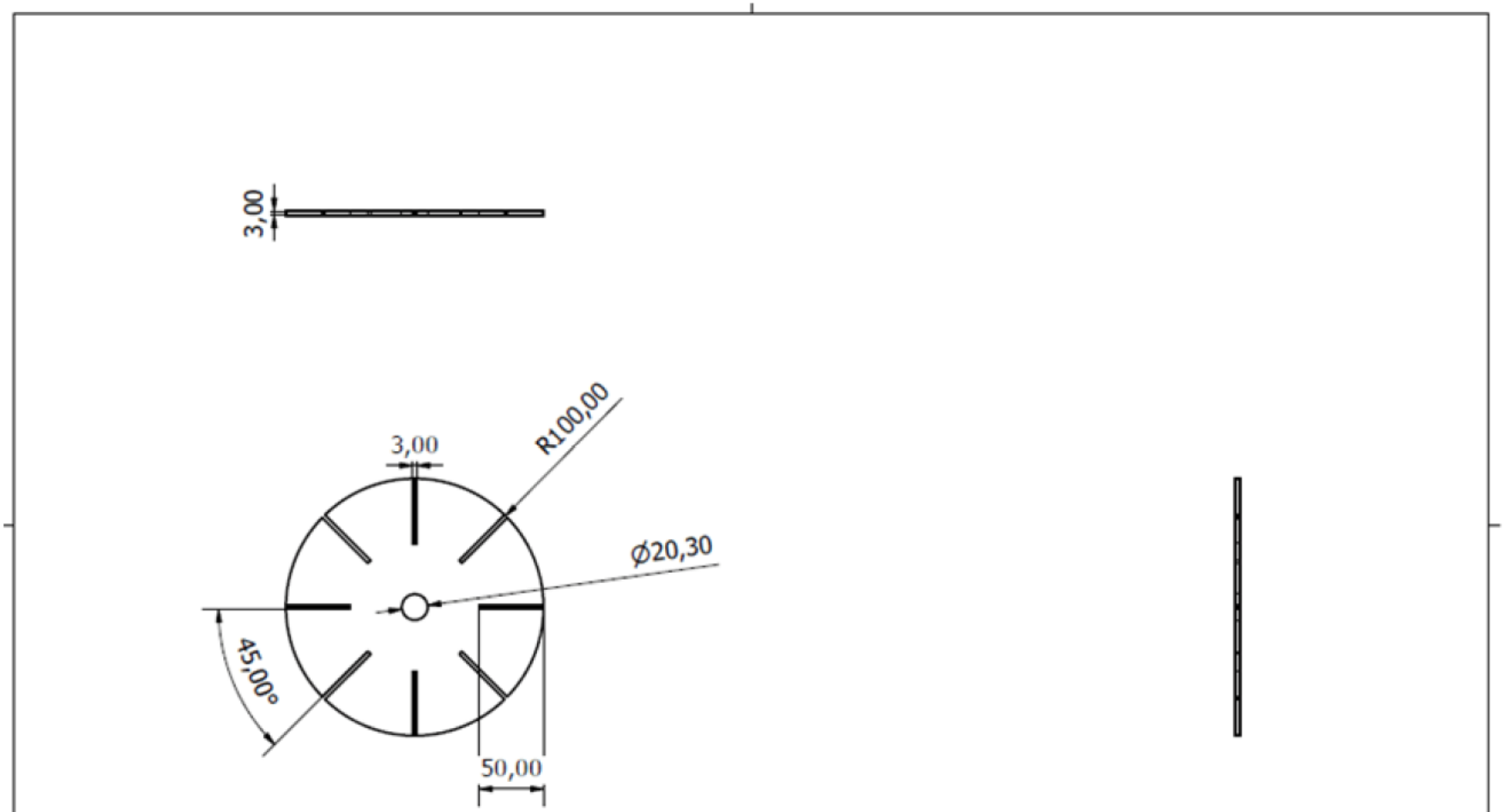

UNLESS OTHERWISE STATED GENERAL TOLERANCES: ±0.05 mm
ANGLES: ± 1 °

UNIVERSITY OF KWAZULU-NATAL	MAT.: Aluminium Sheet		No. REQ.: 4	SCALE: 1:30 UNITS: mm	PROJECT: Greenhouse solar drier
		DATE	CHECKED	STUDENT NAME: Pareshin Naidoo	
SCHOOL OF ENGINEERING	PROJECT SUPERVISOR			STUDENT No.: 212523981	
	WORKSHOP TECHNICIAN			E-MAIL: [redacted]	TITLE: Blade Disks
MECHANICAL ENGINEERING	TECHNICAL OFFICER			TEL. No.: [redacted]	

No.: 11
2021

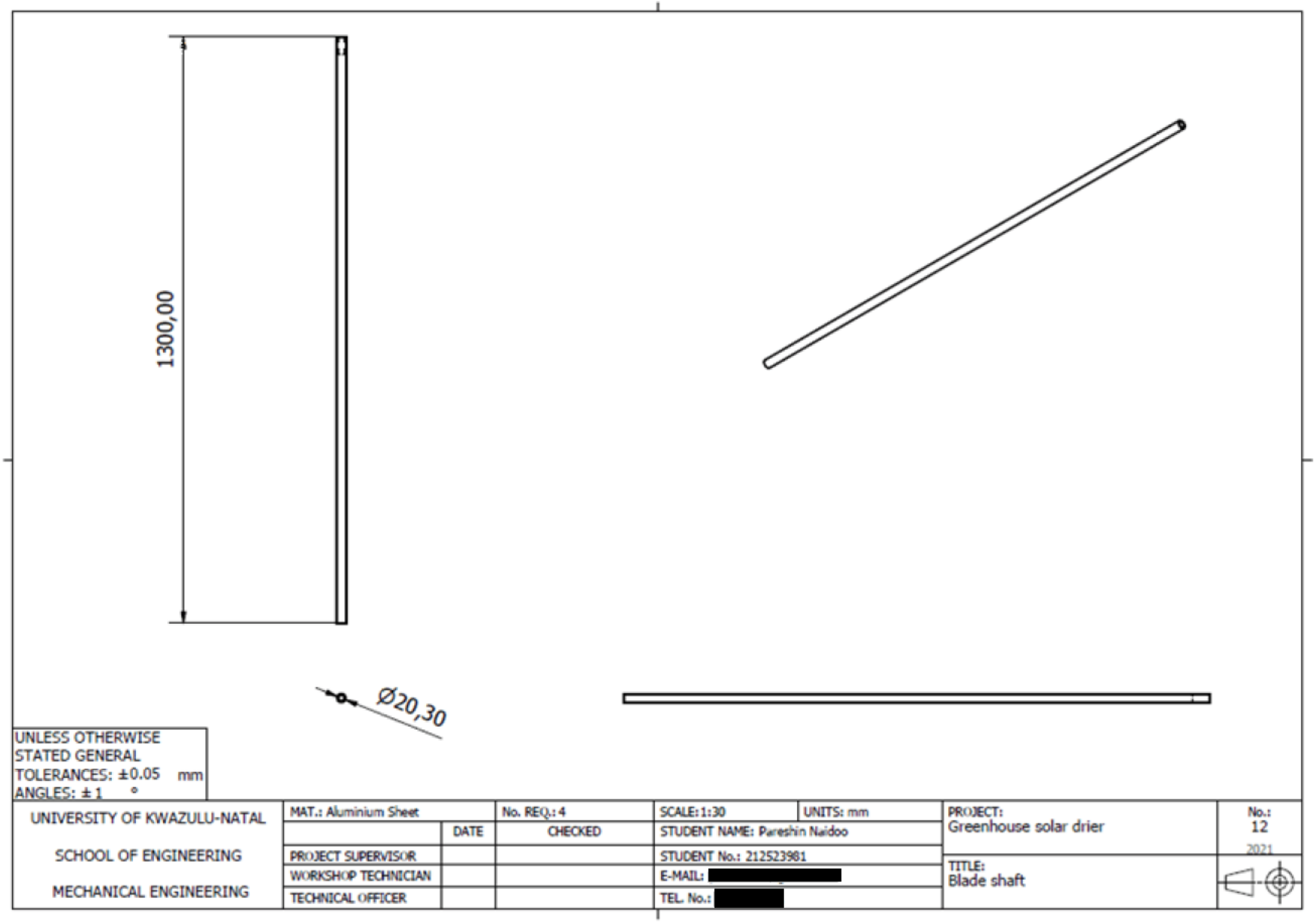
1300,00
Ø20,30
UNLESS OTHERWISE
STATED GENERAL
TOLERANCES: ±0.05 mm
ANGLES: ± 1 °
UNIVERSITY OF KWAZULU-NATAL
SCHOOL OF ENGINEERING
MECHANICAL ENGINEERING
MAT.: Aluminium Sheet
No. REQ.: 4
SCALE: 1:30
UNITS: mm
DATE
CHECKED
STUDENT NAME: Pareshin Naidoo
PROJECT SUPERVISOR
STUDENT No.: 212523981
WORKSHOP TECHNICIAN
E-MAIL: [redacted]
TECHNICAL OFFICER
TEL. No.: [redacted]
PROJECT:
Greenhouse solar drier
No.:
12
2021
TITLE:
Blade shaft

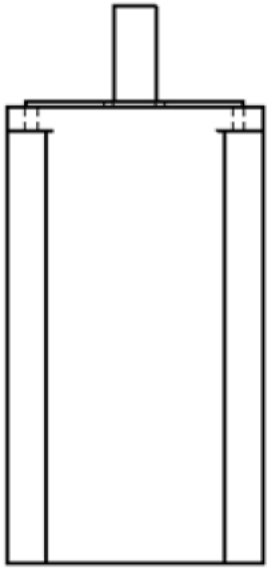

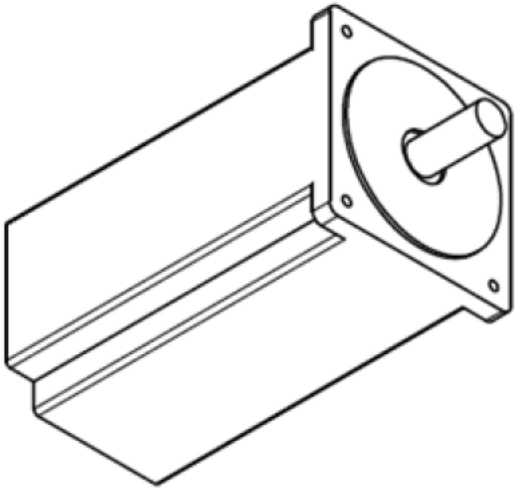

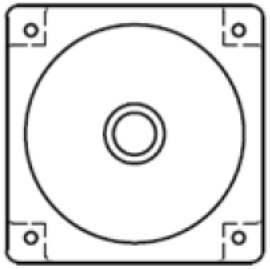

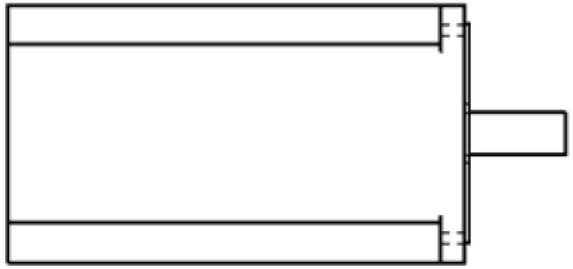

UNLESS OTHERWISE STATED GENERAL TOLERANCES: ±0,05 mm
ANGLES: ± 1 °

UNIVERSITY OF KWAZULU-NATAL	MAT.: Aluminium		No. REQ.: 1	SCALE: 1:15 UNITS: mm	PROJECT: Greenhouse Solar drier
		DATE	CHECKED	STUDENT NAME: Pareshin Naidoo	
SCHOOL OF ENGINEERING	PROJECT SUPERVISOR			STUDENT No.: 212523981	
	WORKSHOP TECHNICIAN			E-MAIL: [redacted]	TITLE: Nema 34 motor
MECHANICAL ENGINEERING	TECHNICAL OFFICER			TEL. No.: [redacted]	

No.: 13
2015

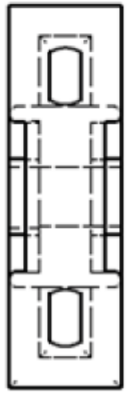

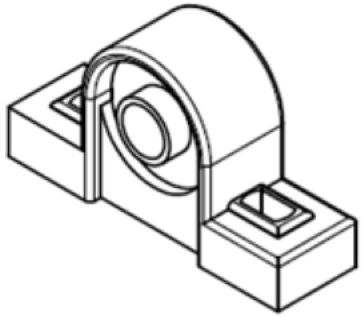

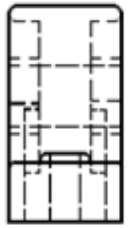

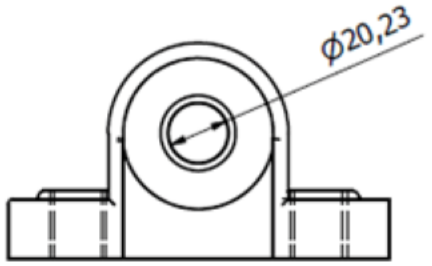

UNLESS OTHERWISE STATED GENERAL TOLERANCES: ±0.05 mm
ANGLES: ± 1 °

UNIVERSITY OF KWAZULU-NATAL	MAT.: Aluminium Sheet		No. REQ.: 1	SCALE: 1:30	UNITS: mm	PROJECT: Greenhouse solar drier	No.: 14
		DATE	CHECKED	STUDENT NAME: Pareshin Naidoo			2021
SCHOOL OF ENGINEERING	PROJECT SUPERVISOR			STUDENT No.: 212523981			
	WORKSHOP TECHNICIAN			E-MAIL: [redacted]		TITLE: Pillow block bearing	
MECHANICAL ENGINEERING	TECHNICAL OFFICER			TEL. No.: [redacted]			

H-4. PMMA Acrylic Sheet

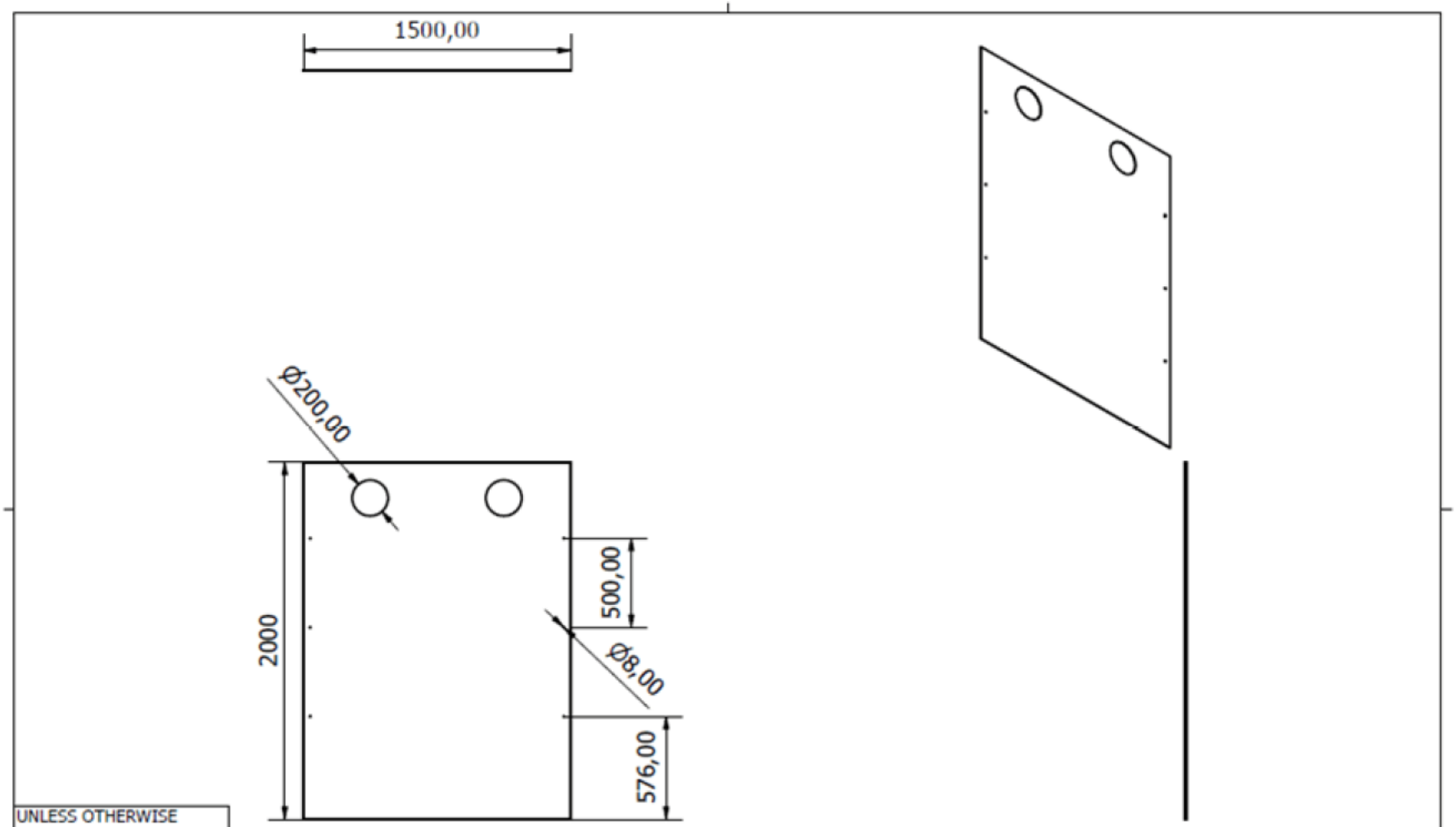

UNLESS OTHERWISE STATED GENERAL TOLERANCES: ±0.05 mm
ANGLES: ± 1 °

UNIVERSITY OF KWAZULU-NATAL	MAT.: PMMA Acrylic		No. REQ.: 1	SCALE: 1:30	UNITS: mm	PROJECT: Greenhouse solar drier
		DATE	CHECKED	STUDENT NAME: Pareshin Naidoo		No.: 15
SCHOOL OF ENGINEERING	PROJECT SUPERVISOR			STUDENT No.: 212523981		2021
	WORKSHOP TECHNICIAN			E-MAIL: [redacted]		TITLE: Back PMMA Acrylic sheet
MECHANICAL ENGINEERING	TECHNICAL OFFICER			TEL. No.: [redacted]		

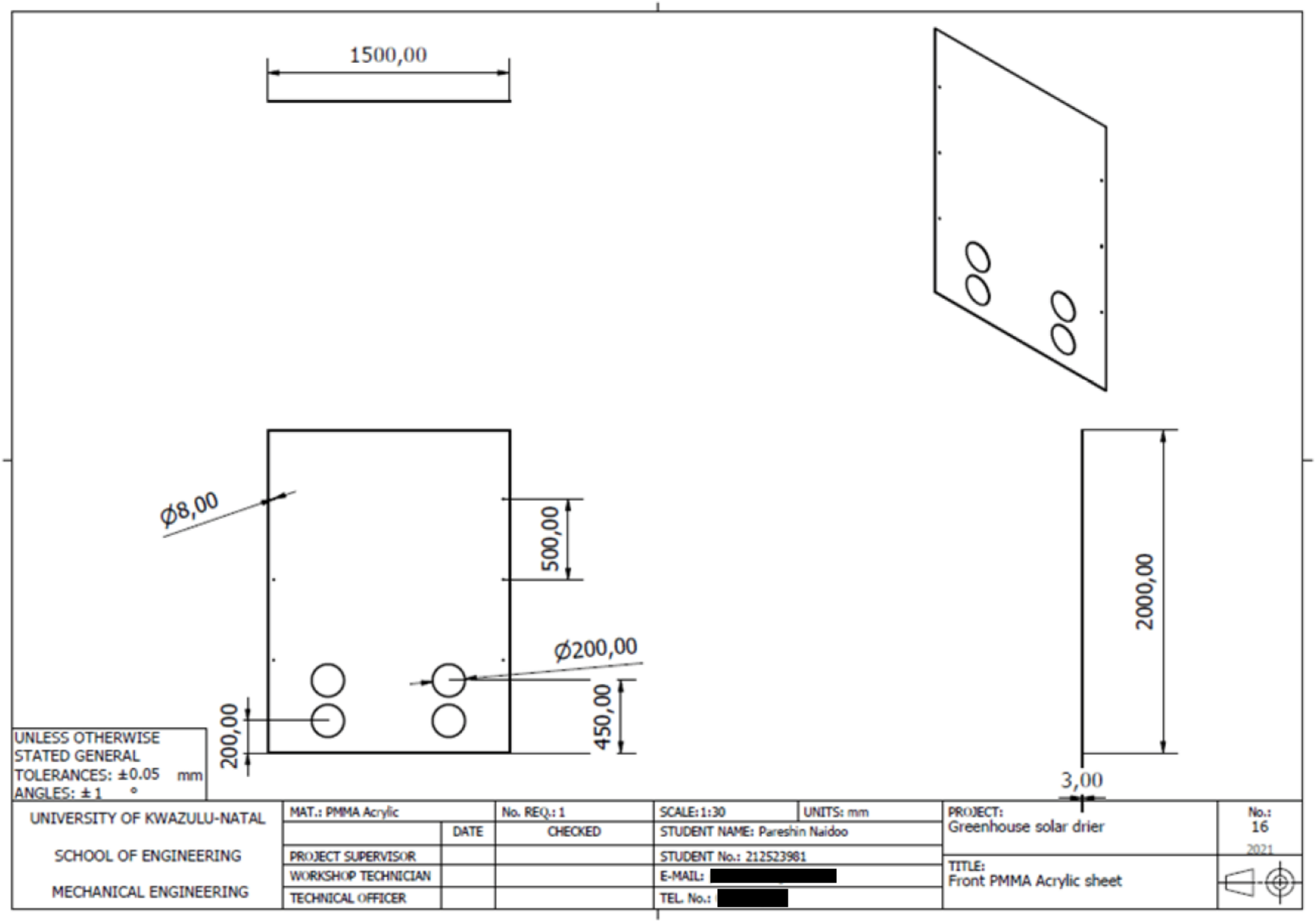
1500,00
Ø8,00
500,00
Ø200,00
450,00
200,00
2000,00
3,00
UNLESS OTHERWISE STATED GENERAL TOLERANCES: ±0.05 mm ANGLES: ± 1 °
UNIVERSITY OF KWAZULU-NATAL
SCHOOL OF ENGINEERING
MECHANICAL ENGINEERING
MAT.: PMMA Acrylic
No. REQ.: 1
SCALE: 1:30
UNITS: mm
DATE
CHECKED
STUDENT NAME: Pareshin Naidoo
PROJECT SUPERVISOR
STUDENT No.: 212523981
WORKSHOP TECHNICIAN
E-MAIL: [redacted]
TECHNICAL OFFICER
TEL. No.: [redacted]
PROJECT: Greenhouse solar drier
No.: 16
2021
TITLE: Front PMMA Acrylic sheet

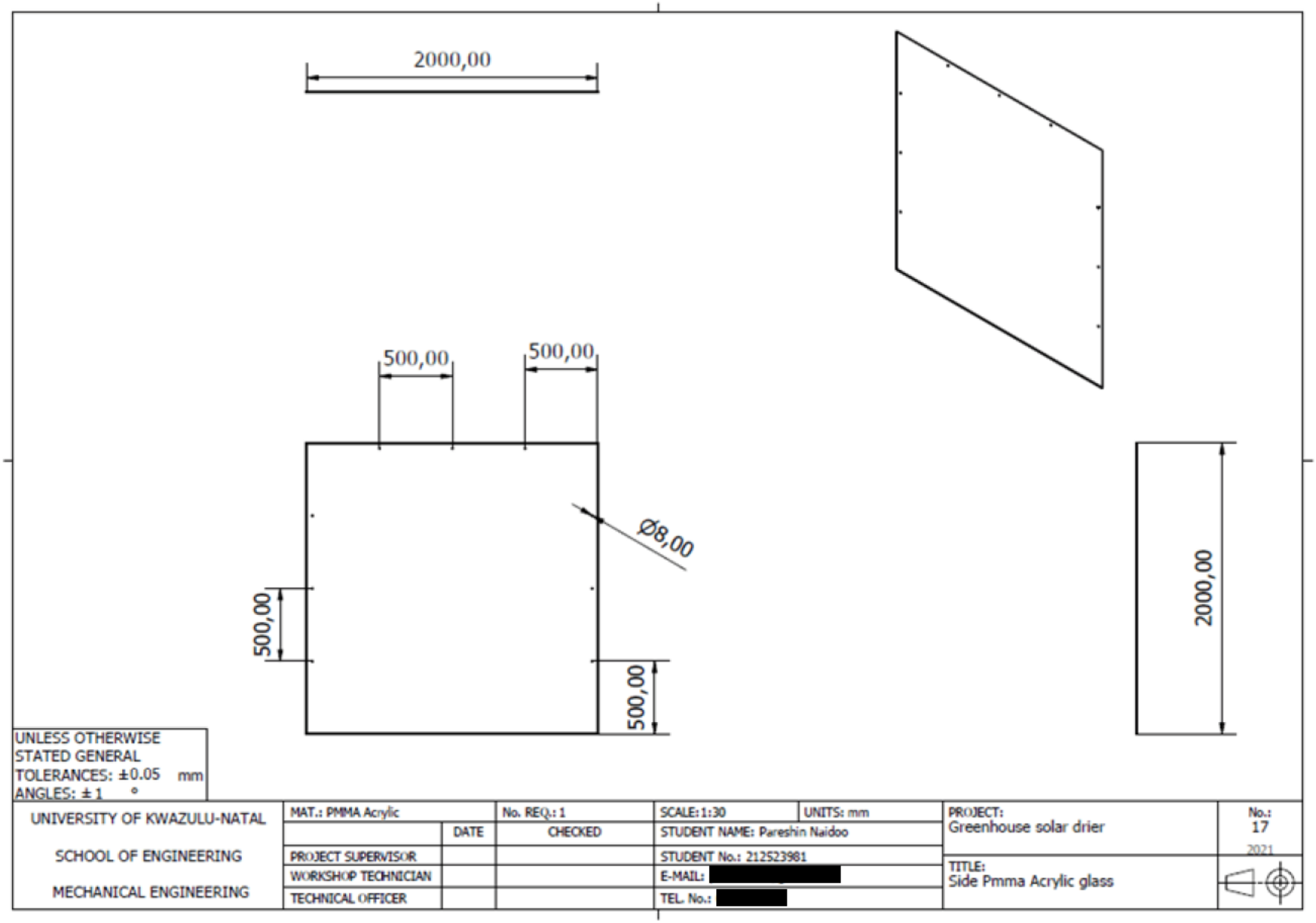
2000,00
500,00
500,00
Ø8,00
500,00
500,00
2000,00
UNLESS OTHERWISE STATED GENERAL TOLERANCES: ±0.05 mm
ANGLES: ± 1 °
UNIVERSITY OF KWAZULU-NATAL
SCHOOL OF ENGINEERING
MECHANICAL ENGINEERING
MAT.: PMMA Acrylic
No. REQ.: 1
SCALE: 1:30
UNITS: mm
DATE
CHECKED
PROJECT SUPERVISOR
WORKSHOP TECHNICIAN
TECHNICAL OFFICER
STUDENT NAME: Pareshin Naidoo
STUDENT No.: 212523981
E-MAIL: [redacted]
TEL. No.: [redacted]
PROJECT: Greenhouse solar drier
No.: 17
2021
TITLE: Side Pmma Acrylic glass

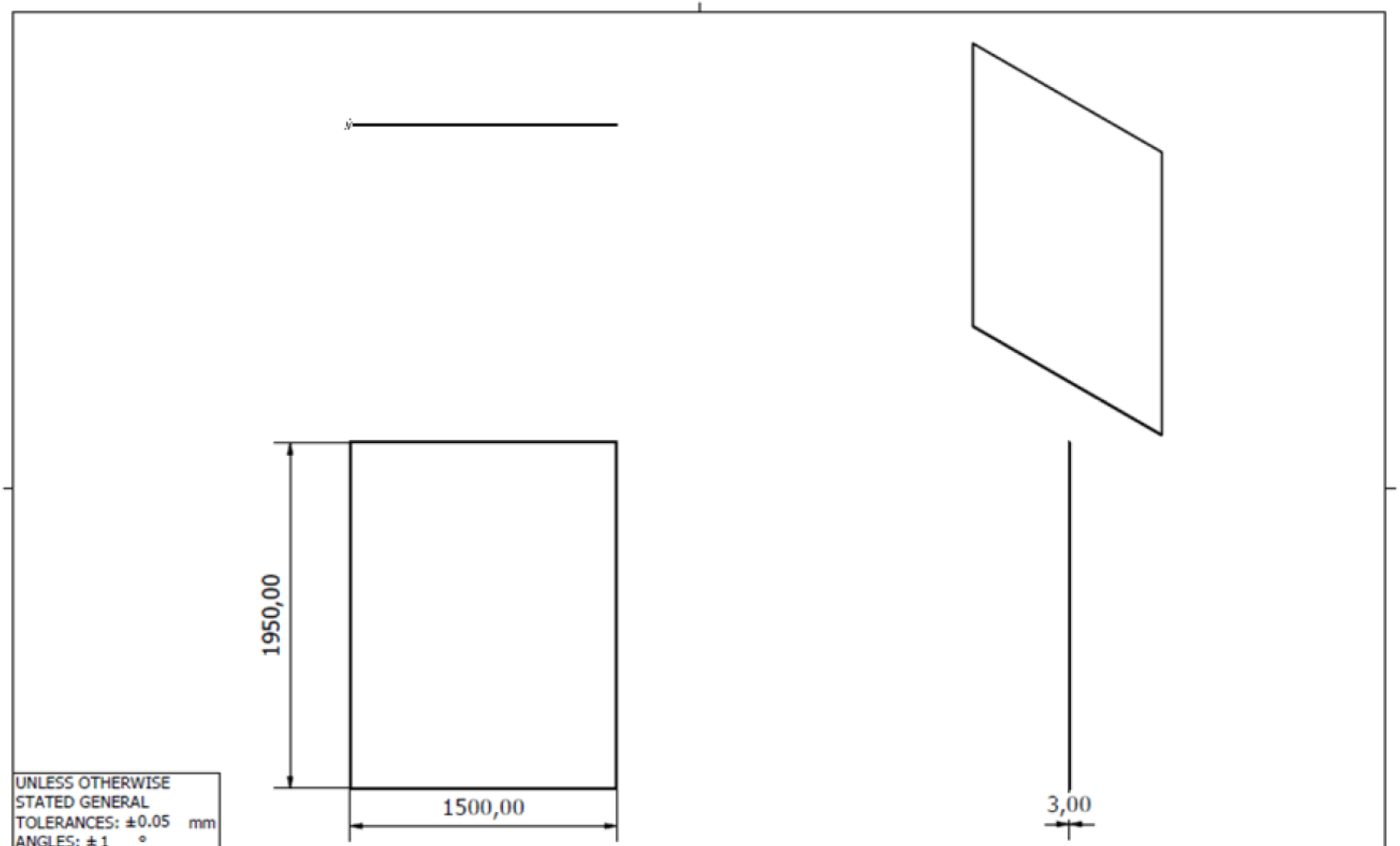

UNLESS OTHERWISE STATED GENERAL TOLERANCES: ±0.05 mm
ANGLES: ± 1 °

UNIVERSITY OF KWAZULU-NATAL	MAT.: PMMA Acrylic		No. REQ.: 1	SCALE: 1:30 UNITS: mm	PROJECT: Greenhouse solar drier
		DATE	CHECKED	STUDENT NAME: Pareshin Naidoo	
SCHOOL OF ENGINEERING	PROJECT SUPERVISOR			STUDENT No.: 212523981	
	WORKSHOP TECHNICIAN			E-MAIL: [redacted]	TITLE: Door PMMA plastic
MECHANICAL ENGINEERING	TECHNICAL OFFICER			TEL. No.: [redacted]	

No.: 18
2021

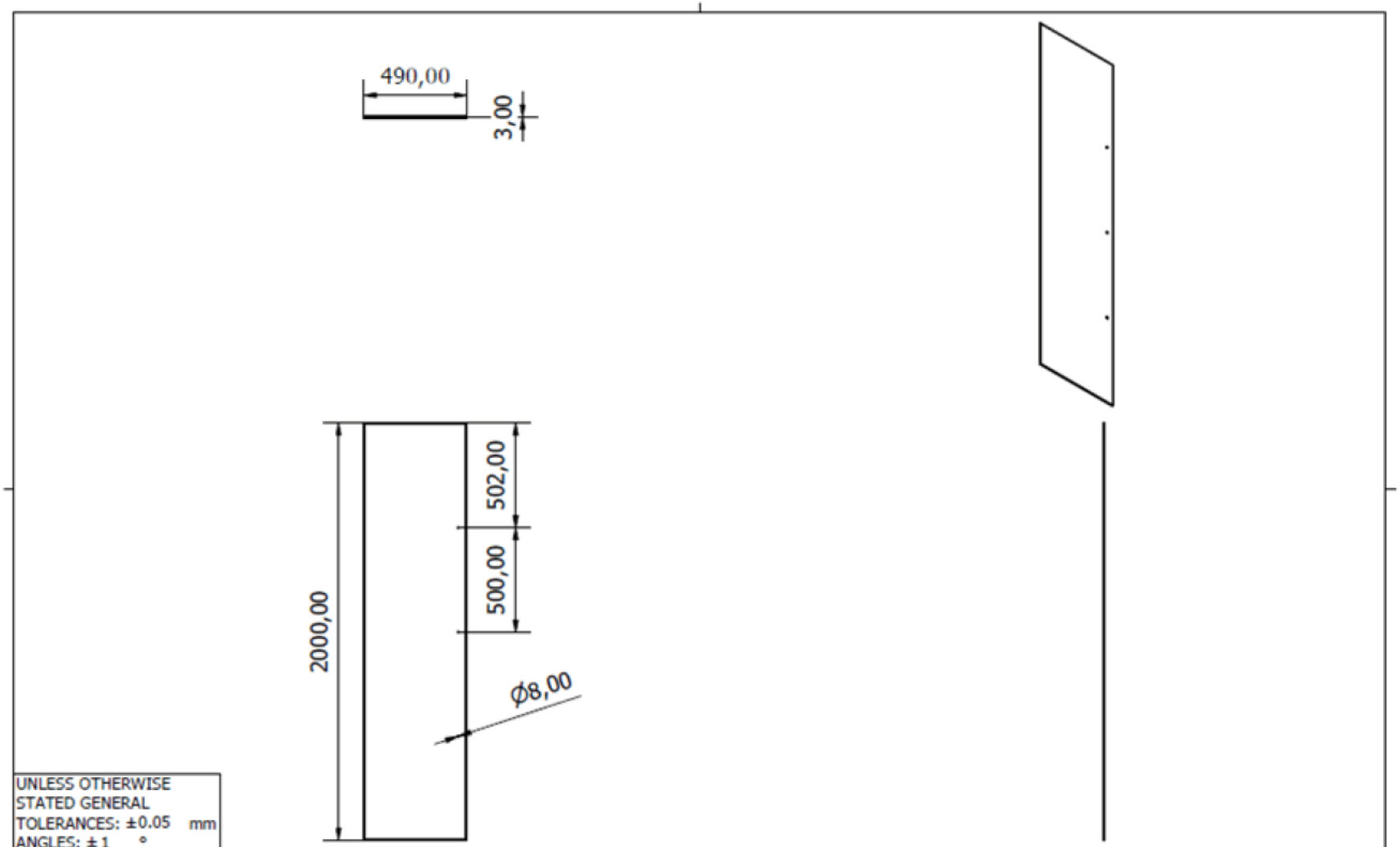

UNLESS OTHERWISE STATED GENERAL TOLERANCES: ±0.05 mm
ANGLES: ± 1 °

UNIVERSITY OF KWAZULU-NATAL	MAT.: PMMA Acrylic		No. REQ.: 1	SCALE: 1:30 UNITS: mm	PROJECT: Greenhouse solar drier
		DATE	CHECKED	STUDENT NAME: Pareshin Naidoo	
SCHOOL OF ENGINEERING	PROJECT SUPERVISOR			STUDENT No.: 212523981	
	WORKSHOP TECHNICIAN			E-MAIL: [redacted]	TITLE: Door Side Acrylic piece
MECHANICAL ENGINEERING	TECHNICAL OFFICER			TEL. No.: [redacted]	

No.: 19
2021

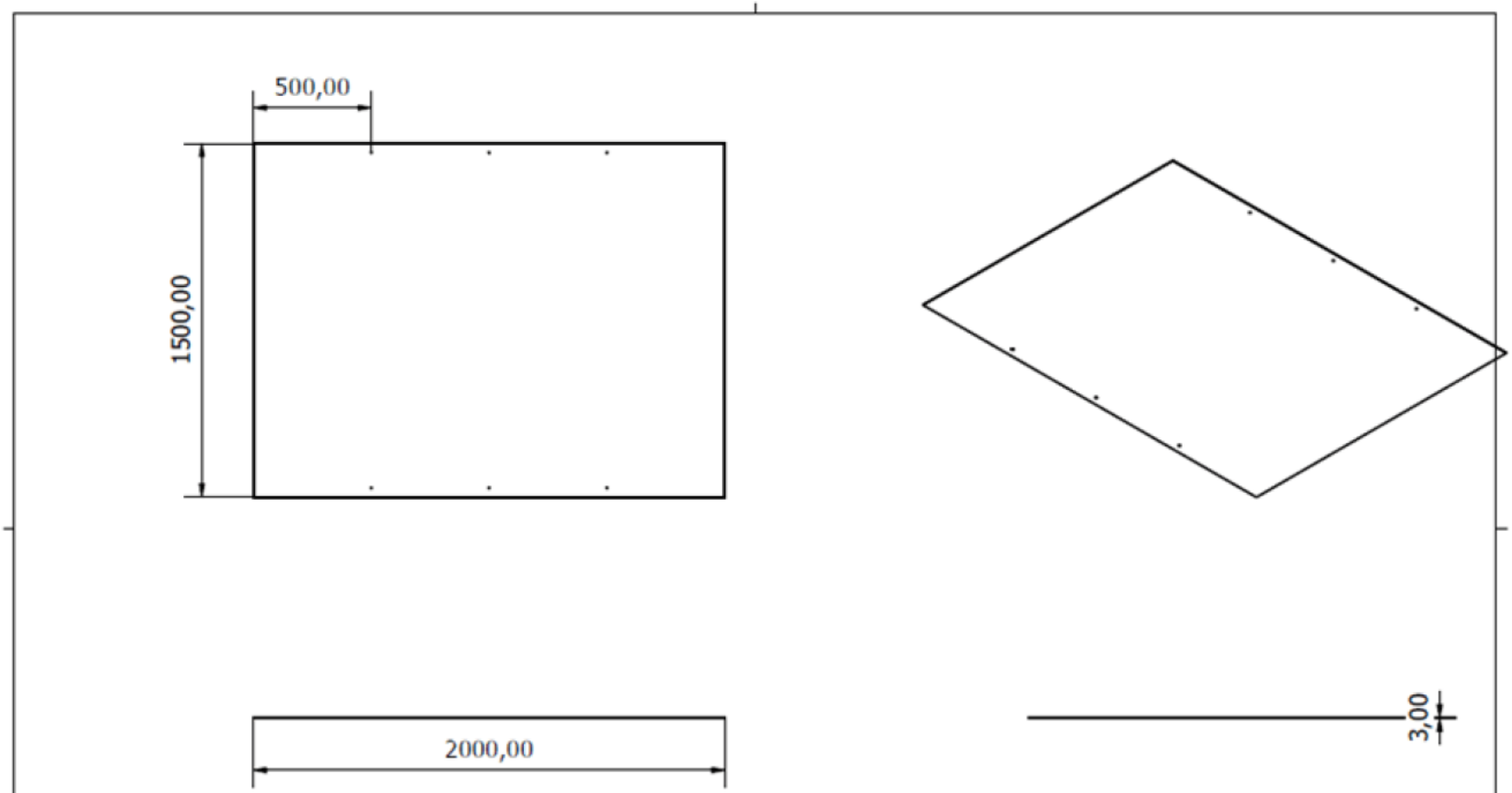

UNLESS OTHERWISE STATED GENERAL TOLERANCES: ±0.05 mm ANGLES: ± 1 °

UNIVERSITY OF KWAZULU-NATAL	MAT.: PMMA Acrylic		No. REQ.: 1	SCALE: 1:30 UNITS: mm	PROJECT: Greenhouse solar drier
		DATE	CHECKED	STUDENT NAME: Pareshin Naidoo	No.: 20
SCHOOL OF ENGINEERING	PROJECT SUPERVISOR			STUDENT No.: 212523981	2021
	WORKSHOP TECHNICIAN			E-MAIL: [redacted]	TITLE: Roof PMMA acrylic
MECHANICAL ENGINEERING	TECHNICAL OFFICER			TEL. No.: [redacted]	

H-5. Drying Tray

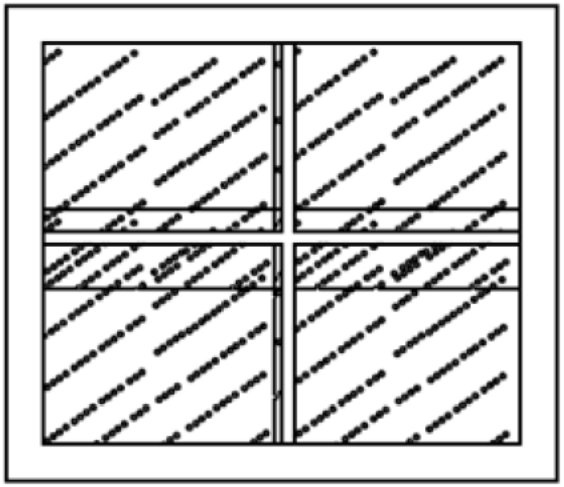

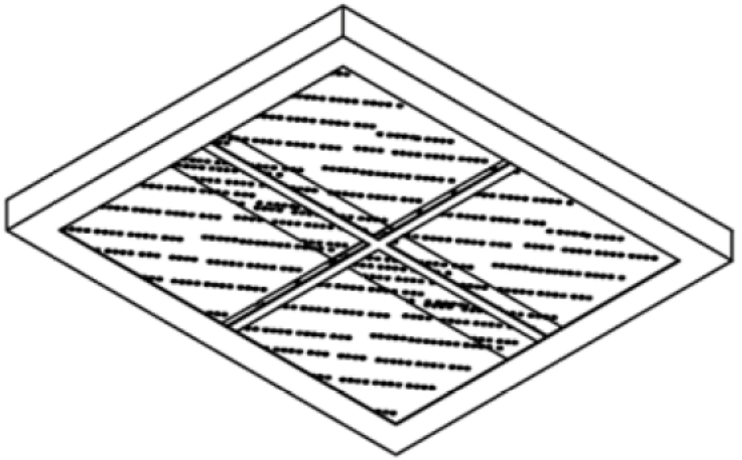

UNLESS OTHERWISE STATED GENERAL TOLERANCES: ±0.05 mm
ANGLES: ± 1 °

UNIVERSITY OF KWAZULU-NATAL	MAT.: Aluminium angle		No. REQ.: 1	SCALE: 1:30 UNITS: mm	PROJECT: Greenhouse solar drier
		DATE	CHECKED	STUDENT NAME: Pareshin Naidoo	
SCHOOL OF ENGINEERING	PROJECT SUPERVISOR			STUDENT No.: 212523981	
	WORKSHOP TECHNICIAN			E-MAIL: [redacted]	TITLE: Drying Tray
MECHANICAL ENGINEERING	TECHNICAL OFFICER			TEL. No.: [redacted]	

No.: 21
2021

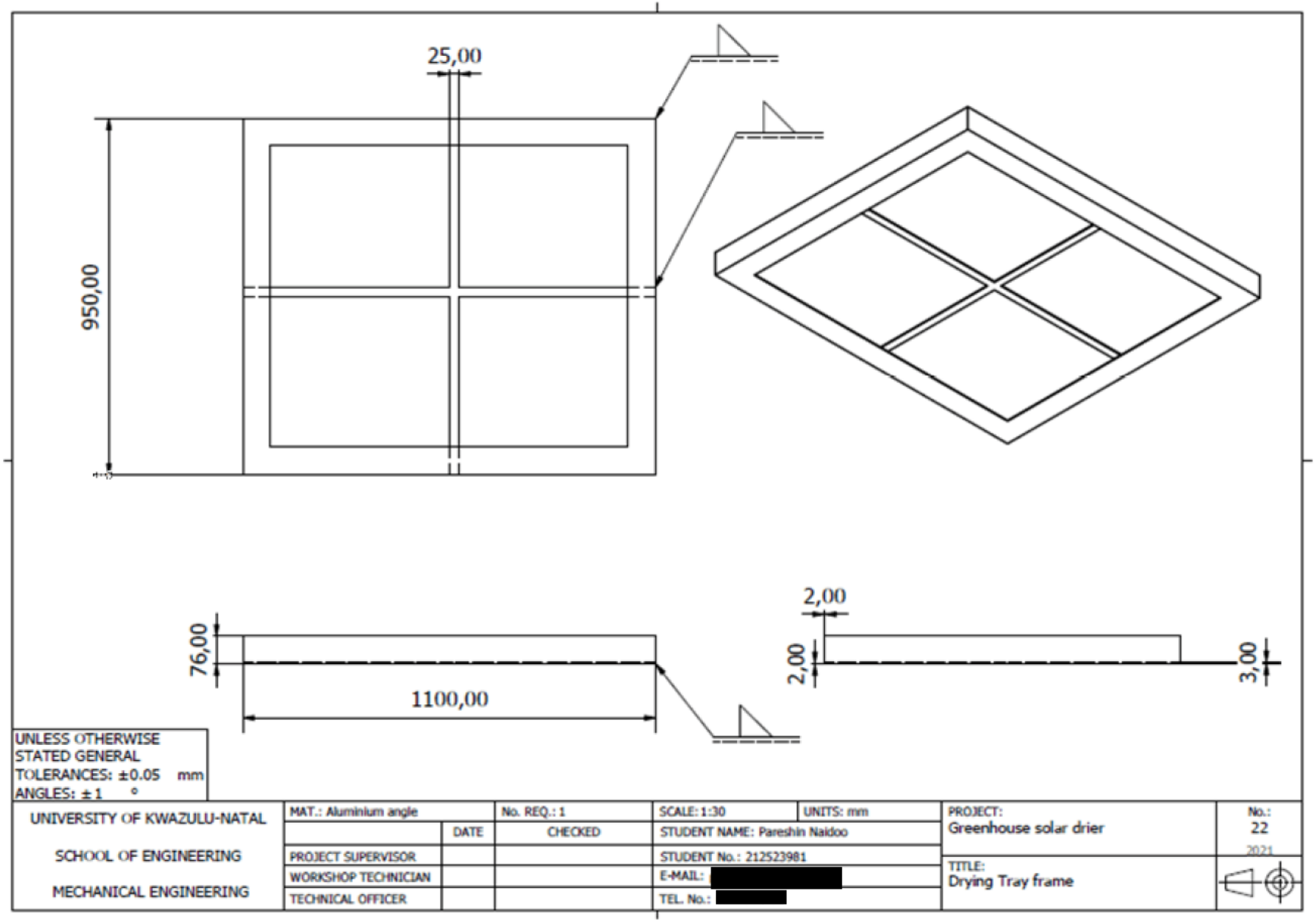
25,00
950,00
76,00
1100,00
2,00
2,00
3,00
UNLESS OTHERWISE STATED GENERAL TOLERANCES: ±0.05 mm
ANGLES: ±1 °
UNIVERSITY OF KWAZULU-NATAL
SCHOOL OF ENGINEERING
MECHANICAL ENGINEERING
MAT.: Aluminium angle
No. REQ.: 1
SCALE: 1:30
UNITS: mm
DATE
CHECKED
STUDENT NAME: Pareshin Naidoo
PROJECT SUPERVISOR
STUDENT No.: 212523981
WORKSHOP TECHNICIAN
E-MAIL: [redacted]
TECHNICAL OFFICER
TEL. No.: [redacted]
PROJECT:
Greenhouse solar drier
No.:
22
2021
TITLE:
Drying Tray frame

H-6. Floor Sheet Metal

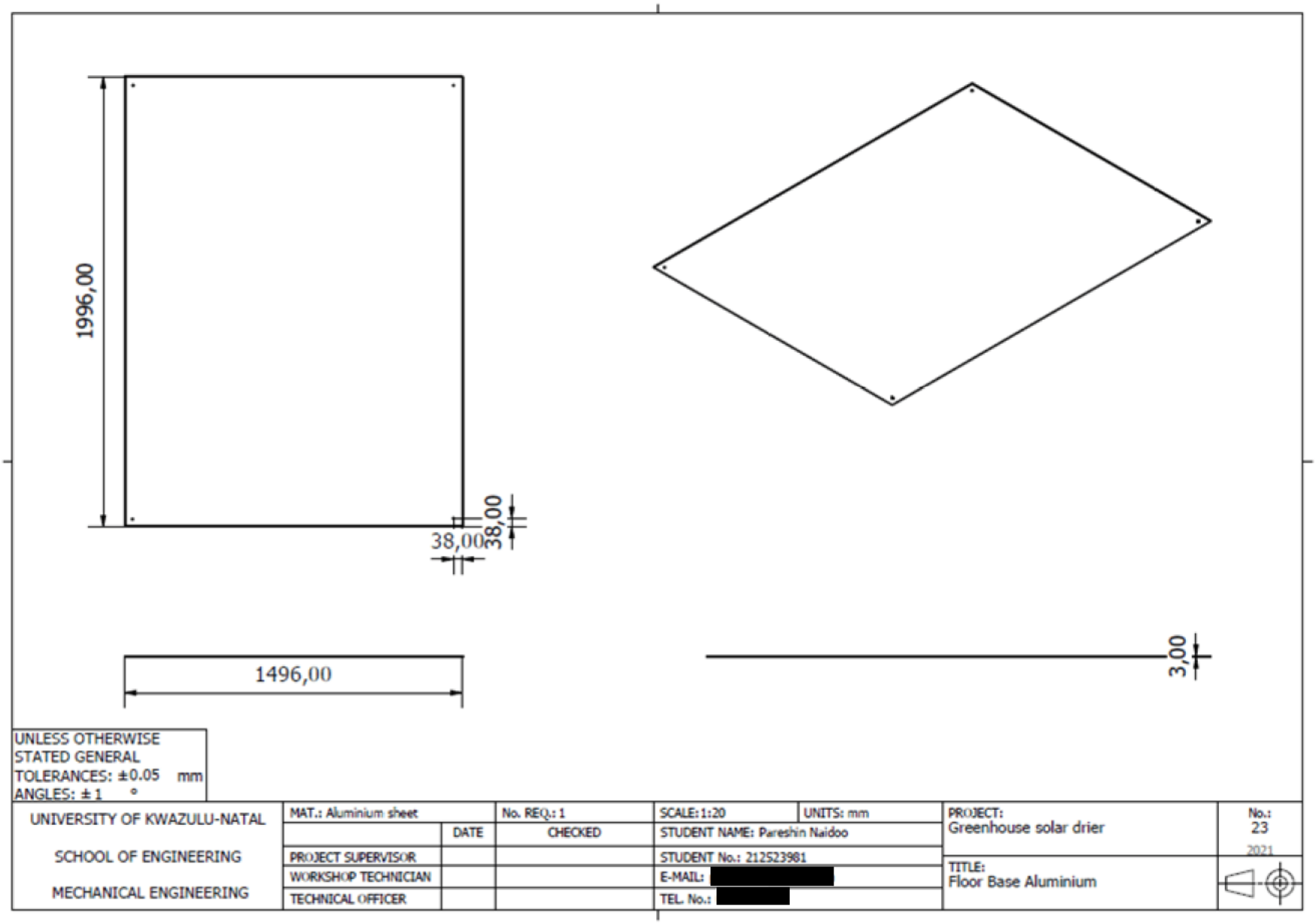
1996,00
38,00
38,00
1496,00
3,00
UNLESS OTHERWISE STATED GENERAL TOLERANCES: ±0.05 mm
ANGLES: ± 1 °
UNIVERSITY OF KWAZULU-NATAL
SCHOOL OF ENGINEERING
MECHANICAL ENGINEERING
MAT.: Aluminium sheet
No. REQ.: 1
SCALE: 1:20
UNITS: mm
DATE
CHECKED
STUDENT NAME: Pareshin Naidoo
PROJECT SUPERVISOR
STUDENT No.: 212523981
WORKSHOP TECHNICIAN
E-MAIL: [redacted]
TECHNICAL OFFICER
TEL. No.: [redacted]
PROJECT: Greenhouse solar drier
No.: 23
2021
TITLE: Floor Base Aluminium

H-7. Final Assembly

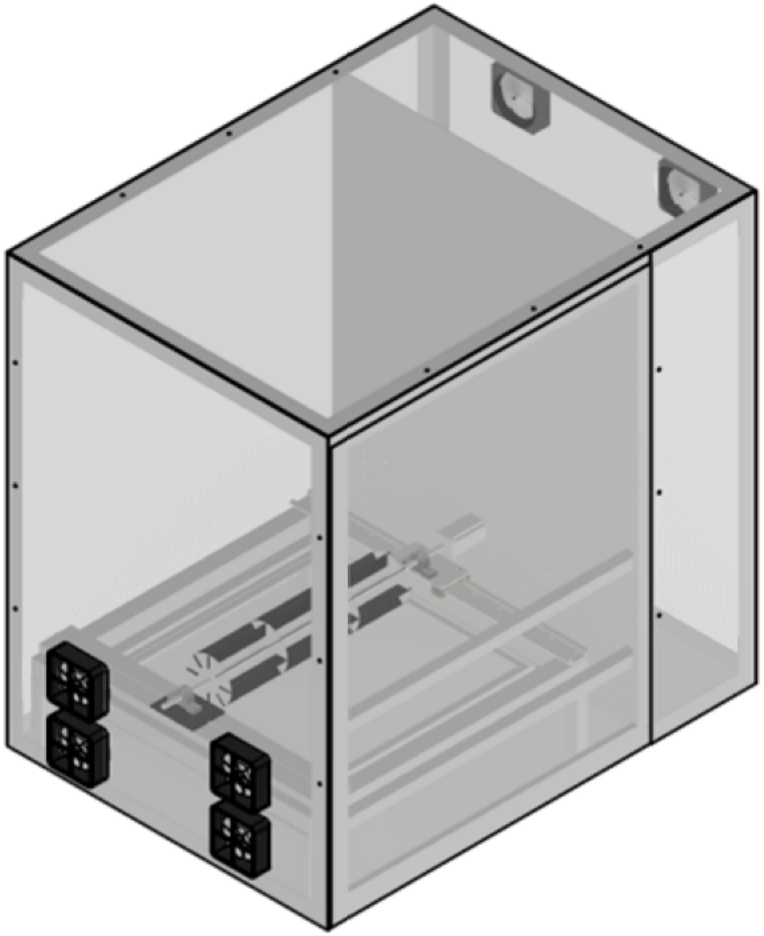

PARTS LIST			
ITEM	QTY	PART NUMBER	DESCRIPTION
1	2	Bottom and top Aluminium frame (enclosure)	
2	4	Vertical braces aluminium frame(enclosure)	
3	1	Door Frame	
4	1	Door hinge support	
5	1	floor aluminium	
6	1	drying table assembly	
7	1	Absorber wall	
8	1	top glass	
9	1	small pmma sheet	
10	1	right glass	
11	1	door PMMA	
12	1	Pmma front glass	
13	1	back glass	
14	6	Fan assembly	

UNLESS OTHERWISE STATED GENERAL TOLERANCES: ±0.05 mm
ANGLES: ± 1 °

UNIVERSITY OF KWAZULU-NATAL SCHOOL OF ENGINEERING MECHANICAL ENGINEERING	MAT.: Aluminium sheet		No. REQ.: 1	SCALE: 1:20	UNITS: mm
		DATE	CHECKED	STUDENT NAME: Pareshin Naidoo	
	PROJECT SUPERVISOR			STUDENT No.: 212523981	
	WORKSHOP TECHNICIAN			E-MAIL: [redacted]	
	TECHNICAL OFFICER			TEL. No.: [redacted]	

PROJECT: Greenhouse solar drier
No.: 24
2021
TITLE: Final Assembly

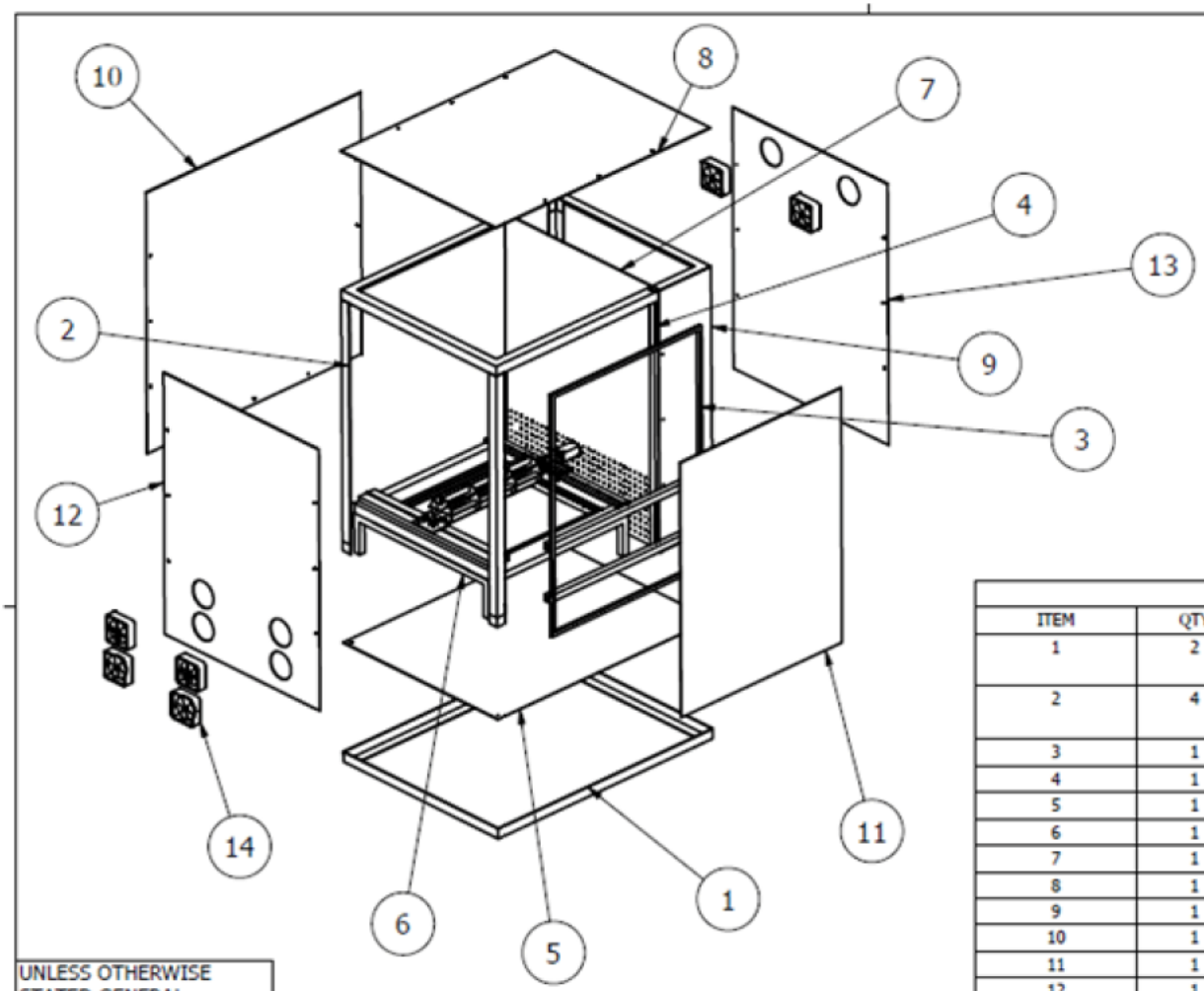

PARTS LIST			
ITEM	QTY	PART NUMBER	DESCRIPTION
1	2	Bottom and top Aluminium frame (enclosure)	
2	4	Vertical braces aluminium frame(enclosure)	
3	1	Door Frame	
4	1	Door hinge support	
5	1	floor aluminium	
6	1	drying table assembly	
7	1	Absorber wall	
8	1	top glass	
9	1	small pmma sheet	
10	1	right glass	
11	1	door PMMA	
12	1	Pmma front glass	
13	1	back glass	
14	6	Fan assembly	

UNLESS OTHERWISE STATED GENERAL TOLERANCES: ±0.05 mm
ANGLES: ± 1 °

UNIVERSITY OF KWAZULU-NATAL SCHOOL OF ENGINEERING MECHANICAL ENGINEERING	MAT.: Aluminium sheet		No. REQ.: 1	SCALE: 1:30	UNITS: mm
		DATE	CHECKED	STUDENT NAME: Pareshin Naidoo	
	PROJECT SUPERVISOR			STUDENT No.: 212523981	
	WORKSHOP TECHNICIAN			E-MAIL: [redacted]	
	TECHNICAL OFFICER			TEL. No.: [redacted]	

PROJECT: Greenhouse solar drier
No.: 25
2021
TITLE: Disconnect Assembly Drawing